THERMODYNAMICS, KINETICS AND MECHANISMS OF THE REACTIONS OF S(IV) WITH Cu(II) AND Fe(III).

Thesis by
Martha Harriet Conklin

In Partial Fulfillment of the Requirements
for the Degree of
Doctor of Philosophy

California Institute of Technology
Pasadena, California

1986

(Submitted June 2, 1986)

ACKNOWLEDGEMENTS

I wish to thank my thesis advisor, Michael Hoffmann, for his interest in my education and his support throughout this research. I would like to thank James Morgan for his helpful insights about my research project. Sunney Chan, Richard Flagan, James Morgan and John Seinfeld kindly served on my examining committee.

The graduate students in the department provided a ready forum to discuss research problems. The students and postdocs who shared the lab with me, Terri Olson, Ken Leung, Andy Hong, Bruce Faust, Alicia Gonzalez, contibuted to this work with their advice and friendship. Particular thanks goes to Eric Betterton who patiently shared his knowledge of chemistry with me.

The entire staff of the Keck have been good friends and helped me throughout my stay at Caltech. Rayma Harrison and Gunilla Hastrup provided expert library assistance. Sandy Brooks and Elaine Granger cheerfully helped me whenever the need arose. The technical support of Elton Daley, Leonard Montenegro, Joe Fontana and Rich Eastvedt in the design and construction of laboratory equipment is also appreciated.

Much of this research was done using resources outside the department. Sunney Chan made the EPR and Raman spectrometers available to me. Members of his group provided frequent assistance and advice.

I owe the completion of this thesis to my friends, Costas Synolakis, Jed Waldman, Roger Bales, Greg McRae, who continually

encouraged me and provided the support network I needed. My parents, Harriet and Roger Conklin, provided much help and understanding.

Generous financial support to Caltech and to this research were made by the U.S. Environmental Protection Agency and the Electric Power Research Institute.

ABSTRACT

Spectrosopic methods are used to determine the stability constant for the formation of $CuSO_3$, $K = 1.8 \pm 0.6 \times 10^4\ M^{-1}$ for $\mu = 0.4$ M. Infrared and Raman measurements indicate that sulfite binds to the metal through both sulfur and oxygen. These results are compared to those of other first-row transition metal-sulfite complexes.

The reduction of Cu(II) is shown to proceed via $(Cu(II))_2SO_3^{2+}$ and $CuSO_3CuOH^+$ intermediates. Copper(I), SO_4^{2-} and a mixed valence compound $Cu^{II}SO_3Cu^{I}_2SO_3 \cdot 2H_2O$ are determined to be the principal products. The rate law is consistent with consecutive first-order reactions. Results are interpreted in terms of the initial formation of an inner-sphere complex which is followed by a rate-limiting electron transfer step. Previously accepted mechanisms for the trace metal catalysis of the autoxidation of SO_3^{2-} are discussed in light of these results.

A conditional stability constant for the formation of a Fe(III)-S(IV) complex at $\mu = 0.4$ M and pH 2.1 was determined spectroscopically. Raman measurements indicate that sulfite binds to the metal through oxygen. EPR experiments show that the reduction of Fe(III) to Fe(II) by S(IV) is a slow reaction at pH 2 ($\tau_{1/2} \simeq 8$ min). Various pathways for the formation of the Fe(III)-S(IV) species are examined to determine the most probable equilibrium species. Results are interpreted by comparing the stability and bonding of Fe(III)-S(IV) species with other Fe(III) complexes.

The rates of these internal redox reactions are too slow for this reaction to be important in the atmospheric autoxidation of S(IV), instead ternary metal-oxygen-sulfito complexes are proposed as the active catalytic species in aqueous atmospheric systems. Calculations based on the equilibrium constants obtained in this study indicate that metal-S(IV) complexes may be important equilibrium species in the absence of α-hydroxyalkylsulfonates. The catalytic autoxidation of SO_2 in aqueous systems appears to proceed via the formation of metal-sulfite complexes as a prelude to electron-transfer.

TABLE OF CONTENTS

	PAGE
ACKNOWLEDGEMENTS	iii
ABSTRACT	v
LIST OF FIGURES	ix
LIST OF TABLES	xv
CHAPTER ONE: THE ROLE OF TRANSITION METALS IN ATMOSPHERIC CHEMISTRY	1
CHAPTER TWO: STRUCTURE AND THERMODYNAMICS OF TRANSIENT Cu(II)-S(IV) COMPLEXES	
Abstract	9
Introduction	9
Experimental	
Reagents and Materials	16
Spectrophotometric Methods	17
Product Identification	18
Results	
Raman and Infrared Spectroscopy Studies	19
Determination of Equilibrium Constant	35
Discussion	42
References	48
CHAPTER THREE: KINETIC STUDIES OF THE REDOX CHEMISTRY OF Cu(II)-S(IV) COMPLEXES	
Abstract	51
Introduction	51
Experimental	
Reagents and Materials	55
Oxygen-free Techniques	56
Spectrophotometric Methods	56
Analyses	57

PAGE

Results 58

Discussion 85

References 92

CHAPTER FOUR: THERMODYNAMICS, STRUCTURE AND KINETICS OF TRANSIENT Fe(III)-S(IV) COMPLEXES

Abstract 95

Introduction 95

Experimental

Reagent and Materials 105

Oxygen-free Techniques 105

Spectrophotmetric Methods 106

Results

Determination of Equilibrium Constant 107

Raman Spectroscopy Studies 114

Spectrophotometric Kinetic Studies 116

Electron Paramagnetic Resonance Kinetic Studies 123

Discussion 125

References 135

CHAPTER FIVE: SUMMARY

Cu(II)-S(IV) System 138

Fe(III)-S(IV) System 139

Comparison between the Fe(III)- and Cu(II)-S(IV) Systems 140

Implications for Atmospheric Systems 141

Suggestions for Future Research 143

References 145

APPENDIX A: SCREENING TECHNIQUES

Electron Spectroscopy for Chemical Analysis 146

Fourier Transform Infrared Spectroscopy 151

Titrations 153

Cyclic Voltammetry 154

Electron Paramagnetic Resonance 156

References 168

APPENDIX B: EXPERIMENTAL DATA FOR CHAPTER THREE 169

LIST OF FIGURES

FIGURE		*PAGE*
2.1	Absorbance spectrum of the Cu(II)-S(IV) complex (recorded immediately after mixing) compared to the absorbance spectrum of a $Cu(NO_3)_2$ solution.	11
2.2	Structure of Chevreul's salt, $Cu^{II}SO_3Cu^{I}_2SO_3 \cdot 2H_2O$ (Nyberg and Kierkegaard, 1968).	15
2.3	Possible structural configurations of metal-sulfite complexes.	20
2.4	Infrared spectra of (a) $Cu_2SO_3(OH)_2 \cdot H_2O$ and (b) $Cu^{II}SO_3Cu^{I}_2SO_3 \cdot 2H_2O$ (* marked bands are due to Nujol).	25
2.5	Raman spectra of 0.2 M (a) $SO_2 \cdot H_2O$, (b) $NaHSO_3$, and (c) Na_2SO_3.	29
2.6	Raman spectra of crystalline $Na_2S_2O_5$.	31
2.7	Raman spectrum of Cu(II)-S(IV) system.	34
2.8	Raman spectrum of $Cu_2SO_3(OH)_2 \cdot H_2O$ after decomposition in spectrometer.	36
2.9	Absorbance (350 nm) of the Cu(II)-S(IV) complex as a function of [S(IV)] at (a) pH 3.6 and (b) pH 4.4.	39
2.10	Equation 2.2 applied to data in Figure 2.9 (a) pH 3.6 and (b) pH 4.4. (Error bars are shown when they exceed symbol size).	40

FIGURE		*PAGE*
3.1	Absorbance spectra of the Cu(II)-S(IV) complex (obtained immediately after mixing) when (a) NO_3^-, (b) ClO_4^-, (c) SO_4^{2-} and (d) Cl^- are present in excess (μ = 0.1 M, $[Cu(II)]_o$ = 1 mM, $[S(IV)]_o$ = 10 mM, pH = 5). Broken line is the aqueous Cu(II) spectrum without S(IV) present.	59
3.2	Absorbance spectra of Cu(II)-S(IV) complexes at different initial pH recorded within 30 sec of mixing.	60
3.3	Changes in the absorbance spectrum of the Cu(II)-S(IV) complex over time.	61
3.4	Cu(II) EPR spectrum for the Cu(II)-S(IV) system in the presence of (a) ClO_4^- and (b) NO_3^-.	66
3.5	Kinetic effects of increasing the photon flux (λ > 300 nm) on the absorbance at 340 nm of the Cu(II)-S(IV) complexes. Sampling interval refers to the interval between measurements when the mixture is exposed to a full spectrum of light (200 to 800 nm).	68
3.6	Effects of adding radical inhibitors, mannitol and methanol, to the Cu(II)-S(IV) system when it is irradiated with light (λ > 300 nm).	70
3.7	Kinetic data obtained at 340 nm on the HP 8450A of a Cu(II)-S(IV) mixture that was kept in the dark. The solid line was fit to the data using a nonlinear least squares double-exponential fitting routine.	71
3.8	Structural representation of the proposed mechanism for the reaction between Cu(II) and S(IV). (Overall charges and coordination waters have been omitted for clarity).	75

FIGURE		PAGE
3.9	Kinetic data obtained at 350 nm for the Cu(II)-S(IV) system at different values of pH (using the Shimadzu MPS-2000).	79
3.10	Appearance of sulfate with time in the Cu(II)-S(IV) system at different values of pH.	81
3.11	The pH dependence of the rate constants (a) k_1 (sec^{-1}) and (b) k_2 (sec^{-1}) for data collected at 350 and 800 nm. The solid curve is a cubic-spline fit to the data.	83
3.12	Kinetic data collected at 350 nm for the Cu(II)-S(IV) system with different anions present in the system.	86
4.1	Absorbance spectra of the Fe(III)-S(IV) complex at two Fe(III)-S(IV) ratios (a) absorbance spectra of whole system and (b) difference spectra of the complex (absorbance due to uncomplexed Fe(III) subtracted). ($[Fe(III)]_o$ = 0.5 mM).	96
4.2	Distribution of Fe(III) species as a function of pH for two different iron concentrations. Shaded area represents saturated solutions (Stumm and Morgan, 1981).	98
4.3	Absorbance of the Fe(III)-S(IV) complex as a function of [S(IV)] at (a) 350 nm and (b) 450 nm.	111
4.4	Equation 4.9 applied to data in Figure 4.3 at (a) 350 nm and (b) 450 nm. (Error bars are shown when they exceed symbol size).	112
4.5	Raman spectrum of Fe(III)-S(IV) system.	115

FIGURE		*PAGE*
4.6	A diagram of a typical kinetic trace obtained with the stopped-flow ($[Fe(III)]_o$ = 1 mM, $[S(IV)]_o$ = 1 mM, pH = 2, μ = 1.3 M).	117
4.7	Kinetic data for disappearance of the absorbance (350 nm) due to the Fe(III)-S(IV) charge transfer complexes, at different Fe(III):S(IV) ratios (μ = 1 M, pH 2).	120
4.8	Kinetic data for disappearance of the absorbance (350 nm) due to the Fe(III)-S(IV) complexes under different light conditions. Sampling interval refers to the interval between absorbance measurements when the mixture is exposed to a full spectrum of light (200 to 800 nm). ($[Fe(III)]_o$ = 5 mM, $[S(IV)]_o$ = 5 mM, pH 2, μ = 1 M).	122
4.9	EPR spectrum of 1 mM Fe(III) compared to the EPR spectra of Fe(III)-S(IV) complexes (pH 2).	124
4.10	Time series of EPR spectra of the Fe(III)-S(IV) system at different Fe(III):S(IV) ratios (a) 1:2, (b) 1:1 and (c) 1:10.	126
4.11	The peak heights of the Fe(III) signal of the time series in Figure 4.7c plotted as a function of time ($[Fe(III)]_o$ = 1 mM, [S(IV)] = 10 mM, pH 2).	127
A.1	ESCA spectrum of $Cu^{II}SO_3Cu^{I}_2SO_3 \cdot 2H_2O$ sample (broad sweep, 1280 eV).	148
A.2	ESCA spectra of $Cu^{II}SO_3Cu^{I}_2SO_3 \cdot 2H_2O$ sample (a) copper peak and (b) sulfur peak (narrow sweeps).	149

FIGURE		*PAGE*
A.3	The copper peak of Fig. A.2 ,smoothed, (a) shown as a function of time and (b) the peaks from (a) are compared for t = 7 min and t = 124 min to show the change in signal shape.	150
A.4	FTIR spectra of (a) H_2O in BaF_2 cells and (b) 0.25 M HSO_3^-, 0.25 M HSO_3^- + 0.25 M Cu(II), pH 1 and H_2O in BaF_2 cells after the cells were exposed to the Cu(II)-S(IV) mixture.	152
A.5	Cyclic voltammetry signal obtained for Cu(II)-S(IV) mixture.	155
A.6	Theoretical line shapes for s = ½ EPR spectra (a) isotropic case, $g_x = g_y = g_z$, (b) axial case, $g_{\parallel} > g_{\perp}$, (c) rhombic case, $g_x \neq g_y \neq g_z$, and (d) axial case, $g_{\parallel} < g_{\perp}$. (Taken from Palmer, 1980).	160
A.7	Simulation of magnetic dipolar interaction between two paramagnets (g_x = 1.5, g_y = 2.2, g_z = 3.5, and g_x = 2.0, g_y = 2.0, g_z = 2.17) at a distance of 5 Å and at various orientations of the g-tensors. The multiplicative factors were employed to scale the spectra to the same size. (Taken from Palmer, 1980).	162
A.8	EPR spectra of Cu(II)-S(IV) mixtures at different ratios (a) S(IV):Cu(II) = 1, (b) S(IV):Cu(II) = 2 and (c) S(IV):Cu(II) = 10. ($[Cu(II)]_T$ = 2 mM, pH = 5).	164
A.9	Cu(II) EPR spectrum for the Cu(II)-S(IV) system in the presence of (a) ClO_4^- and (b) NO_3^-.	165

FIGURE		*PAGE*
B.1	Kinetic data obtained at 350 nm for the Cu(II)-S(IV) system (a) pH 4.9, (b) pH 4.4, and (c) pH 4.4. (The solid line in (c) was fit to the data using a nonlinear least squares double-exponential fitting routine). ($[S(IV)]_o$ = 10 mM, $[(Cu(II)]_o$ = 1 mM).	171
B.2	Kinetic data obtained at 350 nm for the Cu(II)-S(IV) system with different anions present (a) ClO_4^-, pH 4.8 (b) SO_4^{2-}, pH 4.9, and (c) Cl^-, pH 4.9. (The solid line was fit to the data using a nonlinear least squares double-exponential fitting routine). ($[S(IV)]_o$ = 10 mM, $[(Cu(II)]_o$ = 1 mM).	172
B.3	Kinetic data obtained for the Cu(II)-S(IV) system at pH 5.2 (a) 350 nm, (b) 350 nm, and (c) 800 nm. (The solid lines in (b) and (c) were fit to the data using a nonlinear least squares double-exponential fitting routine). ($[S(IV)]_o$ = 10 mM, $[(Cu(II)]_o$ = 1 mM).	173
B.4	Kinetic data obtained for the Cu(II)-S(IV) system at pH 5.7 (a) 350 nm, (b) 350 nm, and (c) 800 nm. (The solid lines in (b) and (c) were fit to the data using a nonlinear least squares double-exponential fitting routine). ($[S(IV)]_o$ = 10 mM, $[(Cu(II)]_o$ = 1 mM).	174
B.5	Kinetic data obtained for the Cu(II)-S(IV) system at pH 6.2 (a) 350 nm, (b) 350 nm, and (c) 800 nm. (The solid lines in (b) and (c) were fit to the data using a nonlinear least squares double-exponential fitting routine). ($[S(IV)]_o$ = 10 mM, $[(Cu(II)]_o$ = 1 mM).	175

LIST OF TABLES

TABLE		PAGE
1.1	Transition metal concentrations in rain and fog for various regions.	3
2.1	Stability constants for sulfate and sulfite complexes.	13
2.2	Vibrational frequencies (cm^{-1}) of the sulfite ion.	21
2.3	Elemental analysis of Cu(II)-S(IV) precipitate.	23
2.4	Vibrational frequencies of metal-sulfite complexes (1105-450 cm^{-1}).	26
2.5	Infrared bands of metal-sulfites (cm^{-1}).	28
2.6	Raman vibrational spectra of meta-bisulfite (cm^{-1}).	33
2.7	Calculated equilibrium concentrations for the Cu(II)-S(IV) system using the determined equilibrium constant for $CuSO_3$.	43
2.8	Calculated stability constants for MSO_3 complexes.	45
2.9	Stability constants for Cu(II) complexes (25 $^{\circ}C$)	47
3.1	Distribution of S(IV) species compared to the initial intensity of the Cu(II)-S(IV) complex absorbance at different values of pH.	64

TABLE		PAGE
3.2	Data based on changes in the areas under the recorded EPR spectra of the Cu(II)-S(IV) system presented in Fig. 3.4 as a function of time.	67
3.3	Values of the observed rate constant for the initial phase of the Cu(II)-S(IV) reaction at different reactant ratios.	73
3.4	Definitions of the constants in equation 3.29 at different experimental conditions.	82
3.5	Self-exchange rate constants and reduction potentials for some copper(II)-(I) couples.	88
4.1	Rate constants for the formation of mono-complexes of Fe(III) (25 $^{\circ}$C).	102
4.2	Observed rate constants for the Fe(III)-S(IV) system in 1 M HCOOH (pH 2).	121
4.3	Stability constants for Cu(II) and Fe(III) complexes (25 $^{\circ}$C)	131
A.1	Data based on changes in the areas under the recorded EPR spectra of the Cu(II)-S(IV) system presented in Fig. A.9 as a function of time.	166
B.1	Experimental data for Table 4.3	170

CHAPTER ONE

THE ROLE OF TRANSITION METALS IN ATMOSPHERIC CHEMISTRY

The fate of SO_2 in the atmosphere has been debated since the nineteenth century when Smith (1872) identified the problem of "acid rain". He observed that the acidity of rain increased in the vicinity of anthropogenic emissions, especially emissions from combustion and manufacturing sources. Both gaseous and aqueous pathways have been identified as possible routes for the oxidation of SO_2 to SO_4^{2-}. Until recently, most discussions of SO_2 oxidation in the atmosphere focused on homogeneous gas-phase oxidation by free radicals $OH^{\bullet}$, $OH_2^{\bullet}$ and $RO_2^{\bullet}$ (Calvert et al., 1978). More recent studies indicate that these radical reactions are slower than previously thought (Burrows et al., 1979; and Graham et al., 1979). The reaction with the primary gas-phase radical, $OH^{\bullet}$, is not sufficiently rapid to account for observed ambient sulfate formation rates (Middleton et al., 1980, Möller, 1980). Cass (1977) found that the rate of aerosol sulfate formation apparently increased with increasing relative humidities. At high relative humidities sub-micron particles are typically in the aqueous droplet rather than the crystalline form. Numerous pathways have been proposed for the aqueous-phase oxidation of S(IV), such as oxidation by H_2O_2, O_3 and O_2. (The term S(IV) includes the aqueous S species in the +4 oxidation state, $SO_2 \cdot H_2O$, HSO_3^- and SO_3^{2-}.) Middleton et al. (1980) suggested that H_2O_2 was the primary contributor to sulfate aerosol production under daytime conditions, and under nighttime conditions, without photochemical reactions, catalytic and

noncatalytic oxidation on wetted aerosols become the important pathways. Möller (1980) developed a kinetic model which included metal-catalyzed autoxidations, O_3 and H_2O_2 reactions (using literature values for rate constants and rate laws) for the production of SO_4^{2-} from SO_2. He predicted that SO_2 would be removed from the atmosphere by gas-phase oxidation (9%), aqueous-phase oxidation (35%), dry deposition (45%) and wet deposition (11%). Graedel et al. (1985) simulated the chemical processes occurring within raindrops falling from the cloud-base to the ground. They reported that transition metal-catalyzed pathways would account for 30-55% of the oxidation of S(IV) to S(VI) at pH 4.

Most of the mechanisms for the metal catalyzed autoxidation of S(IV) can be classified into two categories (Hoffmann and Boyce, 1983), either two-electron polar reactions, which invoke ternary complexes comprised of S(IV), O_2 and the transition metal (e.g. Bassett and Parker, 1951) or one-electron radical chain mechanisms in which an electron transfer from the metal to S(IV) is the first step (Bäckström, 1934). Information about the stability constants of the postulated intermediate complexes and the rate of reduction of the metal by S(IV) is necessary to determine which of these is the more probable pathway.

The metals of particular interest for atmospheric systems are first-row transition metals, such as Fe(III), Mn(II) and Cu(II), which are found in atmospheric systems (see Table 1.1) and they have been shown to be effective catalysts for the autoxidation of S(IV). Of these metals, Fe(III) is perhaps the most important metal catalyst found in atmospheric systems. Hoffmann and Calvert (1985) calculated

TABLE 1.1

Metal concentrations in rain and fog[a] for various regions

Location	Concentrations (μM/l)		
	Fe	Cu	Mn
Minnesota/ Wisconsin[b]	9×10^{-2}-2.5x10	8×10^{-2}-2.4	9×10^{-2}-1.1
Britain[c]	2.3-5.6x10	3.6×10^{-1}-1.3	2.2×10^{-1}-4.2×10^{-1}
Bermuda[d]	3×10^{-2}-2.3×10^{-1}	2×10^{-3}-3×10^{-1}	2×10^{-3}-2×10^{-2}
North/South Atlantic[e]	9×10^{-1}-8.1	8×10^{-2}-8.7	2×10^{-2}-2.2×10^{-1}
Enewetak Atoll[f]	4×10^{-3}-5×10^{-2}	8×10^{-5}-2×10^{-3}	2×10^{-4}-10^{-2}
Southern California[g,h]	1.7-4.3×10^{2}	1.9×10^{-1}-2.4	5×10^{-2}-2.3

[a]The values for Southern California are for fog, the rest are for rain.
[b]Pratt et al. (1984)
[c]Peirson et al. (1974)
[d]Jickell et al. (1984)
[e]Berresheim and Jaeschke (1982)
[f]Arimoto et al. (1985)
[g]Waldman et al. (1982)
[h]Jacob et al. (1986)

that the Fe(III)-catalyzed autoxidation of S(IV) can be the most important aqueous-phase pathway in atmospheric aerosols at pH > 6.

Although, first-row transition metal-sulfite complexes have been studied previously, little information is available about either their structure or their formation constants. If the sulfite ion binds to metals through oxygen, similarity between sulfate and sulfite stability constants could exist. When equilibrium constants for sulfite complexes are compared to equilibrium constants for equivalent sulfate complexes, sulfite complexes have significantly higher equilibrium constants. This difference may be due to metal-S bonding in the metal-sulfite complexes. Sulfur has low-lying d-orbitals available to overlap with the metal, and thus complexes with metal-S bonds would be expected to be more stable complexes than O-bonded counterparts.

Carlyle (1971) and Hansen et al. (1976) have reported stability constants for $FeSO_3^+$. (The waters of hydration will not be included in the chemical representations of metal complexes, e.g. $FeSO_3^+$ actually means $Fe(H_2O)_5SO_3^+$, Cu^{2+} means $Cu(H_2O)_6^{2+}$, etc.). However, their values differ by 10^{12}. The confusion as to the magnitude of the stability constant may be due to the complicated aqueous-phase chemistry of Fe(III) as well as the transient nature of these complexes. One of the most problematic features of Fe(III) chemistry is its tendency to hydrolyze and to polymerize (Stumm and Morgan, 1981). Iron(III) can be distributed between Fe^{3+}, $FeOH^{2+}$, $Fe(OH)_2^+$ and $Fe_2(OH)_2^{4+}$ in aqueous solutions at low pH; the distribution being governed by Fe(III) concentrations and pH. Furthermore, the Fe(III)-S(IV) complexes are unstable species; the Fe(III) is reduced to

Fe(II) while S(IV) is oxidized to S(VI). Electron transfer reactions between S(IV) and first-row transition metals have been proposed as the chain initiation steps for the free-radical chain oxidation of S(IV) by O_2 (Bäckström, 1934). A detailed knowledge of these electron transfer rates are needed to evaluate the importance of free-radical one-electron pathways and two-electron polar pathways.

As noted in Table 1.1 Fe is the most aboundant transition metal present in atmospheric water droplets. However, due to the complicated chemistry of Fe(III) in aqueous solution Cu(II) was selected as a more tractable model for the interaction of S(IV) with first-row transition metals. The hexaquo species of Cu^{2+} is the predominant form of Cu(II) below pH 8. Similar to the Fe(III)-S(IV) system, Cu(II) forms transient charge-transfer complexes with S(IV). The Cu(II) is reduced to Cu(I) as S(IV) is oxidized to S(VI) in this system. The reduction of Cu(II) by S(IV) is a well-known reaction. This reaction has been used in the recovery of Cu from ore (Linkson and Nobbs, 1981) and in the laboratory preparation of Cu(I) (Keller and Wycoff, 1946). However, no information is available about either the stability of the $CuSO_3$ complex or about the kinetics of the electron transfer between Cu(II) and S(IV).

The principal objectives of this research are: (1) to determine the nature of the metal-sulfite bond in metal-sulfite complexes, (2) to determine stability constants for Cu(II)- and Fe(III)-S(IV) complexes; and (3) to determine the rates, rate laws and mechanisms of the reduction of the Cu(II) and Fe(III) by S(IV). Results of this research

will be used to shed light on the potential role of metal-sulfite complexes in aqueous atmospheric systems.

REFERENCES

Arimoto, R., P.A. Duce, B.J. Ray and C.K. Unni, 1985, *J. Geophys. Res.*, **90**, 2391-2408.

Bäckström, H.L.J., 1934, *Z. Phys. Chem. (Leipzig)*, **25B**, 122-138.

Bassett, H. and W.G. Parker, 1951, *J. Chem. Soc*, **46**, 1540-1560.

Berresheim, H. and W. Jaeschke in *Atmospektrom Spurenanai, Vortr. Kolloq.*, B. Weiz, ed. (Verlag Chem., Weinheim, 1982).

Burrows, J.P., D.I. Cliff, G.W. Harris, B.A. Thrush and J.P.T. Wilkinson, 1979, *Proc. Roy. Soc. (London)*, **A368**, 463-481.

Calvert, J.G., F. Su, J.W. Bottenheim and O.P. Strauz, 1978, *Atmos. Env.*, 12, 197-226.

Carlyle, D.W., 1971, *Inorganic Chemistry*, **10**, 761-764.

Cass G.R., *Methods for Sulfate Air Quality Management with Applications to Los Angeles* (Ph.D. Thesis, Env. Eng. Sci., Calif. Inst. Tech., Pasadena, CA, 1977).

Graedel, T.E., C.J. Weshler and M.L. Mandich, 1985, *Nature*, **317**, 240-242.

Graham, R.A., A.M. Winer, R. Atkinson, and J.N. Pitts, Jr., 1979, *J. Phys. Chem.*, **83**, 1563-1566.

Hansen, L.D., Whiting, D.J. Eatough, T.E. Jensen, R.M. Izatt, 1976, *Anal. Chem.*, **48**, 634-638.

Hoffmann, M.R. and S.D. Boyce, in *Trace Atmospheric Constituents, Adv. Environ. Sci. & Tech., Vol. 12*, S.E. Schwartz,ed. (John Wiley & Sons, New York, 1983) pp. 147-189.

Hoffmann, M.R. and J.G. Calvert, *Chemical Transformation Modules for Eulerian Acid Deposition Models, Vol. II. The Aqueous-Phase Chemistry*, (U.S. E.P.A., N.C.A.R. Interagency Agreement DW 930237, 1985).

Jacob, D.J., J.W. Munger, J.M. Waldman, M.R. Hoffmann, 1986, *J. Geophys. Res.*, **91D**, 1073-1088.

Jickells, T.D., A.H. Knap and T.M. Church, 1984, *J. Geophys. Res.*, **89**, 1423-1428.

Keller, R.N. and H.D. Wycoff, 1946, *Inorg. Syn.*, **2**, 1-2.

Linkson, P.B. and D.M. Nobbs in *Proceedings from CHEMECA 81, 9th Australian Conference on Chemical Engineering*, Christchurch, New Zealand, Aug.-Sept., 1981, pp.107-115.

Middleton, P., C.S. Kiang and V.A. Mohnen, 1980, *Atmos. Env.*, **14**, 463-472.

Möller, D., 1980, *Atmos. Env.*, **14**, 1067-1076.

Peirson, D.H., P.A. Carose and R.S. Cambray, 1974, *Nature*, **251**, 675-679.

Pratt, G.C., M.R. Coscio and S.V. Krupa, 1984, *Atmos. Env.*, **18**, 173-182.

Smith, R.A., *Air and Rain: The Beginning of a Chemical Climatology* (Longmans Green, London, 1872).

Waldman, J.M., J.W. Munger, D.J. Jacob, R.C. Flagan, J.J. Morgan and M.R. Hoffmann, 1982, *Science*, **218**, 677-680.

CHAPTER TWO

STRUCTURE AND THERMODYNAMICS OF TRANSIENT Cu(II)-S(IV) COMPLEXES

ABSTRACT

The stability constant for the formation of $CuSO_3$ is determined spectroscopically. The calculated stability constant, $K = 1.8 \pm 0.6 \times 10^4\ M^{-1}$ for $\mu = 0.4$ M, is relatively large compared to the stability constants of simple inorganic complexes of Cu(II) such as $CuSO_4$, $CuCl^+$, $CuClO^+$ and $CuNO_3^+$. Infrared and Raman measurements indicate that sulfite binds to the metal through both sulfur and oxygen. $CuSO_3$ complexes are compared to other first-row transition metal-sulfite complexes.

INTRODUCTION

When blue copper (Cu(II)) solutions were mixed with colorless sodium sulfite (Na_2SO_3) solutions, the resultant solution immediately changed color from blue to green at pH < 6.0. This color change was indicative of the formation of Cu(II)-S(IV) complexes. These complexes underwent a series of redox reactions that resulted in an aqueous mixture of Cu(I), Cu(II), SO_4^{2-} and SO_3^{2-} in apparent equilibrium with a red mixed-valence precipitate of copper, Chevreul's salt ($Cu^{II}SO_3Cu_2^{I}SO_3 \cdot 2H_2O$). The apparent stoichiometry for the reduction of Cu(II) was as follows:

$$2Cu(II) + SO_3^{2-} + H_2O = 2Cu(I) + SO_4^{2-} + 2H^+.$$

The UV/Visible absorbance spectrum of the intermediate species is shown in Fig. 2.1. The absorbance of these complexes appeared as a broad shoulder between 350 nm and 400 nm and a broad peak at 800 nm that is characteristic of Cu(II) ligand-field complexes (and accounts for the green color). When the initial pH of the mixture was greater than 6 ($[Cu(II)]_o$ > 2 mM), a green Cu(II)-S(IV) solid precipitated immediately. The Cu(II)-S(IV) solid reacted further over a period of hours to form a yellow solid which in turn converted into the red crystals of Chevreul's salt ($Cu^{II}SO_3Cu^{I}_2SO_3 \cdot 2H_2O$) within a day. When Cl^- was present, a white precipitate of CuCl was obtained before $Cu^{II}SO_3Cu^{I}_2SO_3 \cdot 2H_2O$ precipitated. The Cu(II)-S(IV) solid was used to obtain information about the bonding of transient aqueous Cu(II)-S(IV) species.

Previous studies have focused on reaction stoichiometry and product determination (Ramberg, 1910; Baubigny, 1912; Albu and Graf von Schweinitz, 1937; and Foffani and Menegus-Scarpa, 1953). Baubigny (1912), who investigated the system under anoxic conditions with [S(IV)] ≃ 1.0 M > [Cu(II)], found the following stoichiometry:

$$2CuSO_4 + 4Na_2SO_3 \rightleftharpoons 2Na_2SO_4 + (Cu_2SO_3 + Na_2SO_3)\downarrow + Na_2S_2O_6.$$

According to Baubigny, the reduction of Cu(II) by S(IV) appeared to be similar to the reduction of Ag(I) by S(IV). The unique features of this reaction were the apparent formation of a precipitate (Cu_2SO_3) and $S_2O_6^{2-}$. Albu and Graf von Schweinitz (1937) repeated Baubigny's experiments and noted that dithionate was only a product under alkaline

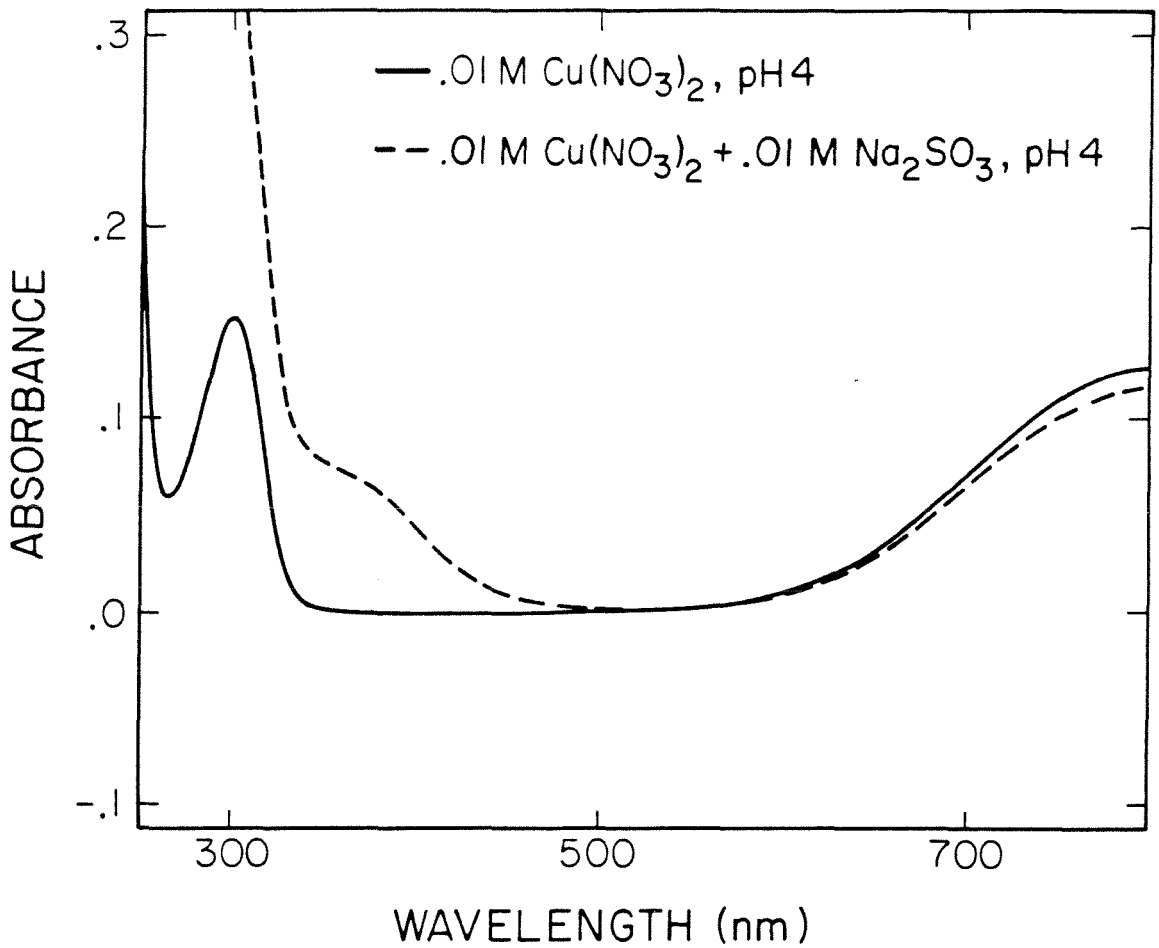

Fig. 2.1 Absorbance spectrum of the Cu(II)-S(IV) complex (recorded immediately after mixing) compared to the absorbance spectrum of a $Cu(NO_3)_2$ solution.

conditions (pH $\simeq$ 10). Ramberg (1910) determined that Cu(I) initially precipitated as $Cu_2SO_3 \cdot 0.5H_2O$ (Étard's salt). It was shown to be unstable with respect to $Cu_2SO_3 \cdot H_2O$ (Rojoski's salt). Dansent and Morrison (1964) showed that $Cu_2SO_3 \cdot H_2O$ was actually a mixture of elemental Cu and $Cu^{II}SO_3Cu^{I}_2SO_3 \cdot 2H_2O$. Foffani and Menegus-Scarpa (1953) ascertained that the green complex was transformed to $Cu(SO_3)_2^{3-}$ under anoxic conditions.

Equilibrium constants for some known metal-S(IV) and metal-S(VI) complexes are listed in Table 2.1. Substantial differences in the stability constants for certain metals are noted. These variations are due to differences in bonding for the two anions. Sulfate is limited to coordination through oxygen whereas sulfite can coordinate through either sulfur or oxygen. The reported stability constants tend to be higher for transition metal complexes with metal-sulfur bonds. Sulfur is more likely to form stronger bonds with metals than oxygen because of its stronger electron-donating ability and higher polarizability. The most pronounced example of the difference between the stability of metal-oxygen and metal-sulfur bonds is given by mercury, which exhibits a difference of 10^{22} between the stability constants of SO_3^{2-} and SO_4^{2-} complexesy. Mercury is known to have a much greater affinity for S than for O; therefore the bonding is assumed to be through S in $Hg(SO_3)_2^{2-}$.

Cu(I) is known to form a salt with S(IV), NH_4CuSO_3, which contains O and S bonds (Nyberg and Kierkegaard, 1968), but little is known about the bonding and stability of aqueous Cu(II)-S(IV) complexes. In $Cu^{II}SO_3Cu^{I}_2SO_3 \cdot 2H_2O$, in which both Cu(I) and Cu(II) are bonded to SO_3^{2-},

TABLE 2.1

Stability constants for sulfate and sulfite complexes[a]

Metal Complex[b]	Ionic Strength (M)	Log of Stability Constant MSO_3	MSO_4
AgL	0.0	5.6	1.3
CdL_2	1.0	4.2	1.6
HgL_2	1.0	24.1	2.4
CeL	0.0	8.0	3.6
UO_2L	1.0	5.26	1.8
Cu(II)L	0.0	4.2[c]	2.36
Cu(I)L	1.0	7.85	

[a]From Smith and Martell (1976) and Sillèn and Martell (1964 and 1971)

[b]L = SO_3^{2-} or SO_4^{2-}

[c]This work (μ = 0.4 M)

the Cu(I) is bonded to the SO_3^{2-} through both O and S bonds; Cu(II) is bonded through O bonds (the structure is presented in Fig. 2.2).

Copper(II) and Cu(I) have different bonding characteristics. Copper(I) is a class b metal, or soft base. Copper(I) follows the trend of increased polarizability over Cu(II), and of having a decreased number of coordination sites (four, instead of five or six). Copper(I) preferentially complexes with "soft" sulfur containing ligands. Copper(II) is sometimes classified as Class b (Gray, 1973), but it can show characteristics of both classes.

The complexes formed by divalent metal ions with many chelating ligands, in which the donors are either oxygen or nitrogen atoms, tend to follow the Irving-Williams order for stability constants:

$$Mn < Fe < Co < Ni < Cu > Zn.$$

As the atomic number increases, changes occur in properties of the metal ion such as its size and electron affinity. These changes explain this sequence, except for Cu(II). Copper(II) is slightly different due to the Jahn-Teller effect. Removal of an electron from the d^{10} Cu(I) leads to the spherically unsymmetrical Cu(II). This assymetry causes the central ion to be less effectively shielded in the x and y directions than in the z direction. The ligands lying in the xy plane are attracted to the central ion by a greater force than those in the z direction. This results in a distorted octahedral symmetry (i.e. tetragonal symmetry) with the four equatorial ligands closer to the Cu(II) than the axial ligands. This distortion leads to the relative

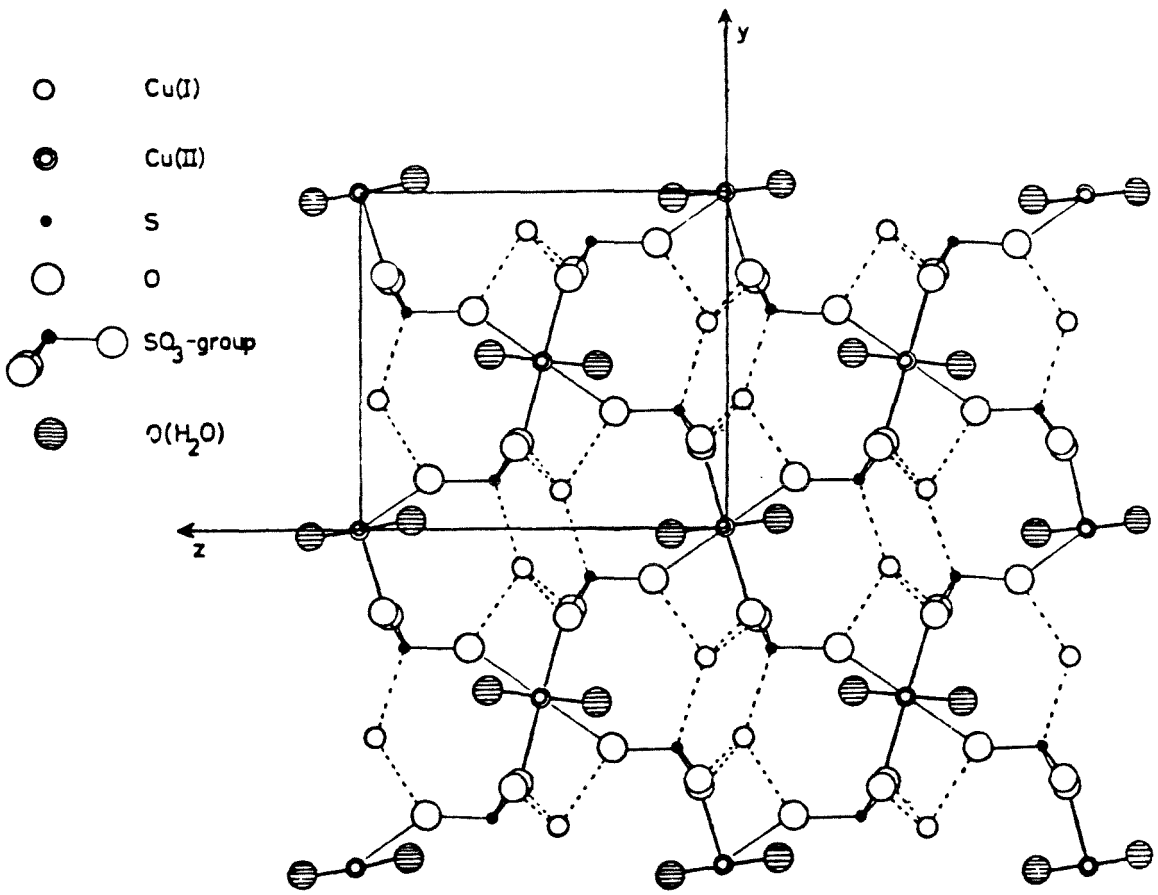

Fig. 2.2 Structure of Chevreul's salt, $Cu^{II}SO_3Cu_2^{I}SO_3 \cdot 2H_2O$ (Nyberg and Kierkegaard, 1968).

positon of Cu(II) in the Irving-Williams series and its ability to form stronger complexes than the other first-row transition metals. This distortion also leads directly to the different behavior for axial coordination sites compared to the equatorial sites. The axial sites, which are weakly polarizing, follow the order of $SO_4^{2-} > H_2O > NH_3$ for ligand preference. The four coordination sites lying on the xy plane are more polarizable and the order of ligand preference is reversed (James and Williams, 1961). Thus Cu(II) could be expected to form either O or S bonds.

An equilibrium constant for the formation of $CuSO_3^o$ has not been determined. Furthermore the nature of the bonding in Cu(II)-S(IV) complexes had not been ascertained. First-row transition metal complexes are of particular importance in aqueous atmospheric systems (e.g., cloud droplets and haze aerosols), where trace metal-catalysis of the autoxidation of S(IV) has been postulated to be an important pathway for SO_2 conversion (Hoffmann and Jacob, 1984). To elucidate the relative importance of this oxidation pathway, information about the equilibrium distribution of these metal-sulfite complexes is needed. The Cu(II)-S(IV) system can be used as a model for first-row transition metals that are active catalysts for SO_2 autoxidation such as Mn(II), Co(II) and Fe(III).

EXPERIMENTAL TECHNIQUES

Reagents and Materials

All reagents were analytical grade. Sodium sulfite (Mallinckrodt), $NaHSO_3$ (J.T. Baker Chem. Co.), $Na_2S_2O_5$ (CMCB

Manufacturing Chemists, Inc.) and $Na_2S_2O_6$ (Fischer Scientific Co.) solutions were prepared gravimetrically. The concentrations of the $NaHSO_3$ solutions were only approximate, as commercially available $NaHSO_3$ is a mixture of $NaHSO_3$ and $Na_2S_2O_5$. These solutions were made fresh for each experiment with water that had been purged with N_2. Copper solutions were made from different salts ($Cu(NO_3)_2 \cdot 2.5H_2O$ (J. T. Baker Chemical Co.), $Cu(ClO_4)_2 \cdot 6H_2O$ (G. Frederick Smith), $CuCl_2 \cdot 2H_2O$ (J. T. Baker Chemical Co.) and $CuSO_4 \cdot 5H_2O$ (Mallinckrodt)). Copper(II) solutions were standardized by iodometric titration (Hammock and Swift, 1949). The concentration of Cu(II) in experimental solutions was determined colorimetrically (Blair and Diehl, 1961) with bathocuproine disulfonate, 2,9-dimethyl-4,7-diphenyl-1,10-phenan- throlinedisulfonic acid, disodium (Sigma Chemical Co.). The sulfite solutions were acidified to the desired pH using the corresponding acid of the Cu(II) counterion. Ionic strength, μ (M), was held constant with either $NaNO_3$ (Mallinckrodt), Na_2SO_4 (Mallinckrodt), $NaClO_4$ (G. Frederick Smith Co.), or NaCl (J.T. Baker Co.). High-purity (18 MΩ-cm) water was obtained from a Millipore Milli-Q system.

Spectrophotometric Methods

UV/Visible absorbance spectra were recorded with a Hewlett-Packard dual beam diode array spectrophotometer (HP 8450A) in 1 cm quartz cells and at 21.0 ± 0.4 °C. A Dionex Stopped-Flow spectrophotometer (D-100) was used for the equilibrium studies of short-lived species. Data were collected at 350 nm at 25°C in a 2 cm Kel-F cell. Variable Cu(II):S(IV) ratios were examined at μ = 0.4 M and pH = 3.6 and 4.4.

Each data point represented at least three repeatable absorbance readings.

Raman spectra were collected at room temperature on a SPEX model 1402 double-monochromator Raman Spectrometer. Spectra were recorded using the 488 nm line of a Spectra-Physics Model 170 argon ion laser. The laser power incident upon the sample was $\simeq$ 400 mW, a 10 nm interference filter was used to remove stray light, and the spectral resolution was 0.25 cm^{-1}. The frequency was calibrated using known frequencies for carbon tetrachloride and sodium sulfate. Solid samples were in sealed glass capillaries. Aqueous samples were introduced in a flow apparatus. Separate solutions of copper and S(IV) were fed into a junction where they were mixed approximately 30 seconds before they entered the sampling capillary. Copper chloride was used in the Raman studies since Cl^- does not have a Raman signal. All the spectra were represented as a summation of repetitive scans. These spectra were smoothed by a four-point averaging technique.

Infrared spectra of $Cu_2(OH)_2SO_3 \cdot H_2O$ were taken in KBr pellets. No interaction with KBr was observed. On the other hand, IR spectra of $Cu^{II}SO_3Cu^{I}_2SO_3 \cdot 2H_2O$ were obtained with a Nujol mull on KBr plates. Spectra were recorded with a Beckman IR 4240 spectrophotometer.

Product Identification

Elemental analysis was performed by Galbraith Laboratories, Inc. Magnetic susceptibilities were measured on a Cahn Electrobalance DTL 7500-7 with $HgCo(SCN)_4$ as a standard.

RESULTS

Raman and Infrared Spectroscopy Studies

Sulfite can bind to metals in a variety of structures. Sidgwick (1951) has reviewed the structures for different sulfite complexes. Possible modes of bonding are depicted in Fig. 2.3. The IR frequency of the S-O stretches yields information about the structural configuration of the S(IV) complex. The S-O stretching frequencies are expected to shift depending on the type of coordination. Cotton and Francis (1960) observed the S-O stretching frequencies in sulfoxide complexes shifted to higher frequencies for metal-sulfur bonding and to lower frequencies for metal-oxygen bonding; this result agreed with their theoretical predictions. Thiosulfate complexes (Freedman and Straughan, 1971) and sulfite complexes (Newman and Powell, 1963 and Nyberg and Larsson, 1973) have been shown to follow the same trend.

Free sulfite ion has C_{3v} symmetry, which gives rise to four IR and Raman active fundamental modes: υ_1 (symmetric stretch), υ_2 (symmetric bend), υ_3 (asymmetric stretch) and υ_4 (asymmetric bend) (see Table 2.2). The two asymmetric modes are doubly degenerate. This symmetry is essentially preserved if the sulfite bonds to a metal through the sulfur. The sulfite symmetry will be lowered to C_3, C_s or C_1, if it is bound through the oxygen, or is bound as a bidentate ligand. For the lower symmetry groups, the degenerate modes, υ_3 and υ_4 will split, giving six vibrations.

Nyberg and Larsson (1973) found that the structures of metal-sulfite compounds can be divided into three groups based on

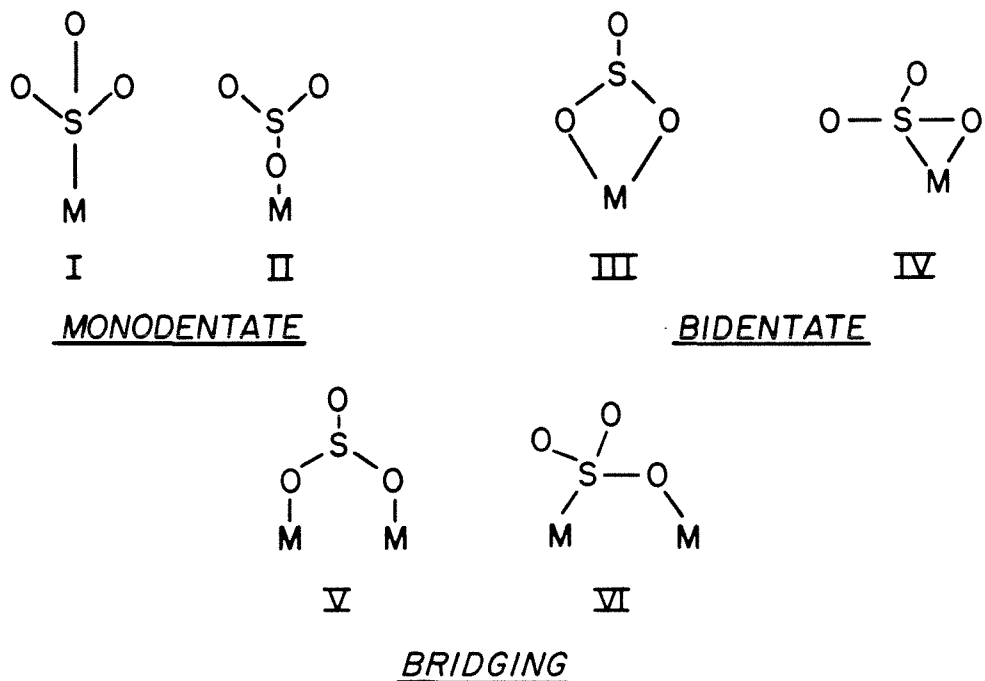

Fig. 2.3 Possible structural configurations of metal-sulfite complexes.

TABLE 2.2

Vibrational frequencies (cm^{-1}) of the sulfite ion

	υ_1	υ_2	υ_3	υ_4
Raman[a] (solution)	967s	620w	933m	469m
Raman[b] (solid)	981s	639w	949m	497m
IR[a] (solution)	1002m	632w	954s	

[a]Nyberg and Larsson (1973)
[b]This work
s=strong, m=medium, w=weak

sulfite coordination. They classified these groups as I (compounds without sulfur coordination), II (compounds with sulfur and oxygen coordination) and III (compounds with dominant sulfur coordination). Compounds in Group I have spectra which resemble the sodium sulfite spectra, with at least one lower stretching mode, and perhaps splitting of υ_3 and υ_4. Spectra of Na_2SO_3, $(NH_4)_2SO_3 \cdot H_2O$, $NiSO_3 \cdot 6H_2O$ and $ZnSO_3 \cdot 2.5H_2O$ fall into this group. Compounds in Group II with known metal-sulfur and metal-oxygen bonds are NH_4CuSO_3, Ag_2SO_3, $Cu^{II}SO_3Cu^{I}_2SO_3 \cdot 2H_2O$ and $Tl_2[Cu(SO_3)_2]$; these have stretching frequencies of high intensity above and below 975 cm^{-1}. Group III compounds have strong stretching frequencies above 975 cm^{-1}; known species include $PdSO_3(NH_3)_3$ and $Co(en)_2SO_3NCS \cdot 2H_2O$.

An unstable green solid formed when Cu(II) and S(IV) were mixed at pH $\geq$ 6. This solid continued to react to form a yellow solid. The composition of the yellow solid has been studied previously by Dasgupta et al. (1979), who determined that the composition of the solid varied with the initial pH of the system. The solid composition varied according to the formula $CuSO_3 \cdot xCu_2SO_3$, where $0 \leq x \leq 1$. Above pH 5, they verified by elemental analysis that the solid was Cu_2SO_3. However, if the precipitate was dried immediately upon formation by washing sequentially with absolute ethanol and anhydrous ether, then the green solid was stabilized. The stoichiometry of the green solid corresponded most closely to $Cu_2SO_3(OH)_2 \cdot H_2O$ (see Table 2.3).

Simple Cu(II) complexes, those lacking Cu-Cu interactions, have magnetic moments in the range of 1.75 to 2.20 B.M.. The magnetic moment of $Cu_2SO_3(OH)_2 \cdot H_2O$ has been measured and found to to be 2.07 $\pm$

TABLE 2.3

Elemental analyis of Cu(II)-S(IV) precipitate

Element	Measured[a]	$Cu_2(OH)_2SO_3 \cdot H_2O$	$Cu_2(OH)_2SO_3$	$CuSO_3$	Cu_2SO_3
H	1.6±0.5	1.56	0.84		
Cu	42.2±0.4	49.04	52.70	44.25	61.35
S	14.2±1.0	12.37	13.29	22.32	15.48
O	40.9±1.7	37.94	33.17	33.42	23.17

[a]An average of three determinations

0.04 B. M.; a molecular weight of 257.9 gm for $Cu_2SO_3(OH)_2 \cdot H_2O$ was assumed.

The IR spectrum of $Cu_2SO_3(OH)_2 \cdot H_2O$ is shown in Fig. 2.4a. The reported frequencies are listed in Table 2.4 together with the frequencies observed for the other metal-sulfite compounds. The IR spectra for $Cu_2SO_3(OH)_2 \cdot H_2O$ can be compared to the spectra for $Cu^{II}SO_3Cu^{I}_2SO_3 \cdot 2H_2O$, shown in Fig. 2.4b. The S-O stretching frequencies for $Cu_2SO_3(OH)_2 \cdot H_2O$ are higher (995 - 1300 cm^{-1}) than those for $Cu^{II}SO_3Cu^{I}_2SO_3 \cdot 2H_2O$ (900 - 1113 cm^{-1}), which is a Group II compound. The frequencies observed for the $Cu_2SO_3(OH)_2 \cdot H_2O$ are similar to those observed for $PdSO_3(NH_3)_3$ and Ag_2SO_3, both of which contain metal-sulfur bonds (Newman and Powell, 1963 and Nyberg and Larsson, 1973). Electrochemical studies of the Pd(II)-S(IV) complexes indicated the existence of a strong bond between S(IV) and Pd(II), so a sulfur-metal bond was postulated (Earwicker, 1960). Potentiometric titration of disulfito-palladates showed only one inflection point, which indicates that one of the sulfite bonds must be very weak. Earwicker (1960) suggested a polymeric structure for the solid, each sulfite forming a bridge between two palladium ions, one being attached through a sulfur bond and the other attached through oxygen. The oxygen bond was thought to be weaker than the sulfur bond and Earwicker suggested that it was broken during dissolution of the complex. Lebedinskii and Shenderetskaya (1957) have noted bonds of different strength in rhodium-sulfito complexes and postulated both sulfur and oxygen bonding in these complexes. The similarity between the palladium-S(IV) and

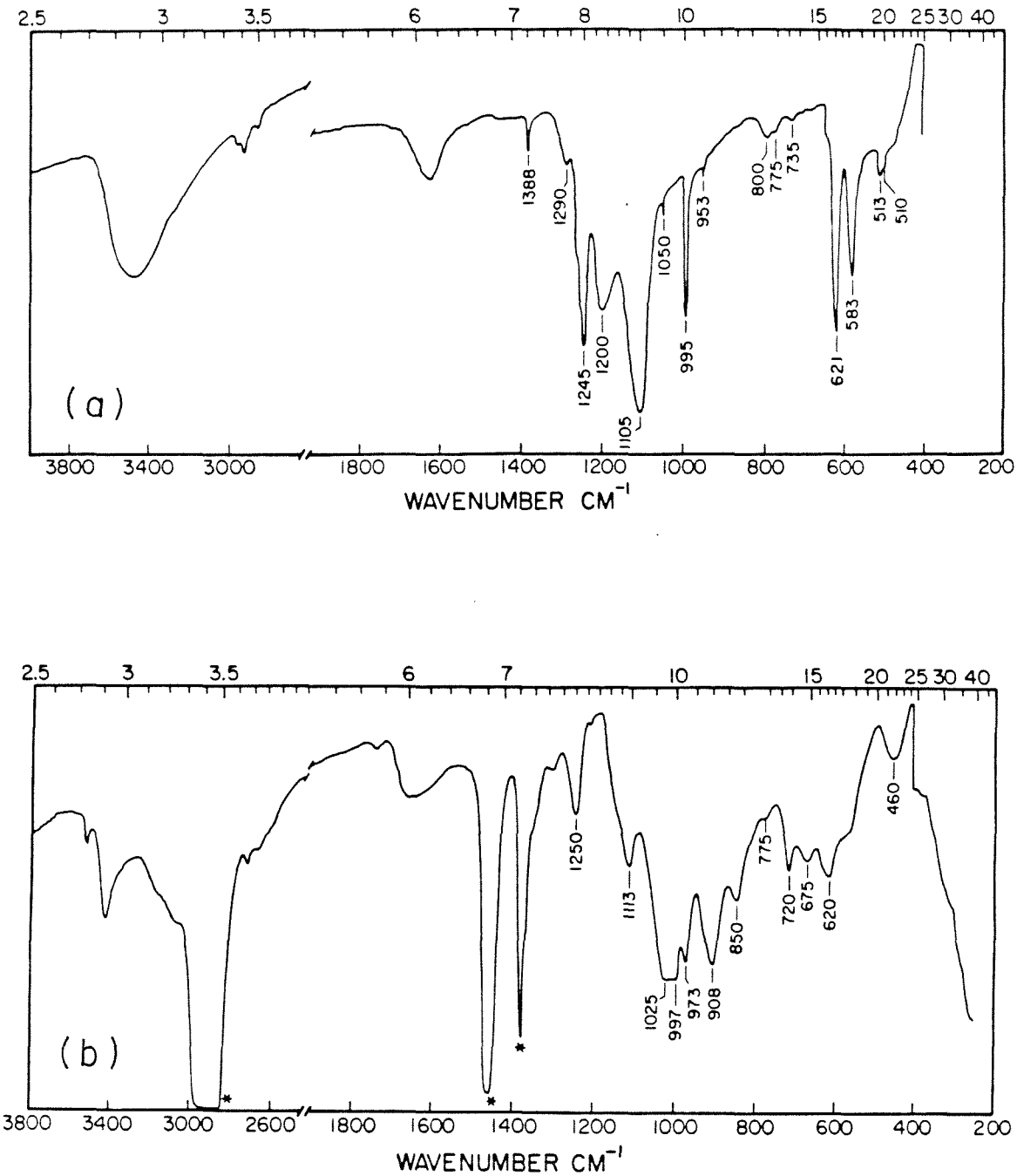

Fig. 2.4 Infrared spectra of (a) $Cu_2SO_3(OH)_2 \cdot H_2O$ and (b) $Cu^{II}SO_3Cu^{I}_2SO_3 \cdot 2H_2O$ (* marked bands are due to Nujol).

TABLE 2.4

Vibrational frequencies of metal-sulfite complexes (1105-450 cm^{-1})

Compound	Group	Observed Frequencies (cm^{-1})														
		ν_1 and ν_3[a]							ν_2[a]					ν_4[a]	
Na_2SO_3[b,c]	I	975s								630m				496s	
$(NH_4)_2SO_3 \cdot H_2O$[d]	I		968s	935s					662w	650w	613s		515w	498m	480m
$ZnSO_3 \cdot 2\frac{1}{2}H_2O$[e]	I	984vw		925s					681s		619w	532m		501vw	
$NiSO_3 \cdot 6H_2O$[d]	I			960s	870vw				660m					494m	
NH_4CuSO_3[b,f]	II		965s						660m	638w	615vw		505w	480w	483m
$Cu^{II}SO_3Cu^{I}_2SO_3 \cdot 2H_2O$[d]	II	1025m	1008m	977m	912m	860w		684w	636m		564m	519w	499w	480w	
$Tl_2[Cu(SO_3)_2]$[d]	II		981s		894s	860s			670vw		590w		510w	498m	453m
Ag_2SO_3[d]	II	1035s		970s		908s			665w	632s			500m	494m	478vw
Cis $K_2[Pd(SO_3)_2(NH_3)_2]$[b]		1093-1056s	995m	977m	958s	831w	797w	771m	655m	622w	568w	522w	506w		
Trans $K_2[Pd(SO_3)_2(NH_3)_2$[b]		1074s	986s		958s	837w	812w			646s		525w	511w		
$PdSO_3(NH_3)_3$[b]	III	1095s 1077s	989s			840vw	818vw		600w	643s		522w	510m		481s
$Co(en)_2SO_3NCS \cdot 2H_2O$[s,h]	III	1095a 1089s	1050s	977s	965s	877w	805w	780s 705w	660w	625s	586vw	545vw	510vw	500m	475m
$Cu_2SO_3(OH)_2 \cdot H_2O$[i]		1105s	1050w	995m	953vw		800w	775w 735vw		621m	583m		513w	510w	

[a] Tentatively assigned using information in Nyberg and Larsson (1973)

[b] Newman and Powell (1963)

[c] Evans and Bernstein (1955)

[d] Nyberg and Larsson (1973)

[e] Pannitier et al. (1964)

[f] Nyberg and Kierkegaard (1968)

[g] Baldwin (1961)

[h] Baggio and Becka (1969)

[i] This work

s = strong, m = medium, w = weak, vw = very weak

en = ethylenediamine

$Cu_2SO_3(OH)_2 \cdot H_2O$ spectra suggests that the bonding might be similar in these two compounds.

Harrison et al. (1983) conducted IR studies on simple metal-sulfite and metal-sulfite-hydroxide crystals. The S-O stretching frequencies for these solids appeared at lower frequencies than observed in this study for the Cu(II)-S(IV) solid (see Table 2.5). In the latter case, the strong peaks for υ_1 and υ_3 occurred below 975 cm^{-1}; this result was consistent with metal-O bonding. Lutz et al. (1983) determined crystal structures for $NaM_2OH(SO_3)_2 \cdot H_2O$ (M = Mg, Fe, Co, Mn, Ni, Zn). Metal-O bonding was proposed for all of these solids (and the IR stretching frequencies for these solids show the major stretching frquencies to be below 975 cm^{-1}).

Raman spectroscopy was used to determine the mode of sulfite bonding to Cu(II). However, Raman spectroscopy is not sufficiently sensitive to probe the Cu(II)-S(IV) system at low concentrations; concentrations of the reactants that were used to obtain well-resolved spectra were $[S(IV)]_T$ = 0.1 M, $[Cu(II)]_T$ = 0.25 M. Copper(II) was used in excess of S(IV) to promote the formation of dimeric Cu(II)-S(IV) complexes. At these concentrations, both the Cu(II) and the S(IV) are expected to dimerize. Therefore the speciation of the system at pH 2.5 may have had an added degree of complexity. To clarify which S(IV) species were present before Cu(II) was added to the system, Raman spectra of $SO_2 \cdot H_2O$, HSO_3^-, and SO_3^{2-} were taken (see Fig. 2.5). In these spectra, the peaks are very broad; this is probably due to solvent effects, such as hydrogen bonding with water. Davis and Chatterjee (1975) recorded spectra of the three S(IV) species in D_2O

TABLE 2.5

Infrared bands of metal sulfites (cm^{-1})[a]

	υ_1, υ_3	υ_2	υ_4
$MnSO_3$	1015m, 960s, 890s	645s	470w
$MgSO_3$	942m	625m	480w
$FeSO_3$	980sh, 942s 900s	620s	470m
$CaSO_3$	970s,950s	665m, 650 m	520w, 480w 458w
$MnSO_3 \cdot H_2O$	1040sh, 975m 880s	635s	470w
$FeSO_3 \cdot 3H_2O$	1020sh, 950s 880s	630s	480s
$MgSO_3 \cdot 3H_2O$	940s	620m	480w
$CaSO_3 \cdot \frac{1}{2}H_2O$	975s, 950s	668m, 650m	520w, 485w 455w

[a]Harrison et al. (1983)

s=strong, m=medium, w=weak and sh=shoulder

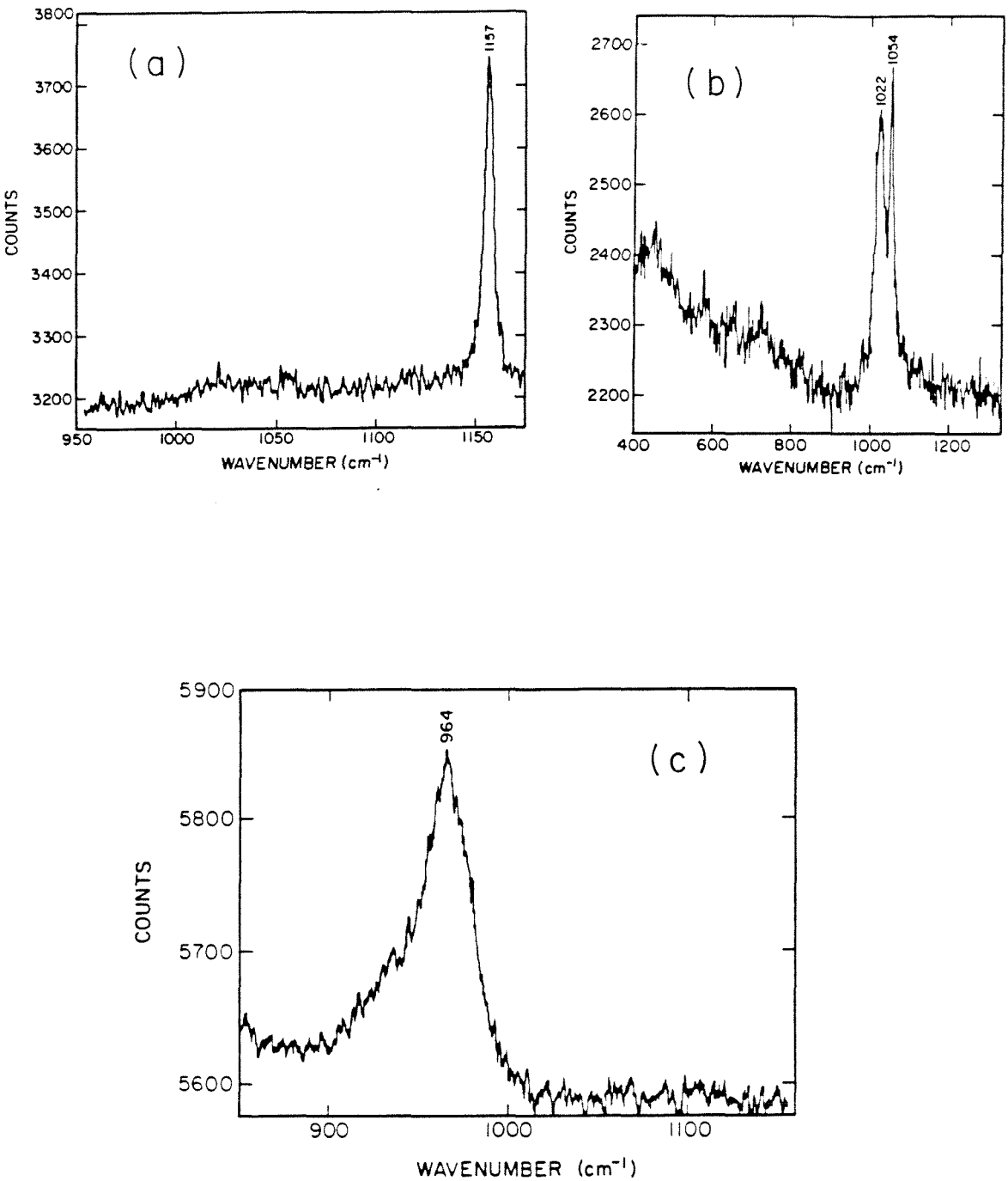

Fig. 2.5 Raman spectra of 0.2 M (a) $SO_2 \cdot H_2O$, (b) $NaHSO_3$, and (c) Na_2SO_3.

and H_2O and they found the peak half-width decreased in D_2O. This was consistent with hydrogen bonding as the cause of peak broadening.

The peak assignment for the HSO_3^- is not straightforward. Bisulfite can exist, theoretically, in the form of two tautomers, $HO-SO_2^-$ or $H-SO_3^-$. Golding (1960) argued that both species co-exist. He suggested that at higher concentrations ([S(IV)] > 10^{-3} M) the two bisulfite tautomers form a dimer which eventually dehydrates to form pyrosulfite, $S_2O_5^{2-}$, as shown below:

$$HO-SO_2^- \overset{K_T}{\rightleftharpoons} H-SO_3^-$$

$$HO-SO_2^- + H-SO_3^- \overset{K_D}{\rightleftharpoons} \text{[dimer]} \overset{K_P}{\rightleftharpoons} S_2O_5^{2-} + H_2O.$$

Based on Raman and IR measurements, Simon and Waldman (1955a, 1955b, 1956a, 1956b) and Simon et al. (1956) analyzed the structure of aqueous $HSO_3^-$and $S_2O_5^{2-}$. They suggested a C_{2v} symmetry group and S-O-S bonding for $S_2O_5^{2-}$. Lindqvist and Mörtsell (1957) determined the crystal structure of $K_2S_2O_5$ and found S-S bonding, agreeing with an earlier study of Zachariasen (1932). The spectrum of crystalline $NaHSO_3$ (or $Na_2S_2O_5$, as commercially prepared $NaHSO_3$ is $Na_2S_2O_5$) is displayed in Fig. 2.6. Using IR and Raman data, Herlinger and Long (1969) agree with Golding as to the probable existence of S-S bonds or hydrogen bonds for the $S_2O_5^{2-}$ species, based on the fifteen IR and Raman peaks they observed. This was the expected number of peaks if the symmetry group for $S_2O_5^{2-}$ were C_s. Using polarization data, Herlinger and Long

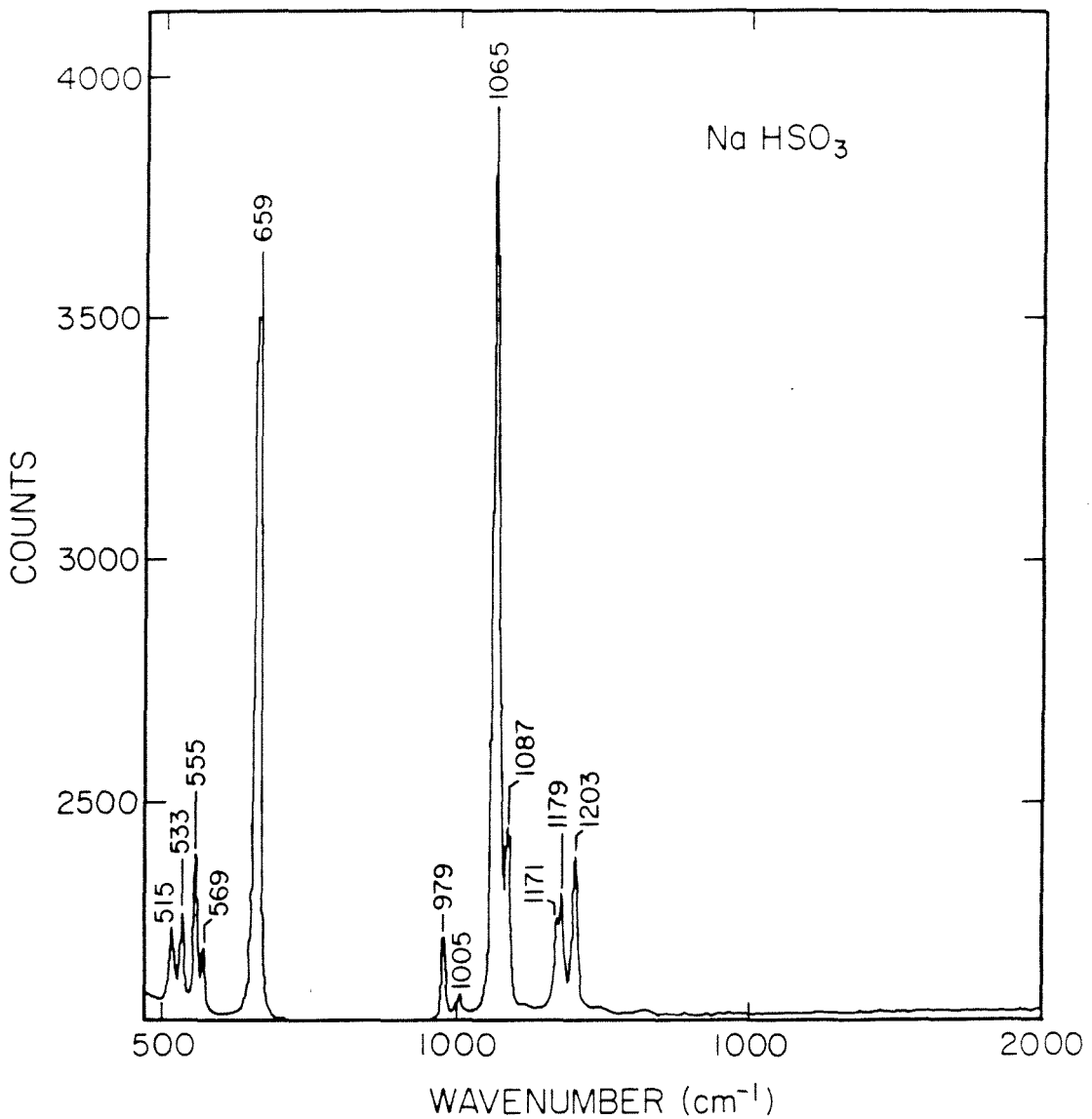

Fig. 2.6 Raman spectra of crystalline $Na_2S_2O_5$.

have assigned 1028 cm^{-1} to HSO_3^- and 1055 cm^{-1} to $S_2O_5^{2-}$ (the two peaks displayed in Fig. 2.5b).

Recent Raman and UV measurements by Connick et al. (1982) substantiate Golding's arguments for the coexistence of both tautomers in aqueous solution. In addition, they determined that the overall formation constant, K_P' ($K_P' = K_T K_D K_P$) is 0.088 M^{-1} compared to Golding's value of 0.07 M^{-1}, and Bourne et al.'s (1974) value of 0.115 at μ = 0.1 M. Rhee and Dasgupta (1985) have determined an overall dimerization constant, K_P' ($K_P' = K_T K_D$) of 1.75 x 10^{-3} M^{-1} at 25 °C. Assuming K_P' is correct, the dimeric form would be the major S(IV) species for the experiments in this section.

The Raman spectra of HSO_3^- obtained in this study and displayed in Fig. 2.5b can be compared to the spectra of solid $Na_2S_2O_5$ (as shown in Fig. 2.6). The aqueous and solid species show substantial differences in the frequency of the S-O stretching peaks which indicates that the $S_2O_5^{2-}$ undergoes a structural change, perhaps partially dissociating in aqueous solution. The Raman spectra shown in Figs. 2.5b and 2.6 compared well with the spectra of Herlinger and Long (see Table 2.6). The lack of detail in the weaker peaks for the aqueous species obtained in this study was probably due to the lower concentrations that were employed.

The Raman spectrum for the Cu(II)-S(IV) aqueous system is shown in Fig. 2.7. The S-O stretching frequencies in this case are similar to the HSO_3^- spectrum except for the appearance of a shoulder at 1033 cm^{-1} on the 1024 cm^{-1} peak. The pH of the latter solution was lower than that of the $NaHSO_3$ solution spectrum presented in Fig. 2.5b. The

TABLE 2.6

Raman vibrational spectra of meta-bisulfite (cm^{-1})

$K_2S_2O_5$[a]		$Na_2S_2O_5$[b]		Assignment[a]
solid	aqueous solution (1 M)	solid	aqueous solution (0.1 M)	
147s	168s			$S_2O_5^{2-}$
218s,195w	200s			$S_2O_5^{2-}$
245vs	235vs			$S_2O_5^{2-}$
317s	309s			$S_2O_5^{2-}$
	395w			HSO_3^-
433s	424s			$S_2O_5^{2-}$
	467m			SO_3^{2-}, HSO_3^-
517w,507vw	510m	515w		$S_2O_5^{2-}$
558m	558w	533m,555m		$S_2O_5^{2-}$
569w,564w	587w	569w		$S_2O_5^{2-}$, HSO_3^-
645w	637w			$S_2O_5^{2-}$, HSO_3^-
653s	655s	659s		$S_2O_5^{2-}$
	685vw			HSO_3^-
	709w			HSO_3^-
	740w			HSO_3^-
	933vw			SO_3^{2-}
971w	966w	979w,1005vw		$S_2O_5^{2-}$, SO_3^{2-}
	1021s		1022s	HSO_3^-
1059s	1052vs	1065vs	1054vs	$S_2O_5^{2-}$
1088m	1085s	1087m		$S_2O_5^{2-}$, $S_2O_6^{2-}$
1178m	1170w	1171w,1179m		$S_2O_5^{2-}$
1202w	1196w	1203m		$S_2O_5^{2-}$

[a]Herlinger and Long (1969)

[b]This work

vs = very strong, s = strong, m = medium, w = weak, vw = very weak

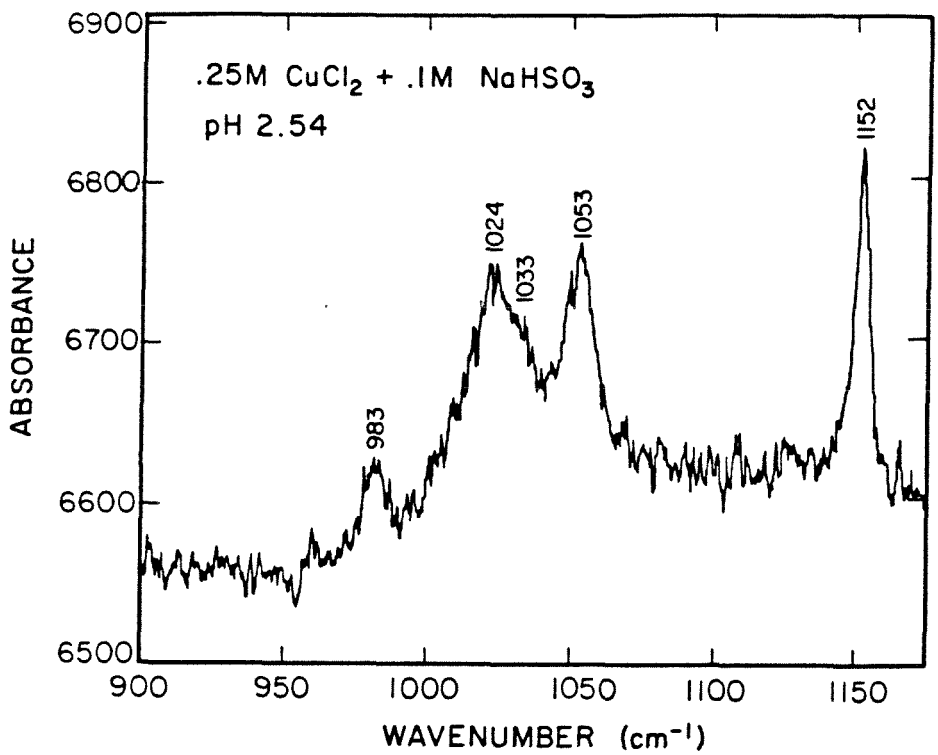

Fig. 2.7 Raman spectrum of Cu(II)-S(IV) system.

presence of a 1152 cm^{-1} peak indicated that an equilibrium with $SO_2 \cdot H_2O$ had been established. Low pH conditions were necessary to prevent precipitation. The existence of a peak at 983 cm^{-1} indicated the presence of SO_4^{2-} as a result of the oxidation of S(IV) by Cu(II). No evidence for $S_2O_6^{2-}$, which has a peak at 1090 cm^{-1}, was obtained. The lack of change of the S-O stretching frequencies would indicate that the Cu(II)-S(IV) complex, at the concentration the spectra were taken, has a symmetry very similar to that of aqueous HSO_3^-, with either Cu-S bonding or a dimeric form with Cu-O and Cu-S bonding such as the structures shown in drawings I and VI in Fig. 2.1. The other possibility is that the Cu(II)-S(IV) complexes are simple ion pair complexes, but this is unlikely since the experimental stability constant for $CuSO_3$ was too high for an ion pair complex (*vide infra*). Attempts to take the Raman spectra of $Cu_2SO_3(OH)_2 \cdot H_2O$ were unsuccessful; it decomposed upon irradiation. The decomposed solid had a very strong peak at 729 cm^{-1} (Fig. 2.8) that did not correspond to the S-O stretching frequencies of any known metal-sulfite complex.

Determination of Equilibrium Constant

Equilibrium studies on the Cu(II)-S(IV) system were performed with a Dionex Stopped-Flow spectrophotometer. The concentrations used in these studies were much lower than those used for Raman spectroscopy. An equilibrium constant was calculated based on observed changes in the absorbance at 350 nm measured 20 msec after mixing (see Fig. 2.1) Cu(II)-S(IV) solutions. The S(IV):Cu ratio was increased by varying [S(IV)]; $[Cu(II)]_T$, pH and ionic strength were held constant (Newton

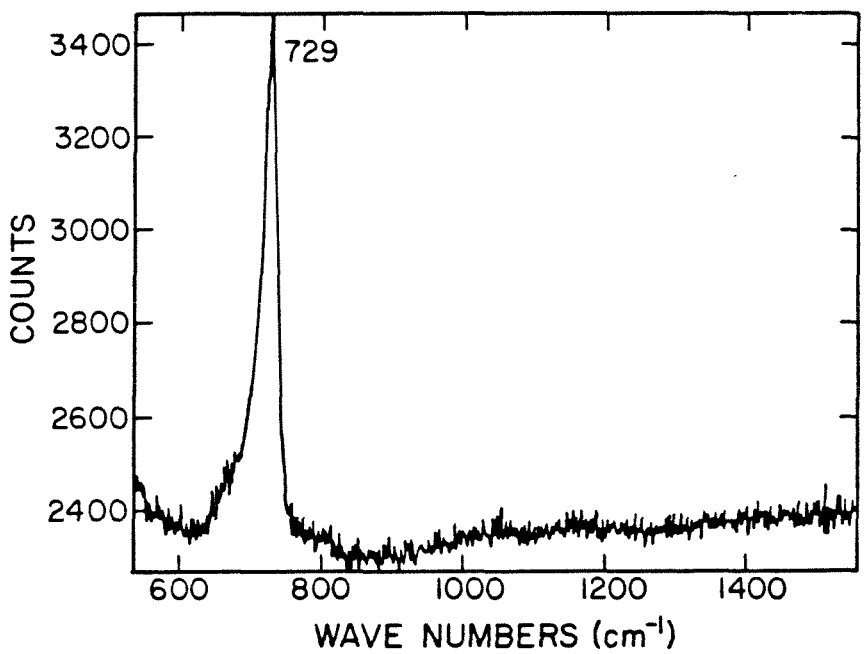

Fig. 2.8 Raman spectrum of $Cu_2SO_3(OH)_2 \cdot H_2O$ after decomposition in spectrometer.

and Arcand, 1953). In this case we have assumed that the reaction can be written as

$$Cu^{2+} + nSO_3^{2-} \rightleftharpoons Cu(SO_3)_n^{2-2n} \qquad (2.1)$$

where n = 1,2,3... If the total copper concentration is held constant and Beer's Law holds for the system then:

$$A = -K^{-1}\frac{(A - A_o)}{[S(IV)]^n} + A_\infty \qquad (2.2)$$

where

A = absorbance;

$K^{-1} = \dfrac{[Cu^{2+}][S(IV)]^n}{[Cu(SO_3)_n^{2-2n}]}$;

A_∞ = absorbance of complex, if all the copper was complexed;

The SO_3^{2-} concentration is related to [S(IV)] by the following relationship:

$$SO_3^{2-} = \alpha_2[S(IV)] \qquad (2.3)$$

where

$$\alpha_2 = \frac{1}{[H^+]^2/K_{a_1}K_{a_2} + [H^+]/K_{a_2} + 1};$$

where K_{a_1} and K_{a_2} are the first and second acid dissociation constants for $SO_2 \cdot H_2O$. Since pH was constant in this experiment, α_2 was a constant. A plot of A vs $(A-A_o)/[S(IV)]^n$ should give a straight line

(if n = 1) with a slope of $-K^{-1}$ and an intercept of A_{∞}. Fig. 2.9 shows absorbance as a function of [S(IV)] for two values of pH (3.6 and 4.4). Data were plotted using Eqn. 2.2 (Fig. 2.10), which was found to be valid at intermediate ratios of S(IV):Cu(II).

As shown in Fig. 2.10, deviations from Eqn. 2.2 were apparent at low S(IV):Cu(II) ratios. This departure from Eqn. 2.2 at low S(IV):Cu(II) ratios was expected. Uncertainty about the free [S(IV)] as well as competition from dimeric Cu(II)-S(IV) species contributed to this deviation. The Cu(II)-S(IV) system consisted of several Cu(II)-S(IV) species: $CuSO_3$, $Cu_2SO_3^{2+}$, and $Cu_2OHSO_3^{+}$. The latter two species were expected to exist as their stoichiometry was similar to the green precipitate, $Cu_2SO_3(OH)_2 \cdot H_2O$. These species were expected to be of greater importance at lower S(IV) concentrations for which the 2:1 Cu:S stoichiometry was satisfied. When these species were present, Eqn. 2.1 was an invalid representation of the system. At pH 3.6, the absorbance was very low for the complex at low S(IV):Cu(II) ratios. The error bars on Fig. 2.9 represent instrument noise. The signal-to-noise ratio decreased at low Cu(II):S(IV) ratios. Data points for which the noise was greater than 10% of the signal were not used in the analysis. At both pH values, the solutions were unbuffered in an attempt to avoid the introduction of competitive complexes into the solution. For the experiment at pH 4.4 the formation of the complex at S(IV):Cu(II) ratios above 4:1 caused the the pH of the solution to decrease significantly (from pH 4.4 to pH 4.0), data points for Cu(II):S(IV) ratios below this value were used in the analysis.

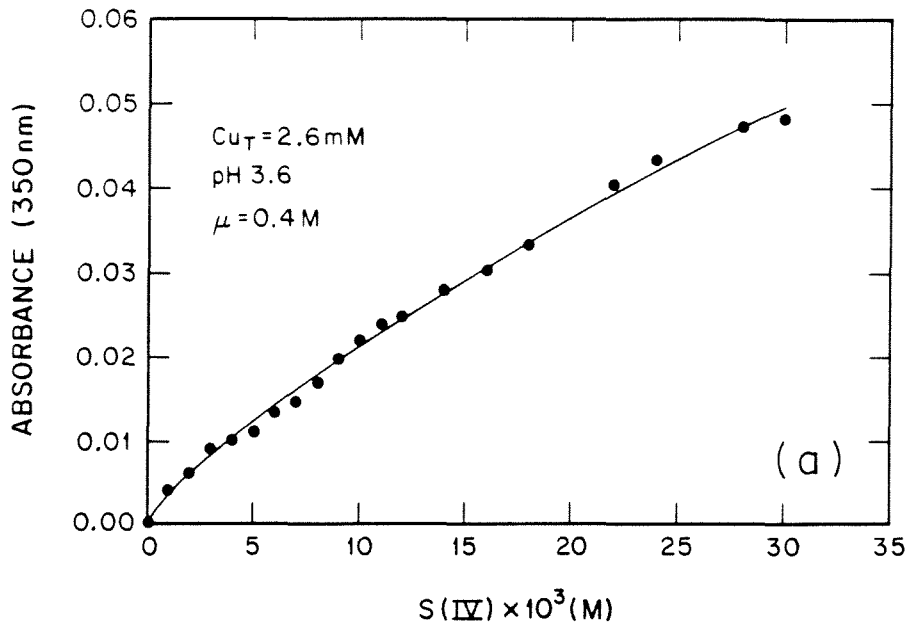

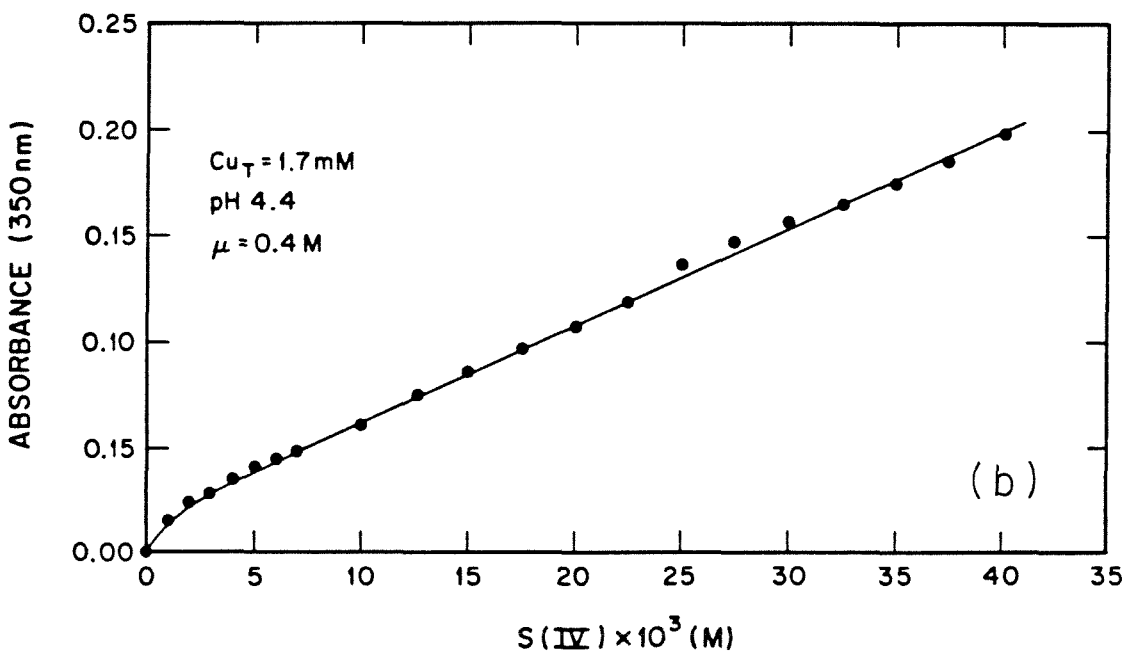

Fig. 2.9 Absorbance (350 nm) of the Cu(II)-S(IV) complex as a function of [S(IV)] at (a) pH 3.6 and (b) pH 4.4.

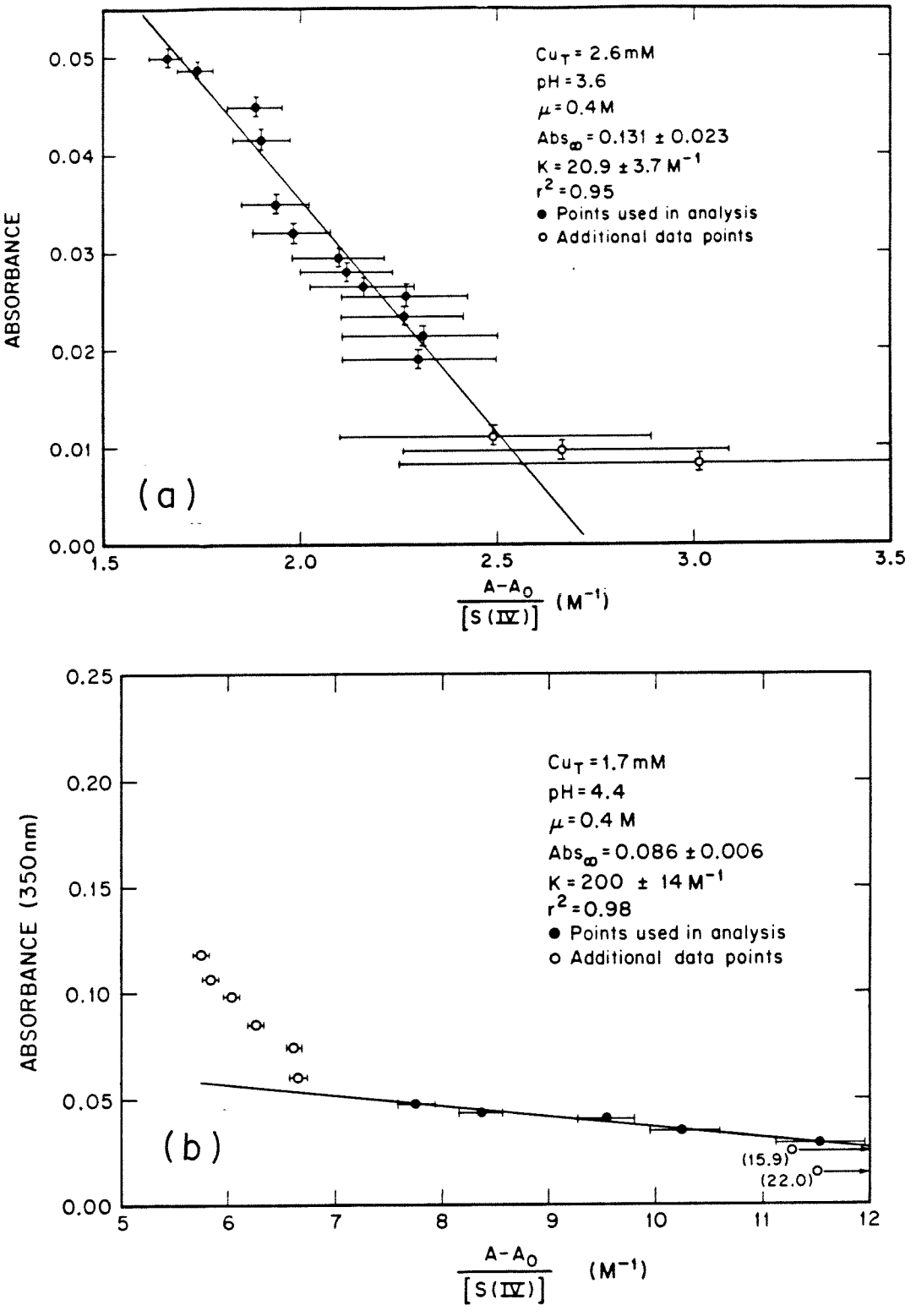

Fig. 2.10 Equation 2.2 applied to data in Figure 2.9 (a) pH 3.6 and (b) pH 4.4. (Error bars are shown when they exceed symbol size).

This decrease in pH would account for the deviation of the data in Fig. 2.10b from Eqn. 2.2 at high S(IV):Cu(II) ratios.

The conditional stability constant as defined for formation of $CuSO_3$ is:

$$K = \frac{[CuSO_3]}{[Cu^{2+}][S(IV)]}. \qquad (2.4)$$

For the pH range of this study, $\alpha_2 \cong \frac{K_{a_2}}{[H^+]}$, therefore we can write

$$K_1 = \frac{[CuSO_3]}{[Cu^{2+}][SO_3^{2-}]} = K\,\frac{[H^+]}{K_{a_2}}. \qquad (2.5)$$

Log K_{a_2} (pK_{a_2} = 7.18, Smith and Martell (1976)) was adjusted using the Davies Equation (Stumm and Morgan, 1981):

$$\log \gamma = -0.5\, z^2 \left[\frac{\sqrt{I}}{1 + \sqrt{I}} - 0.2I \right] \qquad (2.6)$$

where

z = charge of the ion;
I = ionic strenth (M);
γ = activity coefficient.

This yielded log K_{a_2} = -6.6 (μ = 0.4 M). The stability constant was obtained by application of Eqn. 2.2 to the data to obtain initial estimates of K and A_∞. These estimates were then substituted back into Eqn. 2.2 until the result converged on a value of K. Once K was obtained, K_1 was calculated. The constants determined by this method

were $K_1 = 2.1 \pm 0.4 \times 10^4\ M^{-1}$ at pH 3.6 and $K_1 = 1.3 \pm 0.1 \times 10^4\ M^{-1}$ at pH 4.4 The best estimate which can be given here is $K_1 = 1.7 \pm 0.5 \times 10^4\ M^{-1}$, $\mu = 0.4$ M.

The above model is valid only if Eqn. 2.1 is valid, or in other words, there are no other Cu(II)-S(IV) species contributing significantly to the absorbance measurements that were made. An estimation of the relative importance of the other postulated Cu(II)-S(IV) species, $Cu_2SO_3^{2+}$ and $Cu_2SO_3OH^+$, equilibrium computations were made using MINEQL, a computer program designed to solve chemical equilibrium problems (Westall et al., 1976). The computations were done on the Cu(II)-S(IV) system with the equilibrium constant determined in this work and adjusted to $\mu = 0.0$ M (i.e. log K = 5.5). The computational cases were simulations of actual laboratory experiments when the composition of the Cu(II) and S(IV) solutions were known before mixing and the pH was measured immediately after mixing. As was noted previously, the pH was lowered upon mixing. This was attributed to a shift in the SO_3^{2-}/HSO_3^- equilibrium which was perturbed by the formation of the complex. Thus the pH drop was a measure of the degree of complexation. Formation of $CuSO_3$ adequately accounted for the observed drop in pH upon mixing Cu(II)-S(IV) for the conditions of the calculations (10:1 S(IV):Cu(II)). The predicted and calculated pH values are presented in Table 2.7 along with speciation.

DISCUSSION

The Cu(II)-S(IV) complexes appear to be different from the other metal-sulfite complexes in the Irving-Williams series. Stable

TABLE 2.7

Calculated equilibrium concentrations for the Cu(II)-S(IV) system using the determined equilibrium constant for $CuSO_3$[a]

pH		Cu(II) distribution (%)			S(IV) distribution (%)		
predicted	measured	Cu^{2+}	$CuNO_3^+$	$CuSO_3$	HSO_3^-	SO_3^{2-}	$CuSO_3$
6.3	6.1	1.3		98.5	66.7	23.3	10.1
6.2	6.0	1.5		98.3	69.7	20.3	10.0
6.0	5.9	2.1		97.7	75.2	14.8	10.0
5.8	5.8	3.4		96.3	81.3	8.9	9.8
4.7	5.2	24.8	2.5	72.7	91.6		6.8
4.2	4.9	49.8	5.0	45.2	94.9		4.6
4.0	4.7	58.5	5.8	35.6	95.8		3.6
3.5	3.8	77.2	7.7	15.0	97.2		1.5

[a]Concentrations and stability constants (for μ = 0.0 M) used are:

S_T = 9.9 mM

Cu_T = 1.01 mM

μ = 0.1 M

log K_{CuOH^+} = 6.03 (Paulson and Kester, 1980)

log $K_{CuNO_3^+}$ = -0.4 (Smith and Martell, 1976)

log K_{CuSO_3} = 5.5 (this work)

log $K_{HSO_3^-}$ = 7.18 (Smith and Martell, 1976)

metal-sulfite crystals have been isolated for all of these metals except Cu(II) (e.g., Klasens et al., 1936; Lutz et al., 1980; and Harrison et al., 1983). In all of the first-row transition metal-sulfite salts, which have been isolated, crystal structure, IR and Raman studies have shown metal-oxygen bonds. The Cu(II)-S(IV) complexes are different in that Raman spectra of the transient Cu(II)-S(IV) complexes suggest the presence of metal-sulfur bonds.

Stability constants for the divalent first-row transition metal-sulfite complexes have not been determined. However they can be calculated using the modified equation of Drago et al. (1971) that can be applied to aqueous systems (Hancock and Marsicano, 1980).

$$\log K_1 = E_A^{aq} E_B^{aq} + C_A^{aq} C_B^{aq} - D_A D_B \qquad (2.7)$$

where E and C represent the tendency to form ionic and covalent bonds of Lewis acid, A, and base, B; and D parameterizes desolvation and steric hindrance effects. This equation is applicable to monodentate ligands. Values used in the calculation with the predicted stability constants are presented in Table 2.8. The predicted stability constants are small when compared to the measured stability constant of $CuSO_3$. The predicted stability constant for Cu(II) is significantly larger than those that are predicted for the other divalent metals ($0.48 < \log K < 1.33$), although the predicted value ($\log K = 3.62$) is smaller than the experimental value ($\log K = 5.5$). The relative magnitude of these stability constants follows the order predicted by the Irving Williams series, which is the order that the metals would

TABLE 2.8

Calculated stability constants for MSO_3 complexes[a]

Metal	E_A	C_A	D_A	Log K
Cu^{2+}	1.27	0.466	6.0	3.62
Ni^{2+}	1.20	0.300	4.5	1.33
Zn^{2+}	1.43	0.312	4.0	1.30
Co^{2+}	1.33	0.276	3.0	1.28
Fe^{2+}	1.59	0.256	2.0	0.77
Mn^{2+}	1.64	0.223	1.0	0.48

For SO_3^{2-}: $E_A = -1.94$, $C_B = 18.2$, $D_B = 0.4$

[a]Hancock and Marsicano (1980)

follow for an oxygen-bonded ligand. First-row transition metal-sulfate complexes have stability constants that are larger than the predicted constants for metal-sulfite complexes. Nonetheless, $K_{CuSO_4} << K_{CuSO_3}$.

The occurrence of metal-sulfur bonds in the $CuSO_3$ may account for its enhanced stability compared to $CuSO_4$. All the metals listed in Table 2.1 show greater stability constants for the metal-sulfite complex than those corresponding to the metal-sulfate complex. Sulfur bonding is likely to occur in the metal-sulfite complexes for Class b metals. When compared to these metals, the difference in stability between $CuSO_3$ and $CuSO_4$ is of roughly the same order of magnitude (excluding Hg).

Even though the stability constant of $CuSO_3$ is relatively large compared to other Cu(II) inorganic complexes, (see Table 2.9), $CuSO_3$ is not expected to be a major S(IV) species in aqueous-phase atmospheric systems unless formaldehyde is not present. Bisulfite adducts, such as the α-hydroxyalkylsulfonates, which are formed with aldehydes, have larger stability constants ($K = [HMSA]/([HSO_3^-][HCHO]) = 10^7$, Munger et al., 1986). To form equivalent amounts of $CuSO_3$ and α-hydroxyalkylsulfonates (HMSA) in the presence of 1 mM S(IV), $[Cu^{2+}]_T/[HCHO]_T \simeq 10^7$ at pH 2 or $[Cu^{2+}]_T/[HCHO]_T \simeq 6.5$ at pH 5. Aldehydes are usually found in much higher concentrations than Cu(II) in cloud-, fog- and rainwater (Munger et al., 1984, 1986), therefore S(IV) speciation is likely to be dominated by $RC(OH)SO_3^-$ rather than $CuSO_3$.

TABLE 2.9

Stability constants for Cu(II) complexes (25 °C)[a]

Ligand	Log K	Ionic Strength (M)
CO_3^{2-}	6.75	0
HPO_3^{2-}	4.57	3.5
SO_3^{2-}	4.2[c]	0.4
N_3^-	2.86[b]	0
SO_4^{2-}	2.36	0
NCS^-	2.33	0
NO_2^-	2.02	0
F^-	1.2	0
NO_3^-	0.5	0
Cl^-	0.4	0
Br^-	-0.3	0

[a]From Smith and Martell (1976)
[b]20 °C
[c]This work

REFERENCES

Albu, H.W. and H.D. Graf von Schweinitz, 1932, *Ber. Deutsch. Chem. Ges.*, **B65**, 729-737.

Baggio, S. and L.N. Becka, 1969, *Acta. Cryst.*, **B25**, 946-954.

Baldwin, M.E., 1961, *J. Chem. Soc.*, 3123-3128.

Baubigny, M.H., 1912, *Comptes Rend.*, **154**, 701-703.

Blair, D. and H. Diehl, 1961, *Talanta*, **7**, 163-174.

Bourne, D.W., T. Higuchi and I.H. Pitman, 1974, *J. Pharm. Sci.*, **63**, 865-868.

Connick, R.E., M. Tam, E. von Deuster, 1982, *Inorg. Chem.*, **21**, 103-107.

Cotton, F.A. and R. Francis, 1960, *J.Am. Chem. Soc.*, **82**, 2986-2991.

Dansent, W.E. and D. Morrison, 1964, *J. Inorg. Nucl. Chem.*, **26**, 1122-1125.

Dasgupta, P.K., P.A. Mitchell and P.W. West, 1979, *Atmos. Environ.*, **13**, 775-782.

Davis, A.R. and Chatterjee, 1975, *J. of Sol. Chem.*, **4**, 399-412.

Drago, R.S., G.C. Vogel and T.E. Needham ,1971, *J. Am. Chem. Soc.*, 93, 6014-6026.

Earwicker, G. A. ,1960, *J. Chem. Soc.*, 2620-2626.

Evans, J.C. and H.J. Bernstein, 1955, *Can. J. Chem.*, **33**, 1270-1272.

Foffani, A. and M. Menegus-Scarpa, 1953, *Gazz.*, **83**, 1068-1081.

Freedman, A.N. and B.P. Straughan, 1971, *Spectrochimica Acta*, **27A**, 1455-1465.

Golding, R.M., 1960, *J. Chem. Soc.*, 3711-3716.

Gray, H.B. *Chemical Bonds: An Introduction to Atomic and Molecular Structure* (Benjamin/Cummins Pub. Co., Menlo Park, CA, 1973).

Hammock, E.W. and E.H. Swift, 1949, *Anal. Chem.*, **21**, 975-979.

Hancock, R.D. and F. Marsicano, 1980, *Inorg. Chem.*, **19**, 2709-2714.

Harrison, W.D., J.B. Gill and D.C. Goodall, 1983, *Polyhedron*, 2, 153-156.

Herlinger, A.W. and T.V. Long, II, 1969, *Inorg. Chem.*, **8**, 2661-2665.

Hoffmann, M.R. and D.J. Jacob in *Acid Rain Precipitation Series Vol.* 3, J.G. Calvert, ed. (Butterworth Publishers, Boston, 1984).

Hunt, J.P. and H.L. Friedman in *Progress in Inorganic Chemistry, Vol.* 30, S.J. Lippard, ed. (Wiley & Sons, New York, 1983) pp. 359-382.

James, B.R. and R.J.P. Williams, 1961, *J. Chem. Soc.*, 2007-2019.

Klasens, H.A., W.G. Perdok, and P. Terstra, 1936, *Z. Krist.*, **94**, 1-6.

Lebedinskii, V.V. and E.V. Shenderetskaya, 1957, *J. Inorg. Chem. U.S.S.R.*, **2**, 1768-1774.

Lindqvist, I. and M. Mörtsell, 1957, *Act. Cryst.*, **10**, 406-409.

Lutz, H.D., W. Eckers, W. Buchmeier and B. Engelen, 1983, *Z. Anorg. Allg. Chem.*, **499**, 99-108.

Lutz, H.D., S.M. El-Suradi, C. Mertins and B.Engelen, 1980, *Z. Naturforsch. B. Anorg. Chem., Org. Chem.*, **35B**, 808-816.

Munger, J.W., D.J. Jacob, J.M. Waldman and M.R. Hoffmann, 1984, *J. Atmos. Chem.*, 1, 335-350.

Munger, J.W., C. Tiller and M.R. Hoffmann, 1986, *Science*, **231**, 247-249.

Newman, G. and D.B. Powell, 1963, *Spectrochim. Act.*, **19**, 213-224.

Newton, T.W. and G.M. Arcand, 1953, *J. Am. Chem. Soc.*, **75**, 2449-2453.

Nyberg, B. and P. Kierkegaard, 1968, *Act. Chem. Scand.*, **22**, 581-589.

Nyberg, B. and R. Larsson, 1973, *Act. Chem. Scand.*, **27**, 63-70.

Pannitier, G., G. Djega-Mariaclasson, and J.M. Bregeault, 1964, *Bull. Soc. Chim. France*, 1749-1756.

Paulson, A.J. and D.R. Kester, 1980, *J. Sol. Chem.*, **9**, 269-272.

Ramberg, L., 1910, *Z. Phys. Chem.*, **69**, 512-522.

Rhee, T.S. and Dasgupta, P.K., 1985, *J. Phys. Chem.*, **89**, 1799-1804.

Sidgwick, N.V., *The Chemical Elements and Their Compounds, Vol.* 2 (University Press, Oxford, 1951) pp. 909-910.

Sillèn, L.G. and A.E. Martell, *Stability Constants of Metal-Ion Complexes* (The Chemical Society, London, 1964).

Sillèn, L.G. and A.E. Martell, *Stability Constants of Metal-Ion Complexes, Supplement No. 1* (The Chemical Society, London, 1971).

Simon, A. and K. Waldman, 1955, Z. *Anorg. Chem.*, **281**, 113-134.

Simon, A. and K. Waldman, 1955, Z. *Anorg. Chem.*, **281**, 135-150.

Simon, A. and K. Waldman, 1956, Z. *Anorg. Chem.*, **284**, 36-46.

Simon, A. and K. Waldman, 1956, Z. *Anorg. Chem.*, **284**, 47-59.

Simon, A., K. Waldman and E. Steger, 1956, Z. *Anorg. Chem.*, **288**, 131-147.

Smith, R.M. and A.E. Martell, *Critical Stability Constants Vol. 4: Inorganic Ligands* (Plenum Press, New York, 1976).

Stumm, W. and J.J. Morgan, *Aquatic Chemistry* (Wiley & Sons, New York, 1981) pp. 134-137.

Westall, J.C., J.L. Zachary, and F.M. Morel, *MINEQL, A Computer Program for the Calculation of Chemical Equilibrium Composition of Aqueous Solutions*, Tech. Note 18 (Dept. of Civil Eng., Mass. Inst. Tech., Cambridge, MA, 1976).

Zachariasen, W., 1932, *Phys. Rev.*, **40**, 923-935.

CHAPTER THREE

KINETIC STUDIES OF THE REDOX CHEMISTRY OF Cu(II)-S(IV) COMPLEXES

ABSTRACT

The redox chemistry of copper(II)-sulfite complexes is examined and the rate of reduction of Cu(II) is determined. The reduction of Cu(II) is shown to proceed via $(Cu(II))_2SO_3^{2+}$ and $(Cu(II))_2SO_3OH^{+}$ intermediates. Copper(I), SO_4^{2-} and a mixed valence compound $Cu^{II}SO_3Cu_2^{I}SO_3 \cdot 2H_2O$ are determined to be the principal products. The rate law is consistent with consecutive first-order reactions. Results are interpreted in terms of the initial formation of an inner-sphere complex which is followed by a rate-limiting electron transfer step. These results are discussed in light of previously accepted mechanisms for the trace metal catalysis of the autoxidation of SO_3^{2-}.

INTRODUCTION

Copper(II) forms transient complexes with S(IV) in solution (as discussed in Chapter 2). These react to form a mixture of Cu(I), Cu(II), SO_4^{2-} and SO_3^{2-} in apparent equilibrium with Chevreul's salt ($Cu^{II}SO_3Cu_2^{I}SO_3 \cdot 2H_2O$), a mixed valence precipitate of copper under anoxic conditions. However, the reduction of Cu(II) by S(IV), in terms of the predominant Cu(II) and S(IV) species, is

thermodynamically unfavorable:

$$\bar{e} + Cu^{2+} \rightleftharpoons Cu^{+} \qquad 0.153 \text{ V (Latimer, 1952)}$$

$$HSO_3^- \rightleftharpoons H^+ + \bar{e} + SO_3^- \qquad -0.84 \text{ V (Huie and Neta, 1984)}$$

$$Cu^{2+} + HSO_3^- \rightleftharpoons Cu^{+} + H^+ + SO_3^- \qquad -0.69 \text{ V.}$$

The unfavorable ΔG° for this reaction, as written, indicates other processes must be taken into account. These processes include the stabilization of the products and the energy released by precipitation.

Many of the previous studies on the Cu(II)-S(IV) system have been focused on reaction stoichiometry and product determination (Ramberg, 1910; Baubigny, 1912; Albu and Graf von Schweinitz, 1937; and Foffani and Menegus-Scarpa, 1953). The first reported study of the kinetics of the reduction of Cu(II) by S(IV) in the absence of O_2 was by Zeck and Carlyle (1974). They assumed that the rate of disappearance of Cu(II) was given by a second-order equation of the following form:

$$\frac{-d[Cu(II)]}{dt} = k[Cu(II)][S(IV)]. \qquad (3.1)$$

The value of k was reported to vary with the ratio of Cu(II) to S(IV), to decrease in the presence of Cu(I) and to vary inversely with $[H^+]$ in a nonlinear fashion (for 10 mM = [Cu(II)], 100 < [S(IV)] < 25 mM, 1.2 < pH < 0.01). Zeck and Carlyle were able to fit their data with Eqn. 3.1 when $k = 1/(m[H^+] + n[H^+]^2)$ where m and n were adjustable coefficients. When the Cu(II):S(IV) ratio was varied, the observed rate constant did not change in a consistent manner. Zeck and Carlyle reported that they had difficulty obtaining reproducible kinetic data.

The kinetics of reduction of Cu(II) by S(IV) are relevant to the chemistry of SO_2 in clouds and haze aerosol (Hoffmann and Jacob, 1984). Copper is present in most aqueous atmospheric systems, and it is known to be an effective catalyst for S(IV) oxidation at pH > 6. Reinders and Vles (1925) investigated the catalytic autoxidation of S(IV) in the presence of Cu(II), Fe(III), Ni(II) and Co(II). Both Cu(II) and Fe(III) were shown to be active catalysts in the pH range of 4 to 12, with catalytic activity reaching a maximum in that range, depending on the species present in solution. At higher pH the catalytic effectiveness of Cu(II) decreased; this was attributed to the formation of $Cu(OH)_2$. Reinders and Vles reported that their data did not fit a second order rate expression. Fuller and Crist (1941) investigated the copper catalyzed autoxidation of S(IV) at pH 8.7 and obtained the following rate law:

$$\frac{-d[SO_3^{2-}]}{dt} = (k_1 + k_2[Cu^{2+}])[SO_3^{2-}] \qquad (3.2)$$

where $k_1 = 0.013\ sec^{-1}$ and $k_2 = 2.5 \times 10^{-6}\ M^{-1}sec^{-1}$. They reported that the observed rate decreased with a decrease in pH. The two-term rate law was proposed to account for non-catalytic autoxidation of S(IV).

Bäckström (1934) has argued that the reduction of Cu(II) by S(IV) is the initial step in the Cu(II)-catalyzed free-radical oxidation of S(IV):

$$Cu(II) + SO_3^{2-} \longrightarrow Cu(I) + SO_3^{\bullet -}. \qquad (3.3)$$

Even though Bäckström did not postulate the pre-equilibrium formation of a Cu(II)-S(IV) complex before the electron transfer, formation of a complex appears to be a necessary step in the mechanism for thermodynamic reasons.

Veprek-Siska and Lunak (1974) noted that cupric ion was "immediately and quantitatively reduced by sulfite to cuprous ion". However they did not report the reaction conditions at which this rapid reduction was observed. Veprek and Lunak proposed the trace metal-catalyzed autoxidation of S(IV) might proceed via the formation of sulfite-cuprous intermediates (such as $O_2Cu(SO_3)_n^{-2n+1}$) rather than a radical reaction pathway. Veprek-Siska and co-workers (Lunak et al., 1978) investigated the effects of 2-propanol on the rate of S(IV) oxidation in the presence of copper. They found that 2-propanol acted as an inhibitor. Their proposed mechanism involved the reduction of Cu(II) to Cu(I) by S(IV) followed by the formation of sulfito-2-propanol cuprous complexes. These complexes then reacted further to produce acetone and SO_4^{2-}.

Baron and O'Hern (1966) and Mishra and Srivatava (1976) reported the following rate law for the Cu(II) catalyzed autoxidation of S(IV):

$$\frac{-d[O_2]}{dt} = 0.5\ k\ [Cu^{2+}]^{0.5}[SO_3^{2-}]^{1.5}. \qquad (3.4)$$

The above investigators were uncertain about the oxidation state of copper during the reaction. The half-order dependence on copper was

inferred from the Bäckström mechanism; it was not experimentally verified.

The present study focused on the identification of Cu(II)-S(IV) complexes and on the determination of the kinetics and mechanism of the disappearance of these transient complexes.

EXPERIMENTAL

Reagents and Materials

All reagents were analytical grade. Sodium sulfite (Mallinckrodt) solutions were prepared gravimetrically. Fresh solutions were prepared and stored inside an N_2-atmosphere glovebox (Vacuum Atmospheres Dri-Lab HE-43-2 with a HE-439 Dri-Train) for each experiment. The pH of the sulfite solutions was found to decrease only slightly with time ($\Delta[H^+] = 4 \pm 2\times10^{-11}$) for a 0.1 M Na_2SO_3 solution during a two week period indicating only a very slow oxidation of S(IV) to S(VI). Copper solutions were made from $Cu(NO_3)_2 \cdot 2.5H_2O$ (J. T. Baker Chemical Co.), $Cu(ClO_4)_2 \cdot 6H_2O$ (G. Frederick Smith), $CuCl_2 \cdot 2H_2O$ (J. T. Baker Chemical Co.) or $CuSO_4 \cdot 5H_2O$ (Mallinckrodt). Copper(II) solutions were standardized by iodometric titration (Hammock and Swift, 1949). The concentration of Cu(II) in experimental solutions was determined colorimetrically (Blair and Diehl, 1961) using bathocuproine disulfonate (2,9-dimethyl-4,7-diphenyl-1,10-phenanthrolinedisulfonic acid, disodium, Sigma Chemical Co.). Sulfite solutions were acidified to the desired pH using the corresponding acid of the copper(II) counter ion before they were mixed with the copper solutions. Ionic strength, μ (M), was fixed with either $NaNO_3$ (Mallinckrodt), Na_2SO_4

(Mallinckrodt), $NaClO_4$ (G. Frederick Smith Co.), or NaCl (J.T. Baker Co.) High-purity (18 MΩ-cm) water was obtained from a Millipore Milli-Q system.

Oxygen-free Techniques

All the kinetic experiments were conducted in an anoxic environment at 21.0 ± 0.4 °C. Dissolved oxygen was removed from solutions using a Schlenk line. In this procedure, a vacuum was drawn above the solution; the solution was then purged with N_2. This vacuum-stripping cycle was repeated three times for each solution. Trace levels of oxygen were scrubbed from the (high-purity) N_2 by reaction with a packed column of solid MnO absorbed on vermiculite. Deoxygenated solutions were placed in a N_2-atmosphere glovebox (Vacuum Atmospheres Dri-Lab HE-43-2 with a HE-493 Dri-Train). Oxygen leakage through the gloves was controlled by passing the N_2 atmosphere continuously through a Cu(I) catalyst bed. Measurements that were performed outside the glovebox were made in sealed containers.

Spectrophotometric Methods

The kinetics of the electron transfer reaction between Cu(II) and S(IV) were determined by following the disappearance of the charge-transfer absorbance band at 340 and 350 nm and the d-d absorbance band at 800 nm. Pseudo first-order conditions were established such that $[S(IV)]_o >> [Cu(II)]_o \simeq 10^{-3}$ M, with NO_3^- as the counter ion, unless otherwise indicated.

Spectrophotometers used for kinetic studies were a Hewlett-Packard

dual beam diode array instrument (HP 8450A) and a Shimadzu (MPS-2000) dual beam monochromatic instrument. Kinetic traces were either collected automatically on a Digital Equipment Corporation (DEC) MINC computer (PDP 11/23) or digitized from recorded spectra for the data obtained on the MPS-2000. Data were processed with either a DEC VAX 780, VAX 730 or PDP 11/23.

Actinometry measurements were conducted to measure the photon flux for each spectrophotometer using Aberchrome 540 ((*E*)-α-(2,5-dimethyl-3-furyl-ethylidine)(isoproylidene) succinic acid anhydride, Aberchronics, Ltd.) by the method of Heller and Langan (1981). Results indicated that the photon flux was a factor of three more intense for the HP 8450A than for the MPS-2000 under the conditions used in these experiments.

Electron paramagnetic measurements (EPR) spectra were recorded on a Varian E-Line Century Series spectrometer. Spectra were taken on quick-frozen anoxic solutions at 77 ^{o}K in 5 mm quartz tubes. Spectra were integrated using the equations of Aasa and Vänngard (1975).

Analyses

Sulfate was analyzed with a Dionex Ion Chromatograph (2020) using AFS-1 and AS-4 columns. Dithionate was analyzed by the cerimetric technique of Nair and Nair (1971). Interference by copper was eliminated by removal of Cu^{2+} with Bio-rad Chelex 100 resin.

Chevreul's salt was identified with single crystal x-ray diffraction using the unit cell dimensions provided by Kierkegaard and Nyberg (1965) Elemental composition was determined by ESCA (Electron

Spectroscopy for Chemical Analysis) with the help of Dr. Grunthaner at Jet Propulsion Laboratory. Samples were mounted on etched silicon pieces using a 20: 1 hexane and vaseline mixture. Spectra were taken at 240 ^{o}K on a HP 5950A electron spectrometer. Elemental analysis was done at Galbraith Laboratories, Co..

Ion exchange columns with lengths of 10 cm and bed volumes of 85 cm^3 were used. Resins were analytical grade Bio-Rad anion exchange resin AG 1-X8 (Cl^- form) and DOWEX 50W-X2 cation exchange resin (H^+ form). The DOWEX resin was conditioned with 0.1 M NaCl before use.

Cyclic voltammetry measurements were made on Cu(II)-S(IV) solutions purged with Ar. The potential of a graphite electrode vs. SCE (Pt working electrode, NaCl salt bridge) was monitored.

RESULTS

Mixing $Cu(II)X_n$ ($X = SO_4^{2-}$, ClO_4^-, Cl^-, or NO_3^-) with Na_2SO_3 solutions at pH < 6 resulted in the formation of a green complex that eventually disappeared with time both in the presence and absence of O_2. The absorbance spectra of these complexes recorded immediately after mixing (t < 30 sec) in the presence of different anions are shown in Fig. 3.1. They exhibit a broad shoulder between 350 nm and 400 nm and a broad peak at 800 nm that is characteristic of Cu(II) d-d transitions. The shape of the shoulder at 350 nm was independent of pH, even though the initial absorbance was pH dependent (Fig. 3.2). Fig. 3.3 illustrates the change that occurred in the UV/Vis spectrum of Cu(II)-S(IV) with time. A mixed-valence precipitate of $Cu^{II}SO_3Cu_2^{I}SO_3 \cdot 2H_2O$ formed within four hours. Analysis of

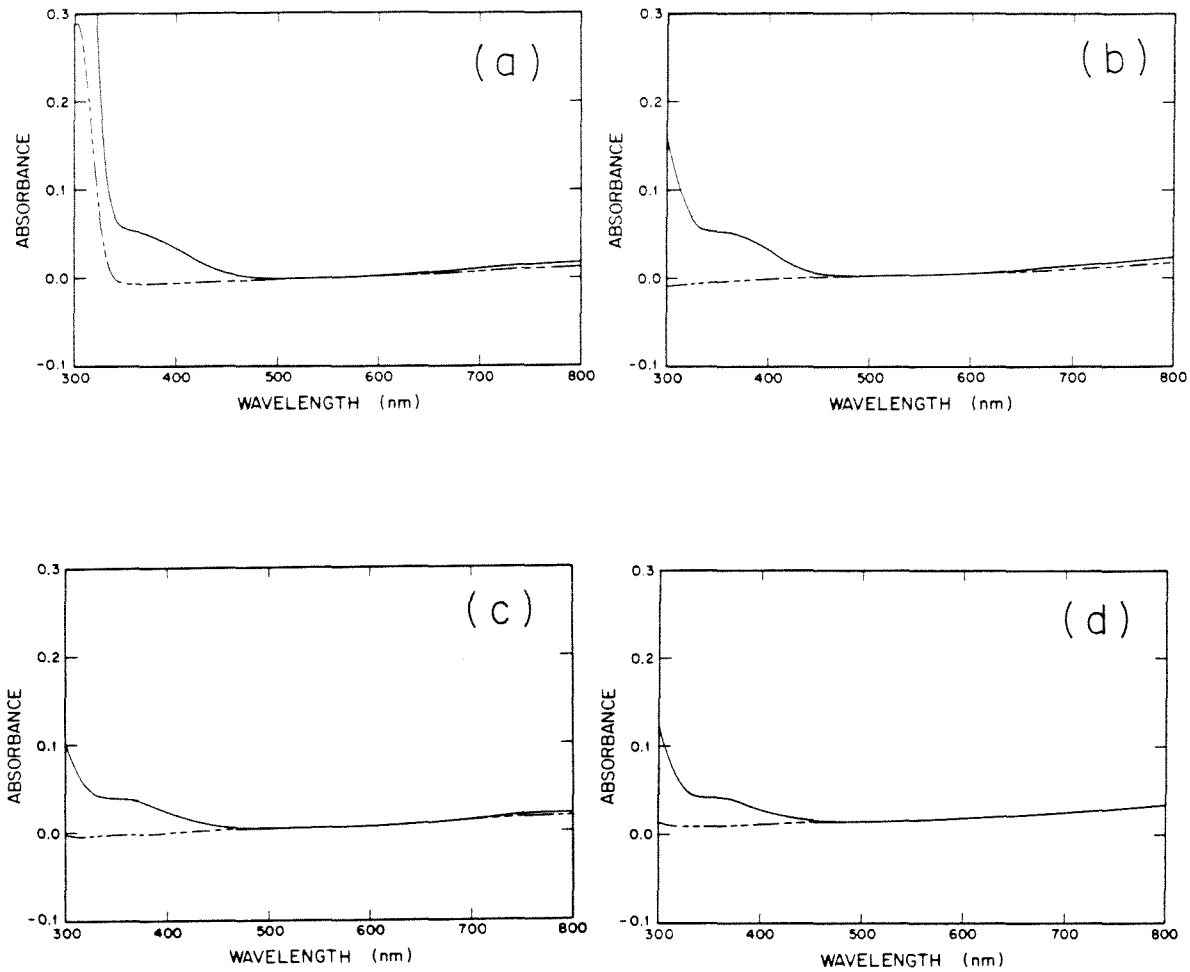

Fig. 3.1 Absorbance spectra of the Cu(II)-S(IV) complex (obtained immediately after mixing) when (a) NO_3^-, (b) ClO_4^-, (c) SO_4^{2-} and (d) Cl^- are present in excess (μ = 0.1 M, $[Cu(II)]_o$ = 1 mM, $[S(IV)]_o$ = 10 mM, pH = 5). Broken line is the aqueous Cu(II) spectrum without S(IV) present.

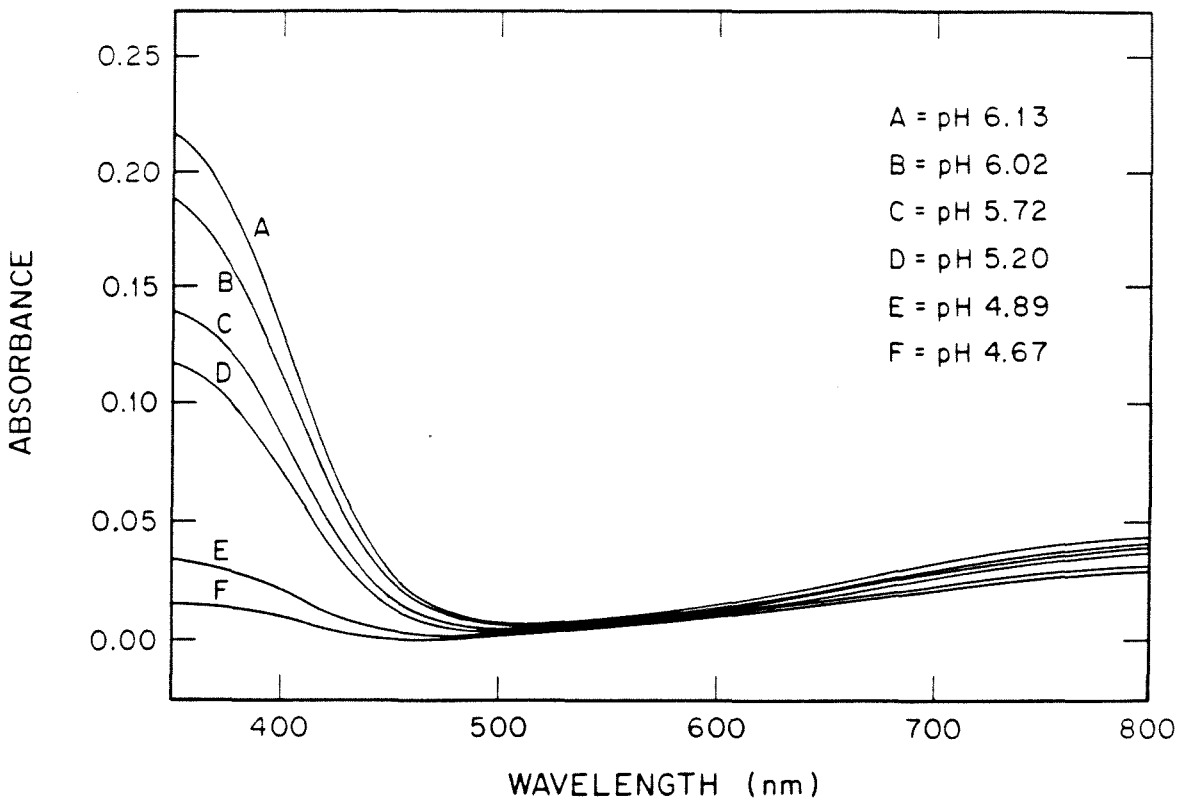

Fig. 3.2 Absorbance spectra of Cu(II)-S(IV) complexes at different initial pH recorded within 30 sec of mixing.

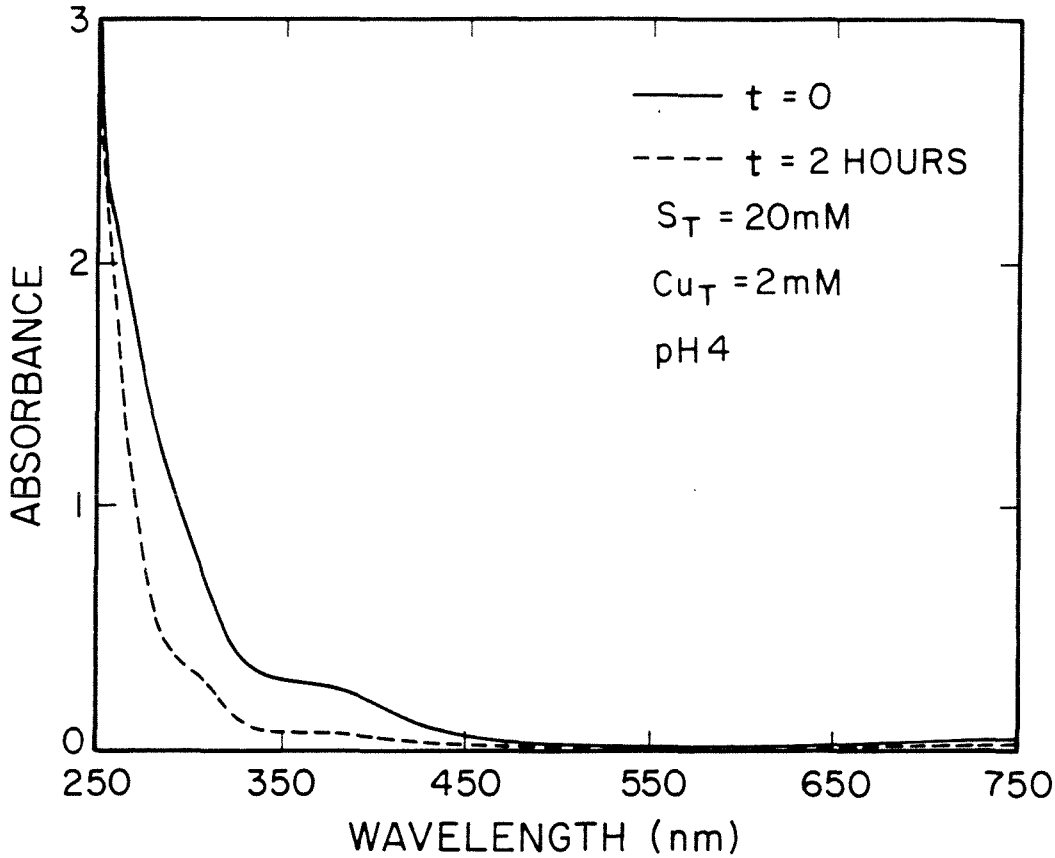

Fig. 3.3 Changes in the absorbance spectrum of the Cu(II)-S(IV) complex over time.

$Cu^{II}SO_3Cu_2^{I}SO_3 \cdot 2H_2O$ by ESCA showed that Na^+ was incorporated to a minor degree into the crystal. Since Na^+ has approximately the same ionic radius as Cu(I) (Basolo and Pearson, 1967) it appeared to be randomly substituted for Cu(I). When the pH of the mixture was greater than 6, a green solid precipitated immediately upon mixing. The solid continued to react with the eventual formation of $Cu^{II}SO_3Cu_2^{I}SO_3 \cdot 2H_2O$ within $\simeq$ 12 hours.

During the course of the above reactions the pH dropped. This can be attributed to a shift in the SO_3^{2-}/HSO_3^- equilibrium, which was perturbed by the formation of the complex and solid products. The products of this reaction have been identified as SO_4^{2-}, Cu(I), and Chevreul's salt. In reactions where Cl^- was the counter ion, insoluble CuCl was also formed. Dithionate formation was not observed. Raman studies of the Cu(II)-S(IV) system have also indicated that SO_4^{2-} was the only oxidation product (Chapter 2). The production of dithionate would have indicated a one-electron transfer reaction occurred between the S(IV) and Cu(II); sulfate production required a two-electron transfer process to take place.

The stoichiometry of the transient green precipitate, $Cu_2SO_3(OH)_2 \cdot H_2O$, suggested that the precursor complex has two copper centers bridged by a sulfite group. The aqueous-phase precursors appeared to be positively charged because they were adsorbed on a cation exchange column and not on an anion exchange column. The Cu(II)-S(IV) complex was retained higher on the column than $Cu(NO_3)_2$ solutions of the same concentration. These results suggested that the

precursor was either a bulkier complex or more highly charged than Cu^{2+}.

The two most likely stoichiometries for a positively charged transient species would be $CuHSO_3^+$ or $Cu_2SO_3^{2+}$. Although the initial UV/Vis absorbance at of the soluble Cu(II)-S(IV) species was highly dependent on pH (Fig. 3.2), the initial absorbance did not vary linearly with $[HSO_3^-]$. In Table 3.1 a comparison between the initial absorbance, A_o, and S(IV) speciation for $3.9 < pH < 6.6$ indicates that the maximum A_o did not overlap with the maximum for $[HSO_3^-]$. Thus $CuHSO_3^+$ does not appear to be the predominant precursor. A more likely precursor complex is a sulfite-bridged Cu dimer. Formation of this precursor is consistent with the observed pH dependence and the required stoichiometry for two-electron transfer. A bridged dimer would also have the same Cu(II):S(IV) stoichiometry as the green precipitate that formed at higher pH. Furthermore, a sulfite-bridged dimer would agree with the Raman and IR study results which suggested that the transient complexes contained both O and S bonds (Chapter 2).

Preliminary EPR experiments on the Cu(II)-S(IV) system supported the observation that a sulfite-bridged dimer was formed. EPR spectra of the Cu(II)-S(IV) system in the presence of ClO_4^- and NO_3^- are shown in Fig. 3.4. The spectra shown are absorption derivatives of the Cu(II) signal and must be integrated to obtain the area under the curves (which is directly proportional to the number of Cu(II) centers contributing to the spectra). These spectra are typical Cu(II) EPR spectra with a g-value of 2.1 and four hyperfine structures. There was an immediate decrease in the magnitude of the Cu(II) signal when S(IV)

TABLE 3.1

Distribution of S(IV) species compared to the initial intensity of the Cu(II)-S(IV) complex absorbance at different values of pH[a]

	Sulfur Solutions[b]			Complex
pH	Sulfur Species Distribution (%)			Initial Absorbance
	$[SO_3^{2-}]$	$[HSO_3^-]$	$[SO_2 \cdot H_2O]$	(350 nm)
6.6	46.0	54.0		0.41
6.2	25.0	75.0		0.24
5.7	9.0	91.0		0.24
5.2	2.6	97.4		0.10
4.9	1.6	98.4		0.07
4.5	0.6	99.3	0.1	0.03
3.9	0.1	99.4	0.5	0.01

[a] μ = 0.1 M
K_{a_1} = 1.91 ± 0.03 (μ = 0.0 M, Smith and Martell, 1976)
K_{a_2} = 7.18 ± 0.02 (μ = 0.0 M, Smith and Martell, 1976)

[b] $[S(IV)]_T$ = 20 mM

was added (within the 30 seconds it took to mix and freeze the solutions); see Fig. 3.4. The times given for each spectrum are the total time for which the sample was at room temperature (21 $^{\circ}$C) before quick-freezing to take the spectrum. The freezing and thawing added ± 30 sec to the indicated times. As the reaction progressed, the hyperfine structure changed, indicating that there were changes in the inner-coordination sphere of the copper. However there was no significant decrease in the number of Cu(II) centers contributing to the spectra (see Table 3.2). The initial decrease indicated that either there was a rapid reduction of the Cu(II) when S(IV) was added to the solution, or else there was spin-coupling of the copper centers by the formation of sulfite-bridged copper dimers.

Initial kinetic data obtained on the HP 8450A diode array spectrophotometer were difficult to interpret because of the apparent lack of reproducibility. The irreproducibility appeared to be due to a light-initiated reaction. The optical configuration of the HP8450A resulted in the reaction being irradiated with the full intensity of the light source (200 to 800 nm) each time an absorbance measurement was taken. The rate of change in the absorbance at 350 nm was observed to be dependent on the sampling interval, which was directly proportional to the photon flux into the cuvette. The light sensitivity was further explored by exposing the reaction mixture to a near-UV light source, a "black light" (300 to 400 nm radiation). The effects of light in this region of the spectrum on the observed kinetics is shown in Fig. 3.5. Upon exposure to this light source the mixture showed an initial decrease in absorbance that was followed by

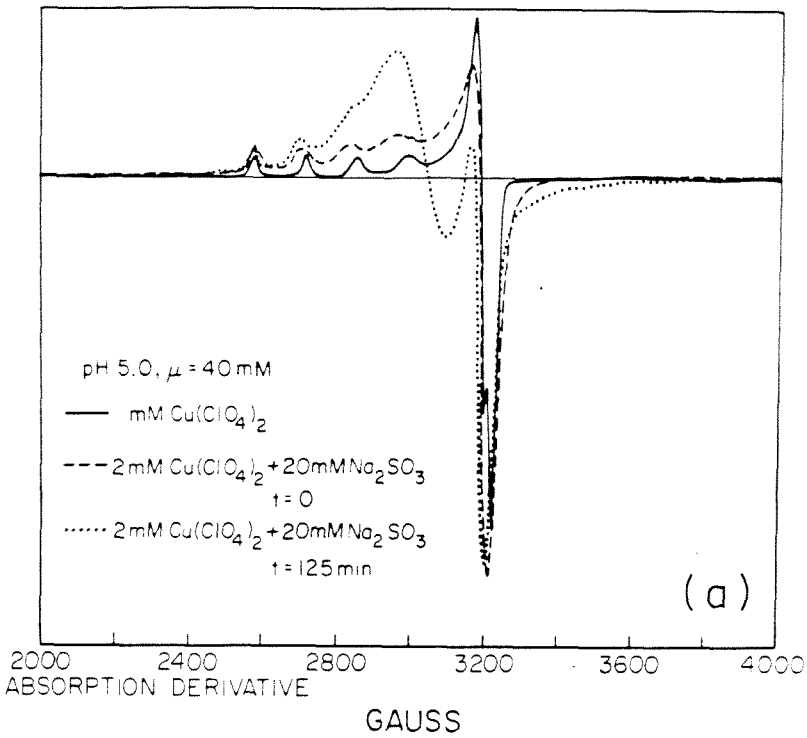

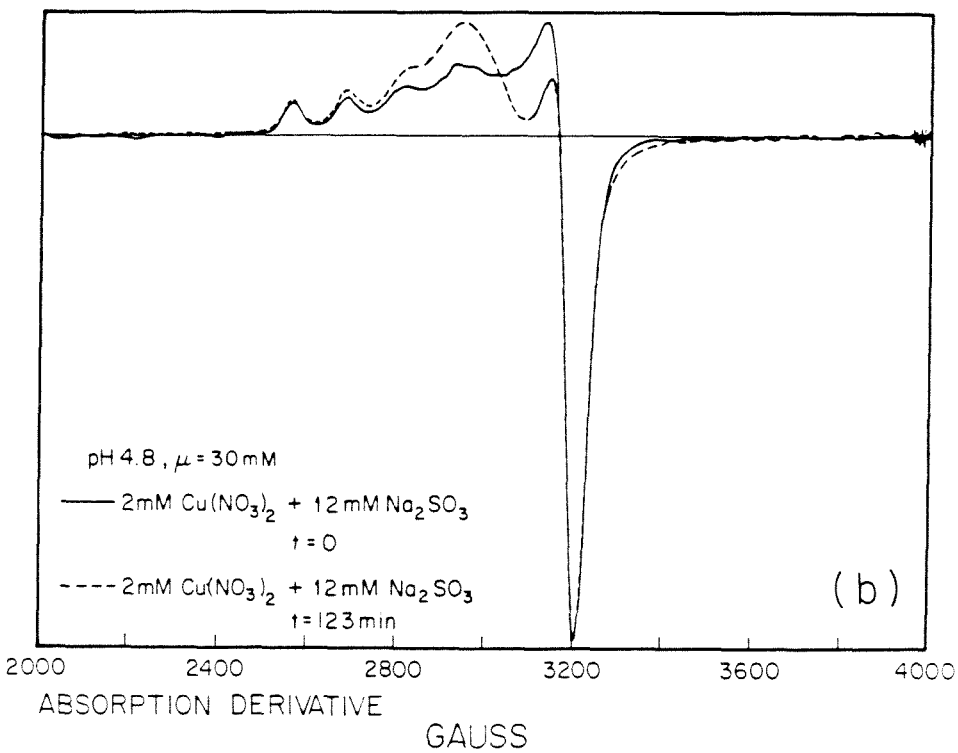

Fig. 3.4 Cu(II) EPR spectrum for the Cu(II)-S(IV) system in the presence of (a) ClO_4^- and (b) NO_3^-.

TABLE 3.2

Data based on changes in the areas under the recorded EPR spectra of the Cu(II)-S(IV) system presented in Fig. 3.4 as a function of time

ClO_4^-		NO_3^-	
Time[a]	% $[Cu(II)]_o$[b]	Time[a]	% $[Cu(II)]_o$[b]
0	51	0	59
25	46	18	64
50	44	42	62
75	49	86	64
100	51	123	62
125	49	>12 hours	58
>26 hours	40		

[a] $[Cu(II)]_o$ was determined from the area under a [Cu(II)] spectrum with no S(IV) present.

[b] Times refer to the length of time the sample was at room temperature before quick-freezing to take spectrum.

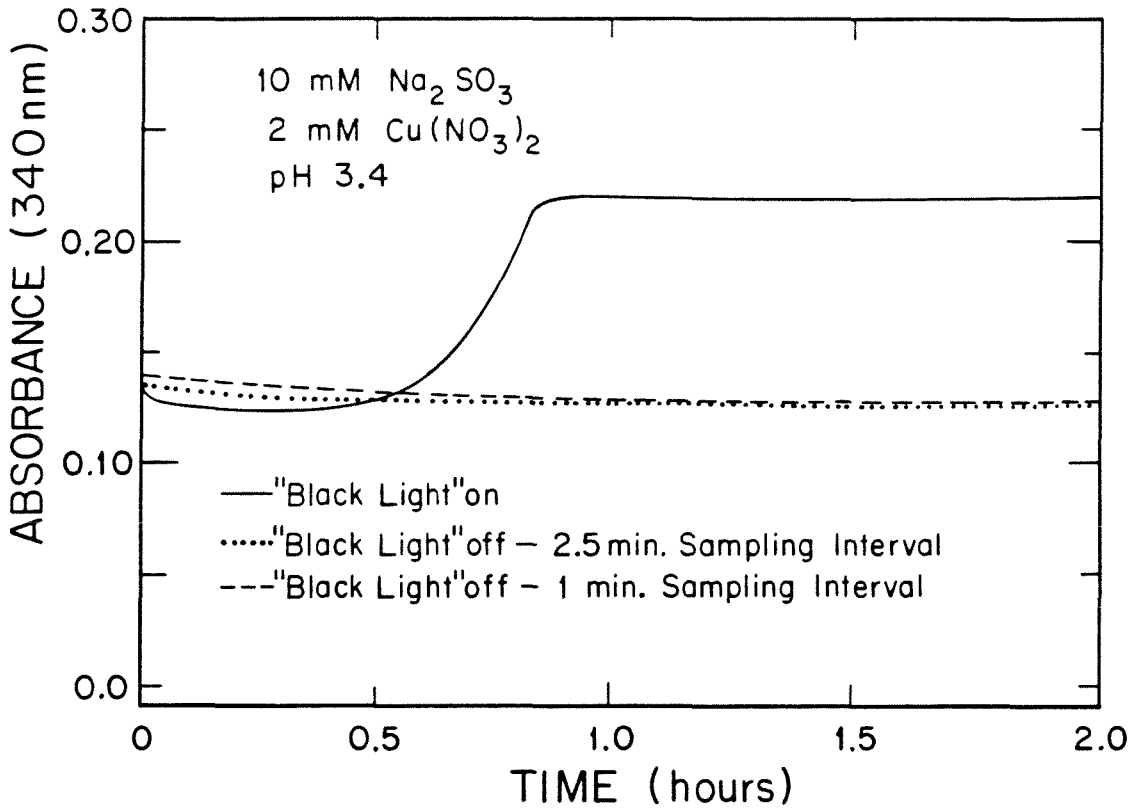

Fig. 3.5 Kinetic effects of increasing the photon flux ($\lambda >$ 300 nm) on the absorbance at 340 nm of the Cu(II)-S(IV) complexes. Sampling interval refers to the interval between measurements when the mixture is exposed to a full spectrum of light (200 to 800 nm).

an increase in absorbance. To see if the light-initiated reaction involved a radical species, two different radical traps, (mannitol and methanol) were added to the solution. The results were inconclusive, mannitol was found to slightly retard the onset of the absorbance increase. Methanol was found to increase the magnitude of the change in absorbance (see Fig. 3.6). Plausible explanations for the light-initiated reactions are a free-radical pathway involving NO_3^-, a metal-to-ligand charge-transfer or a ligand-to-metal charge-transfer. A nitrate-solvent complex forms in aqueous systems. When this complex is irradiated with 308 nm light, the nitrate oxidizes H_2O and a hydroxyl radical is produced (Kotzias et al., 1982). This could be an initiation step for a radical chain reaction. Light-induced ligand-to-metal charge-transfer has been reported for bis (dithiooxalato-S,S')cuprate(III), $Cu(Dto)_2^-$ (Imamura et al., 1984). This anion was shown to undergo a light-activated, intramolecular, Dto $\longrightarrow$ Cu two electron transfer. An analogous reaction may occur in the Cu(II)-S(IV) system.

All subsequent experimental work was done under dark conditions, to eliminate any interference from light induced reactions. Improved reproducibility was obtained when sample aliquots were taken in a time series from a bulk solution, which had been maintained in the dark under anoxic conditions. However, this technique decreased the time resolution of the data sets. Data obtained using the aliquot method are shown in Fig. 3.7. From the data it appears that the reaction is biphasic. There was an initial decrease ($\tau_{1/2} \simeq 15$ min) in absorbance that was followed by a slower second phase which required days to reach

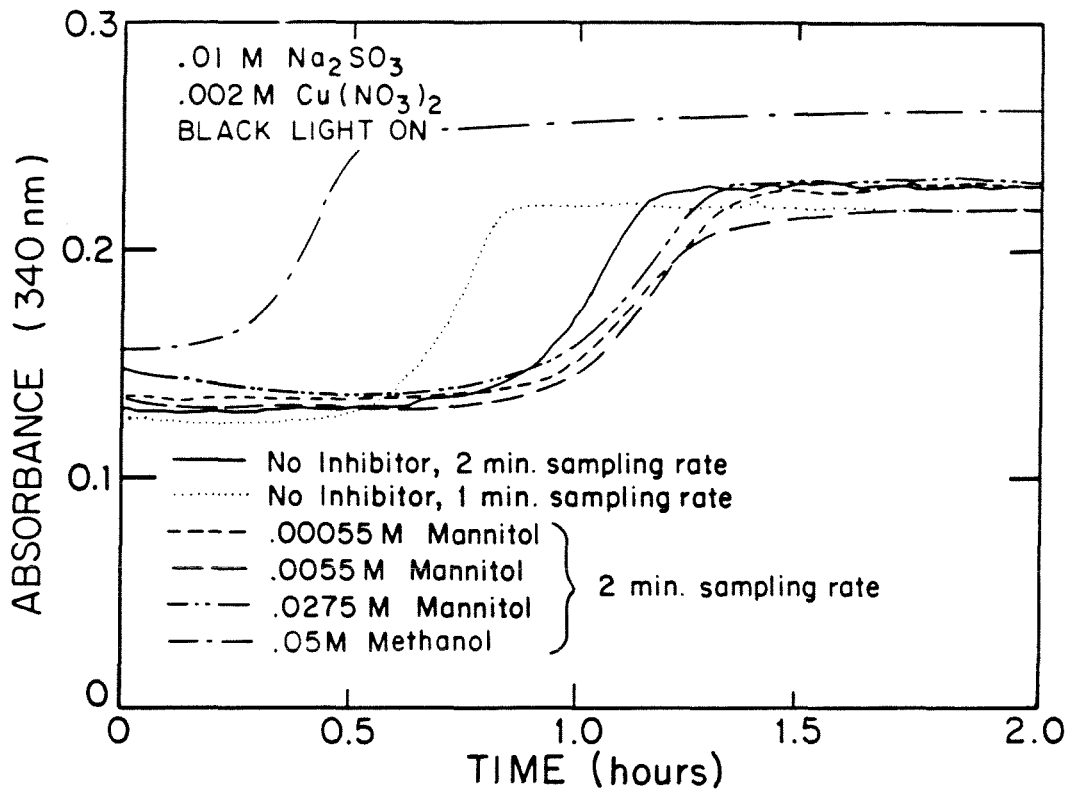

Fig. 3.6 Effects of adding radical inhibitors, mannitol and methanol, to the Cu(II)-S(IV) system when it is irradiated with light ($\lambda > 300$ nm).

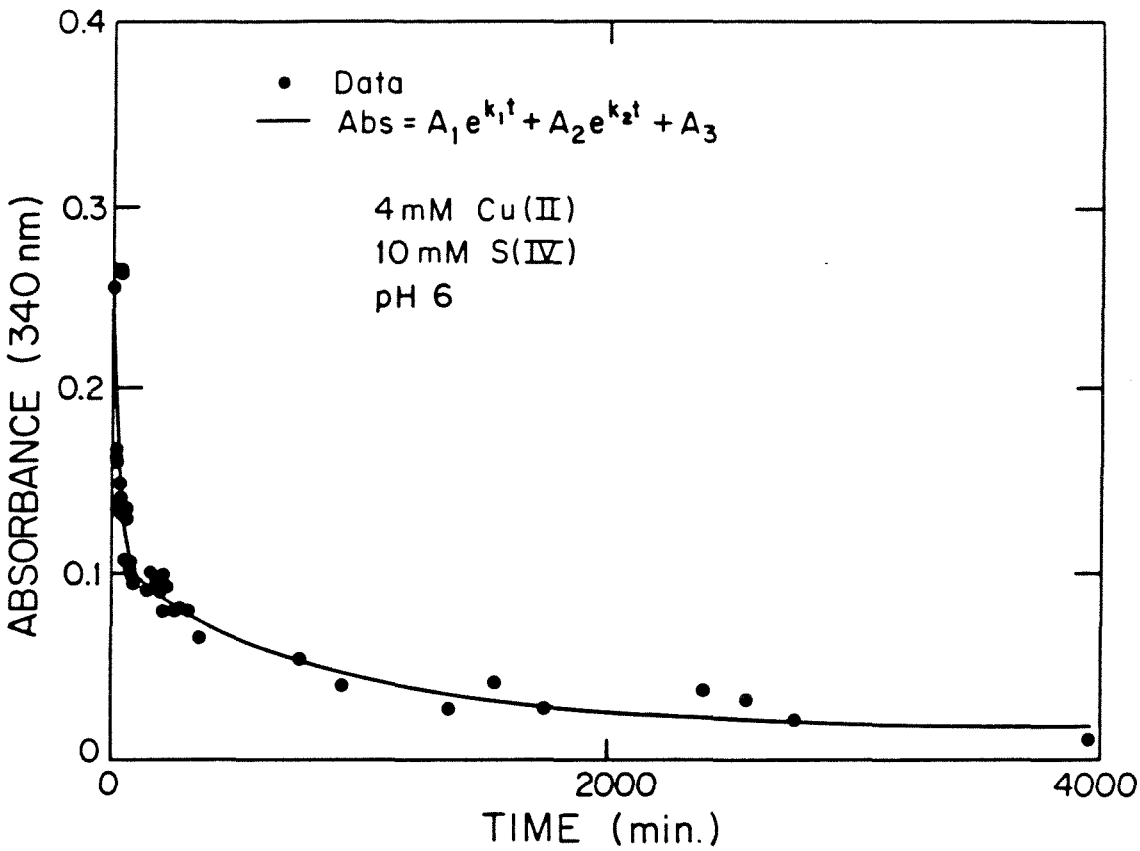

Fig. 3.7 Kinetic data obtained at 340 nm on the HP 8450A of a Cu(II)-S(IV) mixture that was kept in the dark. The solid line was fit to the data using a nonlinear least squares double-exponential fitting routine.

equilibrium. Rate constants for this bi-phasic reaction were determined using a nonlinear least-squares routine fitting a function with two exponential terms[1]. Results of this analysis are shown in Fig. 3.7. Experiments were run with variable Cu(II):S(IV) ratios, at the same pH. The observed constants for the first phase of the reaction were independent of the Cu(II):S(IV) ratio (see Table 3.3); this observation is consistent with a rate-limiting step that involves the reduction of Cu(II) in a Cu(II)-S(IV) complex.

A mechanism for the anoxic reaction between Cu(II) and S(IV) must account for the following observations: (1) positively-charged dimeric Cu(II)-S(IV) complexes were formed upon mixing solutions of Cu(II) and S(IV); (2) the formation of Cu(II)-S(IV) complexes is pH-dependent; (3) the rate of disappearance of the complexes followed bi-phasic first-order kinetics; (4) evidence for a two-electron transfer process with the formation of S(VI) was obtained; and (5) the establishment of an equilibrium mixture of Cu(II), Cu(I), S(IV) and S(VI) with precipitated $Cu^{II}SO_3Cu^{I}_2SO_3 \cdot 2H_2O$ was verified. A mechanism, which is consistent with the above observations, is as follows:

---

[1]The program fits a theoretical function f_i to a set of data d_i by minimizing the following function:

$$\phi = \sum_i \frac{(f_i - d_i)^2}{2\sigma_i^2}$$

where σ_i^2 are weighting factors ($\sigma_i^2 = 1.0$ in this case). The parameters f_i were defined as $f_i = A\exp(kt)$, where k is a first order rate constant, t is time and A is a constant, dependent on the initial absorbance of each species. The search algorithm is described by Marquadt (1963).

TABLE 3.3

Values of the observed rate constant for the initial phase of the Cu(II)-S(IV) reaction at different reactant ratios[a]

[S(IV)] (M)	[Cu(II)] (M)	[S]:[Cu]	pH	k (sec^{-1})
0.005	0.005	1:1	4.5	$5x10^{-4}$
0.01	0.004	2.5:1	4.7	$7x10^{-4}$
0.01	0.004	2.5:1	4.9	$8x10^{-4}$
0.02	0.002	10:1	5.0	$7x10^{-4}$

[a]Cu(II)-S(IV) mixture was kept in the dark during the reaction.

$$HSO_3^- \rightleftharpoons H^+ + SO_3^{2-} \quad (3.5)$$

$$Cu^{2+} + SO_3^{2-} \rightleftharpoons CuSO_3 \quad (3.6)$$

$$Cu^{2+} + CuSO_3 \rightleftharpoons Cu(II)SO_3Cu(II)^{2+} \quad (3.7)$$

$$Cu(II)SO_3Cu(II)^{2+} + H_2O \rightleftharpoons Cu(II)SO_3Cu(II)OH^+ + H^+ \quad (3.8)$$

$$Cu(II)SO_3Cu(II)^{2+} \xrightarrow{k_5} Cu(I)S(V)O_3Cu(II)^{2+} \quad (3.9)$$

$$Cu(II)SO_3Cu(II)OH^+ \xrightarrow{k_6} Cu(I)S(V)O_3Cu(II)OH^+ \quad (3.10)$$

$$Cu(I)S(V)O_3Cu(II)^{2+} \xrightarrow{k_7} Cu(I)S(VI)O_3Cu(I)^{2+} \quad (3.11)$$

$$Cu(I)S(V)O_3Cu(II)OH^+ \xrightarrow{k_8} Cu(I)S(VI)O_3Cu(I)OH^+ \quad (3.12)$$

$$Cu(I)S(V)O_3Cu(II)^{2+} \rightleftharpoons 2Cu(I) + S(VI)O_3 \quad (3.13)$$

$$Cu(I)S(VI)O_3Cu(I)OH^+ \rightleftharpoons 2Cu(I) + S(VI)O_3 + OH^- \quad (3.14)$$

$$S(VI)O_3 + H_2O \rightleftharpoons SO_4^{2-} + 2H^+ \quad (3.15)$$

$$Cu^+ + SO_3^{2-} \rightleftharpoons CuSO_3^- \quad (3.16)$$

$$2Cu^+ + Cu^{2+} + 2SO_3^{2-} + H_2O = Cu^{II}SO_3Cu_2^{I}SO_3 \cdot 2H_2O\downarrow. \quad (3.17)$$

A structural representation of this mechanism is given in Fig. 3.8.

In this mechanism, two parallel pathways involving $Cu_2SO_3^{2+}$ and $Cu_2SO_3OH^+$ were proposed because of the pH dependence of the observed rate constants indicated that there was more than one redox-active species. These transient species have stoichiometries similar to the green precipitate, $Cu_2SO_3(OH)_2 \cdot H_2O$. The first four pre-equilibria were assumed to be fast. For example, the water exchange rate for Cu(II) has been reported to be $\simeq 10^{10}$ sec^{-1} (Hunt and Friedman, 1983). Due to the tetragonal distortion of hexaquo Cu(II), the waters coordinated in the apical positions are less tightly bound and consequently they undergo rapid water exchange. Ligand substitution rates are often

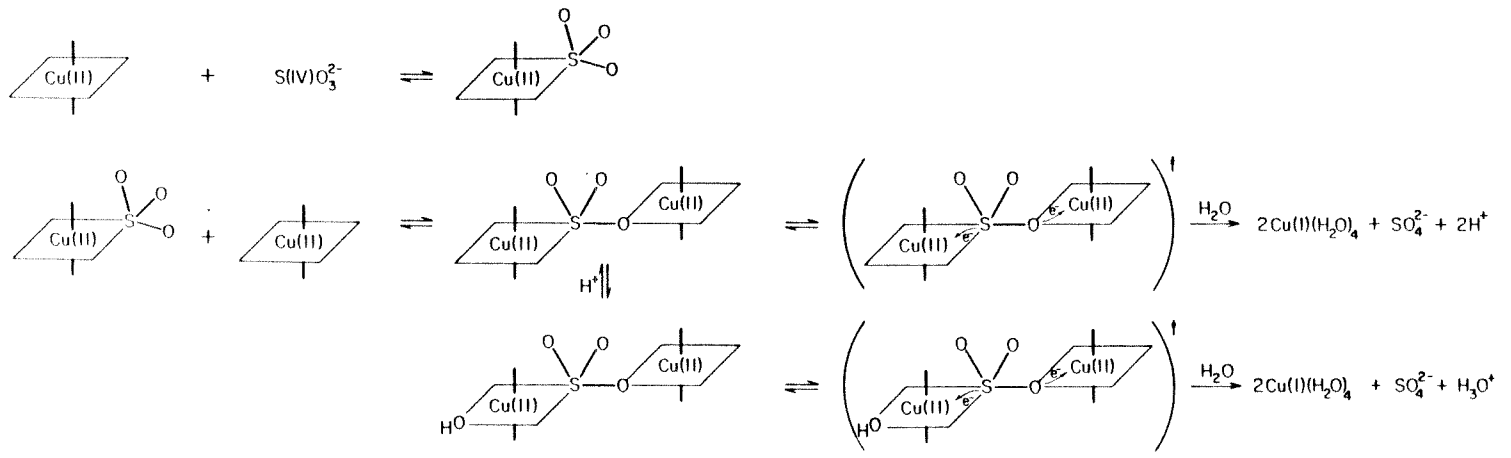

Fig. 3.8 Structural representation of the proposed mechanism for the reaction between Cu(II) and S(IV). (Overall charges and coordination waters have been omitted for clarity).

controlled by the water exchange rate of the central metal (Langford and Gray, 1966).

The rates of electron transfer from S(IV) to Cu(II) in various complexes appeared to be rate-limiting. This was consistent with the slow loss of green color of the Cu(II)-S(IV) complexes. Cyclic voltammetry was attempted on this system, however the preliminary results indicated that there was an irreversible reduction of Cu(II).[2]

Assuming that the electron transfer steps of Eqns. 3.9 to 3.12 are rate-limiting, a rate expression for the above mechanism can be obtained as follows.

$$\frac{d[Cu_2SO_3^{2+}]}{dt} = -k_5[Cu_2SO_3^{2+}] \tag{3.18}$$

$$\frac{d[Cu^{II}Cu^{I}S^{V}O_3^{2+}]}{dt} = k_5[Cu_2SO_3^{2+}] - k_7[Cu^{I}Cu^{II}S^{V}O_3^{2+}] \tag{3.19}$$

$$\frac{d[Cu_2SO_3OH^{+}]}{dt} = -k_6[Cu_2SO_3OH^{+}] \tag{3.20}$$

$$\frac{d[Cu^{II}Cu^{I}S^{V}O_3OH^{+}]}{dt} = k_6[Cu_2SO_3OH^{+}] - k_8[Cu^{I}Cu^{II}S^{V}O_3OH^{+}] \tag{3.21}$$

Integration of Eqns. 3.18-3.21 (from time t=0 to time t) yields:

$$[Cu_2SO_3^{2+}] = [Cu_2SO_3^{2+}]_o\exp(-k_5t) \tag{3.22}$$

$$[Cu_2SO_3OH^{+}] = [Cu_2SO_3OH^{+}]_o\exp(-k_6t) \tag{3.23}$$

$$[Cu^{I}Cu^{II}S^{V}O_3^{2+}] = \left[\frac{k_5[Cu_2SO_3^{2+}]_o}{k_7-k_5}\right][\exp(-k_5t) - \exp(-k_7t)] \tag{3.24}$$

$$[Cu^{I}Cu^{II}S^{V}O_3OH^{+}] = \left[\frac{k_6[Cu_2SO_3OH^{+}]_o}{k_8-k_6}\right][\exp(-k_6t) - \exp(-k_8t)] \tag{3.25}$$

---

[2]Further experiments were not attempted because Cu^o was deposited on the graphite electrode.

Furthermore, if we assume that these species contribute to the net absorption at the wavelengths of interest, λ = 350 and λ = 800 nm then:

$$A = \epsilon_1[Cu_2SO_3^{2+}] + \epsilon_2[Cu_2SO_3OH^+] + \epsilon_3[Cu^{I}Cu^{II}S^{V}O_3^{2+}] + \epsilon_4[Cu^{I}Cu^{II}S^{V}O_3OH^+] + A_\infty \quad (3.26)$$

where

ϵ_n = extinction coefficient for each species;

A_∞ = absorption at time t = ∞.

Substituting Eqns. 3.22 to 3.25 into 3.26 gives:

$$A = A_1\exp(-k_5 t) + A_2\exp(-k_6 t) + A_3\exp(-k_7 t) + A_4\exp(-k_8 t) + A_\infty \quad (3.27)$$

where

$$A_1 = \epsilon_1\left[1 + \frac{k_5}{k_7-k_5}\right][Cu_2SO_3^{2+}]_o;$$

$$A_2 = \epsilon_2\left[1 + \frac{k_6}{k_8-k_6}\right][Cu_2SO_3OH^+]_o;$$

$$A_3 = \epsilon_3\frac{k_5[Cu_2SO_3^{2+}]_o}{k_5-k_7};$$

$$A_4 = \epsilon_4\frac{k_6[Cu_2SO_3OH^+]_o}{k_6-k_8}.$$

Eqn. 3.27 is difficult to solve since multiple species contribute to the total absorbance. The number of species can be reduced by choosing conditions at which $CuOH^+ << Cu^{2+}$ or vice versa.

Detailed studies were conducted on the effects of pH and the

nature of the Cu(II) counter ion on the rate of Cu(II) reduction. A monochromatic spectrophotometer (Shimadzu, MPS-2000) was utilized for these measurements. Reaction mixtures were monitored continuously at a single wavelength (λ = 350 nm or λ = 800 nm). A rapid-mixing cuvette (1 cm) was used for the collection of data during the rapid phase of the reaction. Reproducible kinetics were be obtained under these conditions.

The pH dependence of the reaction was complicated by the number of Cu(II)-S(IV) species present. As illustrated in Fig. 3.9, reactions run at higher pH were faster and had higher A_o values. At lower pH, dA/dt and ΔA were slower and smaller respectively. The strong pH dependence on the formation of the Cu(II)-S(IV) complexes was anticipated given the above mechanism since both reactants, S(IV) and Cu(II), have pH-dependent equilibria. In the proposed rate law, A is a function of Cu(II)-S(IV) complex speciation as well as a function of the rate constants (this can be seen in Eqn. 3.27 where A_n is proportional to $[Cu_2SO_3^{2+}]_o$ and $[Cu_2SO_3OH^+]_o$). The relative concentrations of these two species are related by the following constant, K_a:

$$K_a = \frac{[Cu_2SO_3OH^+][H^+]}{[Cu_2SO_3^{2+}]}. \qquad (3.28)$$

This equilibrium can be shifted by adjusting the pH of the system and the relative importance of different terms in Eqn. 3.27 will thus vary depending on the pH. At lower pH, less oxidation of S(IV) is expected

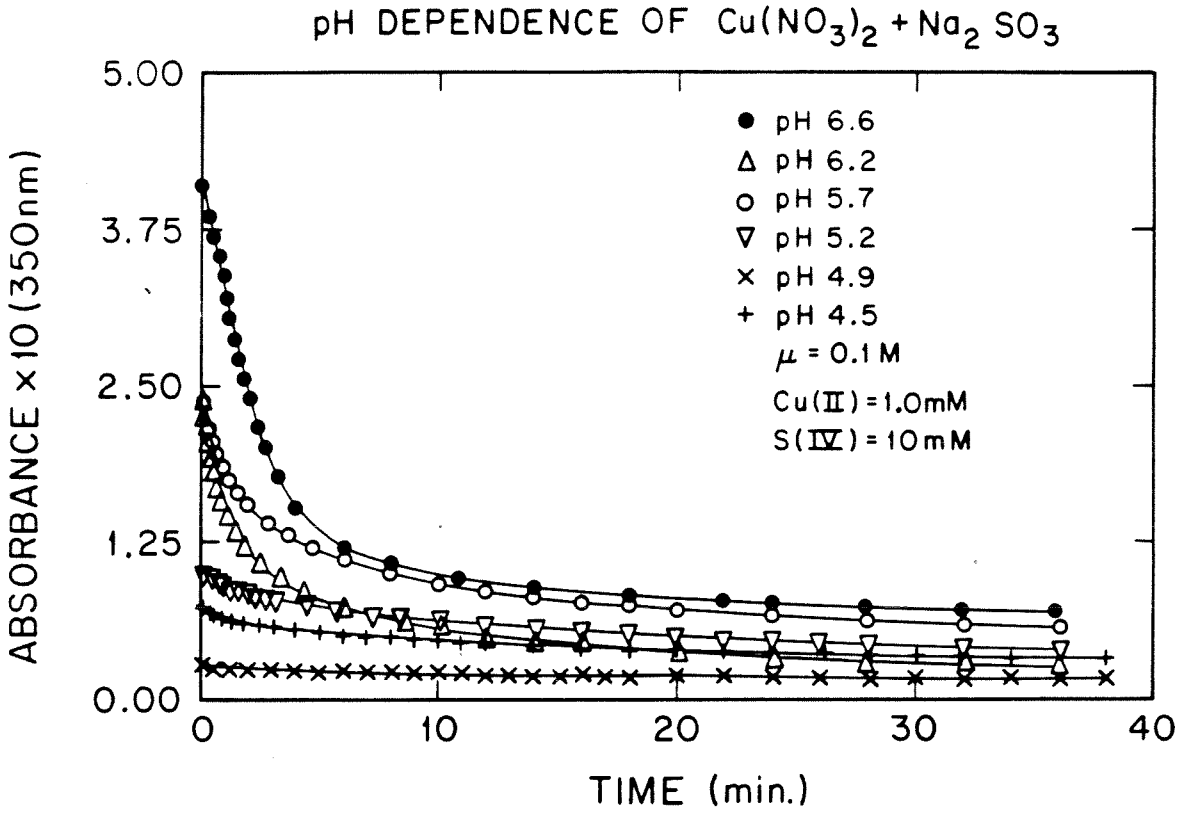

Fig. 3.9 Kinetic data obtained at 350 nm for the Cu(II)-S(IV) system at different values of pH (using the Shimadzu MPS-2000).

to occur because of the low concentrations of the reactive intermediate Cu(II)-S(IV) complexes. This is confirmed in Fig. 3.10 where the rate of sulfate production is presented as a function of time and pH.

The rate expression of Eqn. 3.27 indicates that the kinetic data should be represented by a function with four exponential terms. However, these four separate rate constants are difficult to resolve, since the extinction coefficients for $Cu_2SO_3^{2+}$ and $Cu_2SO_3OH^+$ are approximately equal. To determine the rate constants, it is necessary to simplify this expression by choosing experimental conditions for which some of the terms become unimportant. This can be achieved in the limits $[Cu_2SO_3^{2+}]_o \gg [Cu_2SO_3OH^+]_o \simeq 0$ or $[Cu_2SO_3OH^+]_o \gg [Cu_2SO_3^{2+}]_o \simeq 0$. In either limit, Eqn. 3.27 can be reduced to

$$A = B_1\exp(-k_1 t) + B_2\exp(-k_2 t) \qquad (3.29)$$

where values of B_1, B_2, k_1, k_2 are given in Table 3.4. If the conditions are obtained so that Eqn. 3.29 is a valid approximation for the system, k_1, k_2 should give the values of k_5, k_6, k_7, and k_8. Between these two limits, k_1 and k_2 will be apparent, pH-dependent rate constants. A nonlinear least squares routine was used to fit Eqn. 3.29 to experimental data to determine k_1 and k_2. The pH dependences of k_1 and k_2 are displayed in Fig. 3.11 obtained from absorbance measurements at λ = 350 nm and λ = 800 nm. Both rate constants show the same pH dependence, which appears to be sigmoidal. Extrapolating the data to lower and higher pH, one obtains rate constants of $k_5 \simeq 5.7 \times 10^{-3}$ sec^{-1}, $k_6 \simeq 1.8 \times 10^{-2}$ sec^{-1}, $k_7 \simeq 5.1 \times 10^{-4}$ sec^{-1} and $k_8 \simeq 1.8 \times 10^{-3}$

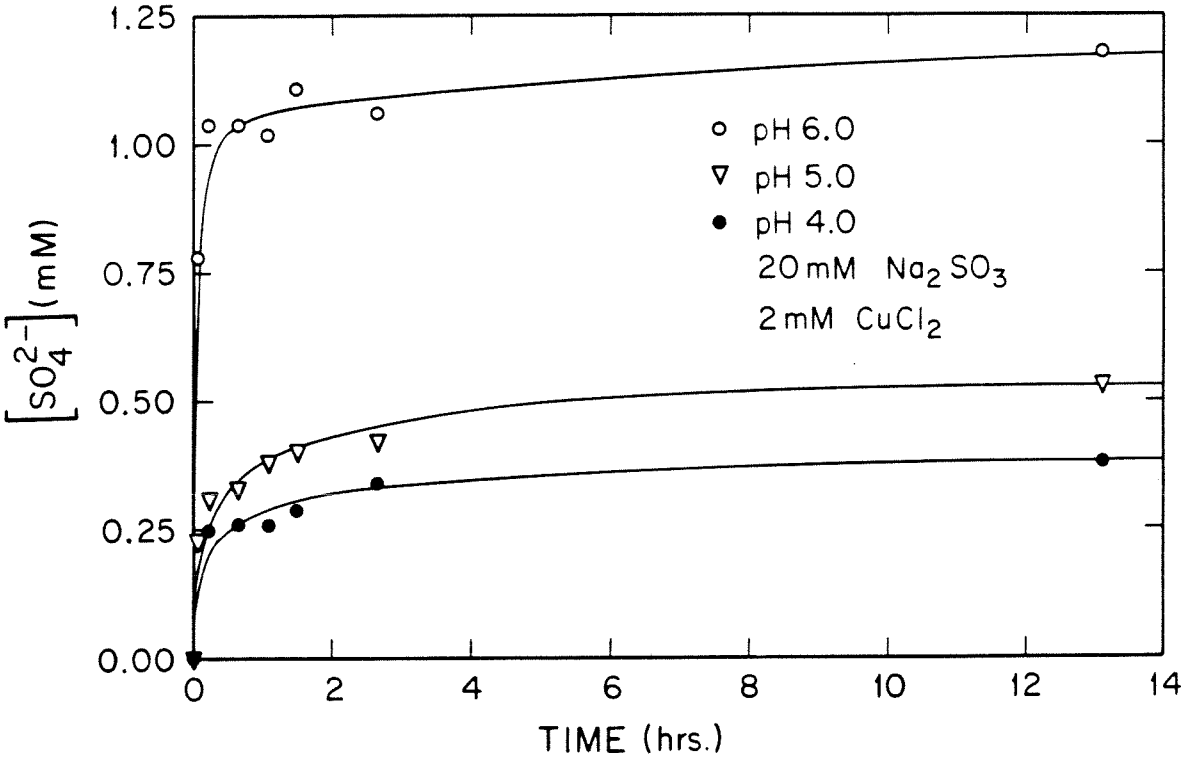

Fig. 3.10 Appearance of sulfate with time in the Cu(II)-S(IV) system at different values of pH.

TABLE 3.4

Definitions of the constants in Eqn. 3.29
at different experimental conditions

Constant				Comment
k_1	k_2	B_1	B_2	
k_5	k_7	A_1	A_3	$[Cu_2SO_3^{2+}] >> [Cu_2SO_3OH^+]$
k_6	k_8	A_2	A_4	$[Cu_2SO_3^{2+}] << [Cu_2SO_3OH^+]$
$f(k_5,k_6)$	$f(k_7,k_8)$	$f(A_1,A_2)$	$f(A_3,A_4)$	$[Cu_2SO_3^{2+}] \simeq [Cu_2SO_3OH^+]$

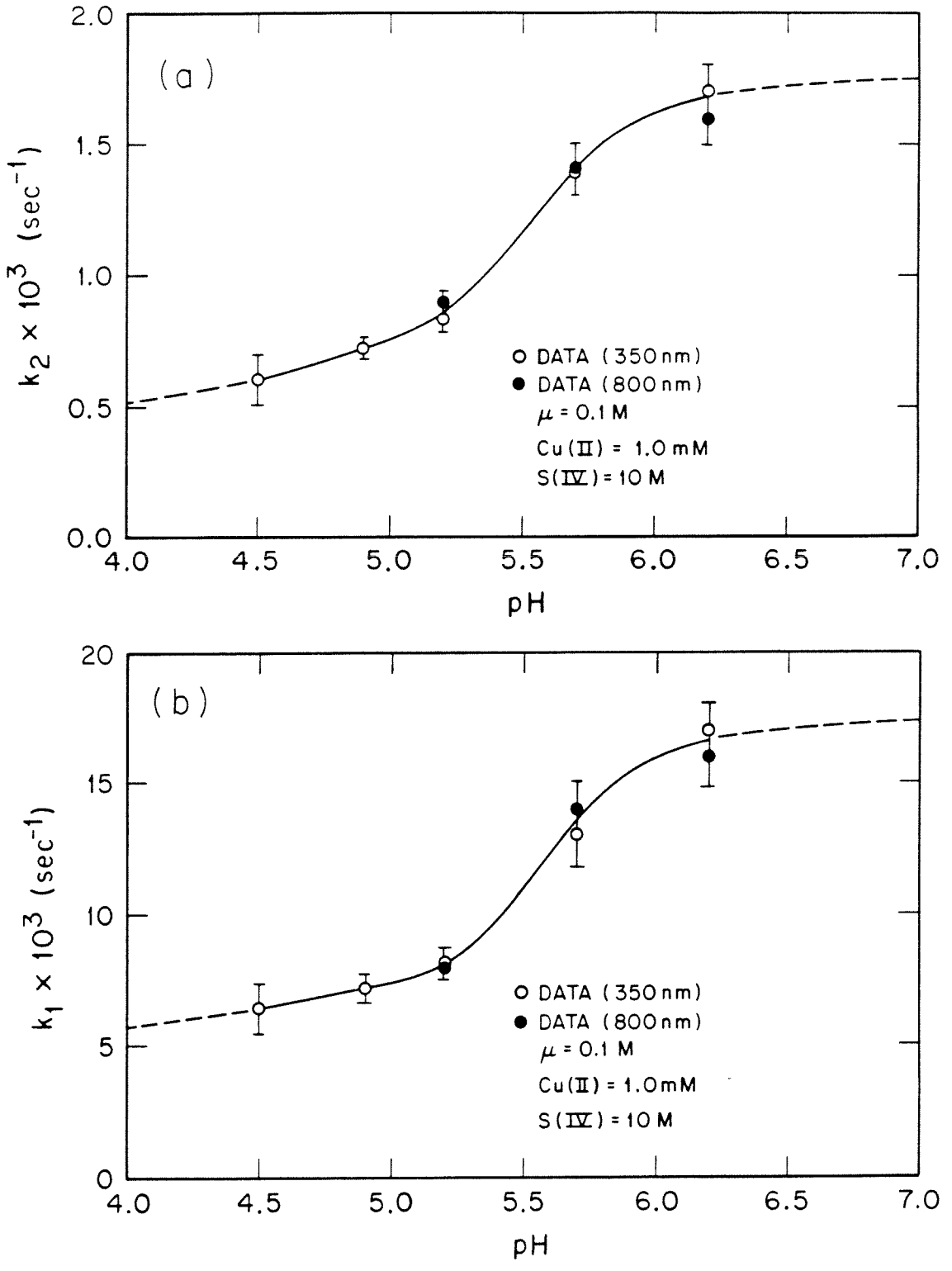

Fig. 3.11 The pH dependence of the rate constants (a) k_1 (sec^{-1}) and (b) k_2 (sec^{-1}) for data collected at 350 and 800 nm. The solid curve is a cubic-spline fit to the data.

sec^{-1}. The value for k_5 is close to the observed rate constant ([S(IV)] = 0.1 M) obtained by Zeck and Carlyle (1974) for pH 1.2, k_{obsd} = 3.6 x $10^{-3}sec^{-1}$. The pH range open to study could not be extended above 6.2 or below 3.5 because of the formation of precipitates and very low absorbances, respectively. The pH profiles show an inflection point at pH 5.5. The existence of an inflection point would indicate that there is a change in speciation over this pH range. If the proposed mechanism is correct, this implies that the pK_a defined in Eqn. 3.28 lies within this range. The pK_a of $Cu_2SO_3^{2+}$ would be considerably lower than the first hydrolysis constant of Cu^{2+} (pK_a = 8.12, μ = 0.1 M, Paulson and Kester (1980)), indicating that $Cu_2SO_3^{2+}$ is a stronger acid than hexaquo Cu(II). This would be the expected trend for a metal sulfito complex that has metal-S bonds. Sulfur is a good π-donor, contributing electron density to the metal center, which would enhance the back-donation from the metal to the oxygen in the hydroxide group. This back-donation would stabilize the Cu-O bond, making $Cu_2SO_3^{2+}$ a stronger acid than Cu^{2+}.

The rates determined for the $Cu(NO_3)_2$-S(IV) system were dependent on the background electrolyte in the system. The oxidizing potential of a metal can be changed if a complex is formed with the metal that preferentially stabilizes the reduced form of the metal. This thermodynamic effect has been observed in the Cu(II)/Cu(I) system in acetonitrile (Dushcek and Gutman, 1972). In this system, the reduced state of Cu(I) was stabilized by acetonitrile and the oxidation potental of Cu^{2+} was increased. If Cu(I)L complexes (L = Cl^-, NO_3^-,

SO_4^{2-}, ClO_4^-) obey a linear free energy relationship, i.e. the rate of formation of Cu(I)L increases with the stability of Cu(I)L, then the rate of Cu(II) reduction in the Cu(II)-S(IV) system would be expected to be greater in the system that more stable Cu(I)L complexes form.

The effects of a variation of the Cu(II) counter ion in the Cu(II)-S(IV) system are illustrated in Fig. 3.12. Both NO_3^- and ClO_4^- appear to have the same kinetic effect; neither anion has a particular affinity for Cu^{2+} or Cu^+. On the other hand, Cl^- substantially increases the reduction rate. Chloride forms highly stable complexes with Cu^+. In the presence of Cl^-, the formation of Cu(I) is thermodynamically more favorable. This effect was previously noted by Dorfman et al. (1977, 1978). They found the rate of oxidation of SO_2 gas by aqueous phase $Cu(II)X_2$, where X = Cl^-, Br^-, I^-, increased with the series $Br^- > I^- > Cl^-$. This is the same order in which the stability constants of $Cu(I)X_n^{n-1}$ increase. Dorfman et al. mentioned that the oxidation of S(IV) was slow in the presence of Cl^-, but in the pH range that they worked (pH < -0.3), the redox reaction is expected to be slow. Conversely, in this present study, sulfate ions were found to inhibit the reaction. Copper(II) forms a more stable complex with SO_4^{2-} than with the other anions investigated. Sulfate appeared to stabilize Cu(II) with respect to reduction.

DISCUSSION

The Cu(II)-S(IV) system was investigated as a model for the electron transfer reactions between S(IV) and other environmentally

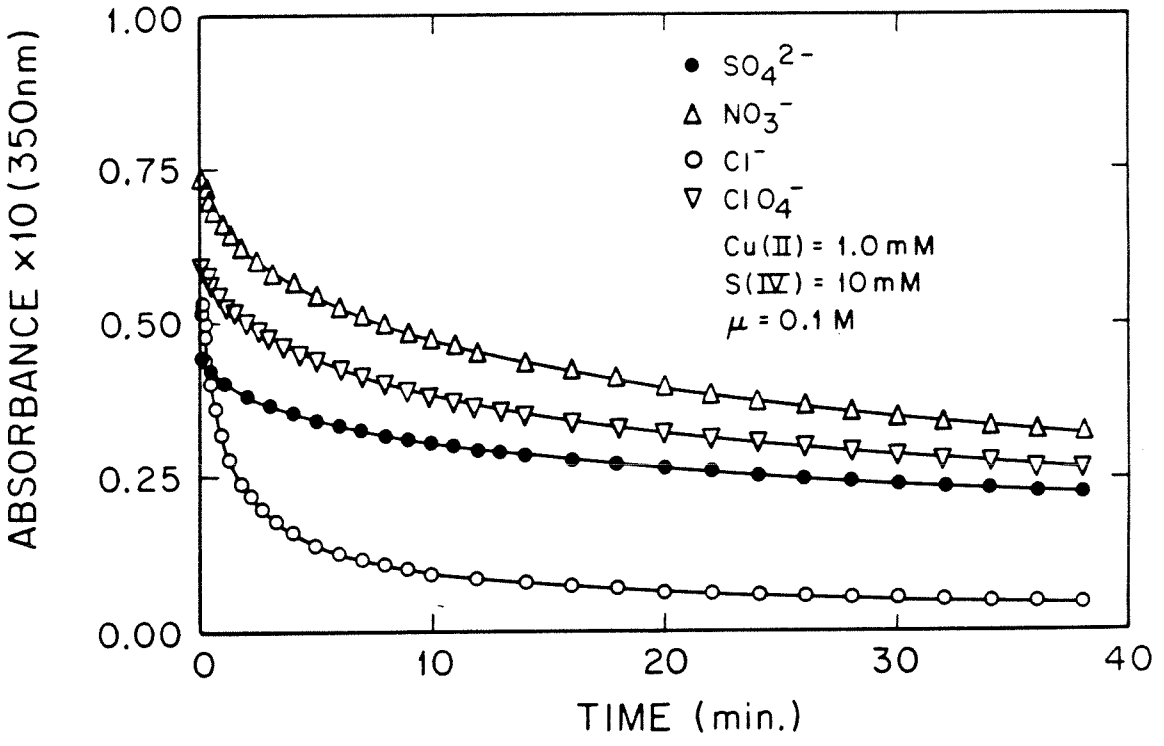

Fig. 3.12 Kinetic data collected at 350 nm for the Cu(II)-S(IV) system with different anions present in the system.

important trace metals, such as Fe(III). Both Cu(II) and Fe(III) form transient complexes with S(IV), that subsequently undergo internal redox reactions. The Cu(II) system is less complex to study than the Fe(III) system in the pH range of interest, $2 < pH < 6$. Over this pH range Fe(III) forms numerous hydrolysis products. Although there are differences between Fe(III) and Cu(II) as catalysts for the autoxidation of S(IV), the reaction of Cu(II) with S(IV) does give some insight into the importance of the electron transfer reaction as the first step in the metal-catalyzed autoxidation of S(IV).

The kinetic data and corresponding mechanism for the Cu(II)-S(IV) redox reaction suggests that the rate-determining step of this reaction is the inner-sphere electron transfer between S(IV) and Cu(II). A slow electron transfer in this case is not unrealistic. The d^9 electron configuration of Cu(II) has substantially different stereochemistry and coordination number than the d^{10} electron configuration of Cu(I). Copper(I) prefers a coordination state of four or less, whereas Cu(II) forms preferably penta or hexa coordinate complexes (James and Williams, 1961; Lewin et al. 1971; Hathaway, 1973).

Self-exchange electron-transfer rate constants and reduction potentials for Cu(II)/Cu(I) systems are given in Table 3.5 (Endicott et al., 1983). As noted in Table 3.5, the self-exchange rate constant for $Cu_{aq}^{2+,+}$ is relatively small at 10^{-5} $M^{-1}sec^{-1}$ (Hoselton et al., 1978). The slow Cu(II) + Cu(I) $\longrightarrow$ Cu(I) + Cu(II) self-exchange rate has been attributed to the reorganizational energies required to form a penta-coordinate transition state from the tetragonal ground state of $Cu(II)(OH_2)_6^{2+}$ to tetrahedral $Cu(I)(OH_2)_4^{+}$ (Endicott et al., 1983).

TABLE 3.5

Self-exchange rate constants and reduction potentials for some copper(II)-(I) couples

Couple	E° (volts)[a]	k[b] ($M^{-1}sec^{-1}$)
$Cu(aq)^{2+,+}$	0.15[c]	10^{-5}[d]
$Cu(byp)_2^{2+,+}$[g]	0.12[e]	160[f]
$Cu(phen)_2^{2+,+}$[h]	0.17[e]	68[f]
$Cu(5\text{-}NO_2phen)_2^{2+,+}$[i]	0.264[f]	93[f]
$Cu(2,9,Me_2phen)_2^{2+,+}$[j]	0.615[e]	2.0×10^{4}[f]

[a] Volts versus NHE

[b] 25°C, μ=0.1 M

[c] Latimer (1952)

[d] Hoselton et al. (1978)

[e] James and Williams (1961)

[f] Augustin and Yandell (1979)

[g] bpy = 2,2'-bipyridine

[h] phen = 1,10-phenanthroline

[i] 5-NO_2phen = 5-nitro-1,10-phenanthroline

[j] 2,9-Me_2phen = 2,9-dimethyl-1,10-phenanthroline

The reorganization energy barrier has been labelled as the "structural barrier". Yandell (1983) has suggested that the structural barrier energy is approximately 30 $kJmol^{-1}$ and that it is roughly independent of the nature of the ligands. The main "structural barrier" can be attributed to changes in solvation energy as Cu(II) is reduced to Cu(I). It is reasonable to assume that this "structural barrier" contributes substantially to the slow reduction of Cu^{2+} by S(IV).

Even though the reduction of Cu(II) by S(IV) occurs, albeit slowly, in this system, the Cu(II) was not completely reduced, even in the presence of excess S(IV). Reduction of HSO_3^- by Cu^{2+} is thermodynamically unfavorable if electron transfer is the only process considered. Energy released upon the formation of precipitates such as CuCl or $Cu^{II}SO_3Cu_2^{I}SO_3 \cdot 2H_2O$ are required to make the overall thermodynamics favorable. As the reaction system approaches equilibrium saturation with respect to solid phases the thermodynamics for electron transfer may become unfavorable. At this stage the reaction stops. The redox-active species appear to be dimeric Cu(II) species. As the concentration of Cu(II) is lowered, these species become less important.

The nature of the counter ion was found to influence the observed rate of electron transfer. Chloride enhanced the rate of reaction whereas SO_4^{2-} lowered the rate. Cheng et al. (1971) observed the reverse anion effect in the heterogeneous catalysis of SO_2 by aqueous $CuSO_4$ and $CuCl_2$ solutions (with O_2 present). Copper sulfate was

reported to be a more effective catalyst. Cheng et al. postulated that Cl^- stabilized Cu(I), which appeared to break the catalytic cycle.

The observed pH dependence of the rate constants and their relative magnitude is in general agreement with the work of Zeck and Carlyle (1974). However, our proposed mechanism is substantially different. The evidence obtained in this study indicated that other Cu(II)-S(IV) species in addition to $CuSO_3$ were important in the overall reaction. Zeck and Carlyle reported that Cu(I) retarded the reaction, although the rate did not vary systematically with [Cu(I)]. The conditions under which they performed these measurements were pH 0.013 with [Cu(I)] $\simeq$ [Cu(II)] and Cl^- as the counter ion. At equivalent concentrations at low pH, Cu(I) may inhibit the formation of $CuSO_3$ since the stability constant for $CuSO_3^-$ (log K = 7.85,, Smith and Martell, 1976) is larger than that for $CuSO_3$ (log K = 4.2, μ = 0.4 M, Chapter 2).

The relatively slow S(IV) to Cu(II) electron transfer rates makes this reaction an improbable initiation step for the Cu(II)-catalyzed chain reaction as proposed by Bäckström (1934). Likewise this electron transfer rate is inconsistent with the suggestion of Veprek-Siska and Lunak (1974) that oxygen reacts with intermediate cuprous sulfito complexes to form catalytically active Cu(I)-dioxygen complexes, $[O_2Cu(SO_3)_n]^{-2n+1}$. In the latter case, Cu(II) must be reduced before the dioxygen complex could be formed. This behavior may explain the apparent induction period that is seen in many metal-catalyzed reactions. Instead, a more likely pathway is the one proposed by Hoffmann and Hong (1985) for the sulfito cobalt(II)tetra-

sulfophthalocyanine (Co(II)TSP) complex. Using electron paramagnetic resonance (EPR) spectra, they showed that the formation of a Co(II)TSP-SO_3^{2-} complex was a necessary step before the formation of a Co(III)TSP-SO_3^{2-}-O_2^- ion, which was found to be the reactive catalytic species. A similar intermediate may be the reactive species in the Cu(II)-S(IV) system in the presence of oxygen:

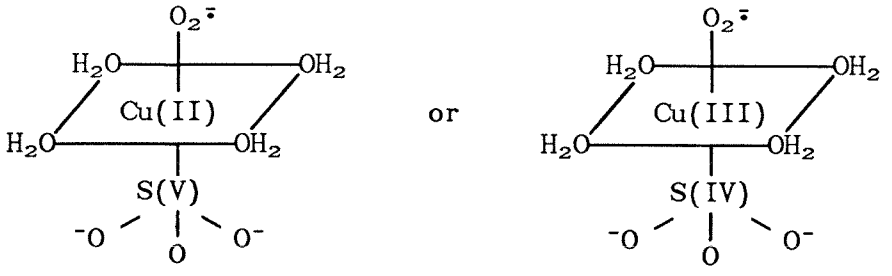

REFERENCES

Aasa, R. and T. Vanngard, 1975, *J. Mag. Res.*, **19**, 308-315.

Albu, H.W. and H.D. Graf von Schweinitz, 1937, *Ber. Deutsch. Chem. Ges.*, **B65**, 729-737.

Augustin, M.A. and J.A. Yandell, 1979, *Inorg. Chem.*, **18**, 577-583.

Bäckström, H. L. J., 1934, Z. *Phys. Chem. (Leipzig)*, **25B**, 122-138.

Barron, C.H. and H.A. O'Hern, 1966, *Chem. Eng. Sci.*, **21**, 397-404.

Basolo, F. and R. Pearson, *Mechanisms of Inorganic Reactions: A Study of Metal Complexes in Solution* (Wiley & Sons, New York, 1967) pp. 81-82.

Baubigny, M.H., 1912, *Comptes Rend.*, **154**, 701-703.

Blair, D. and H. Diehl, 1961, *Talanta*, **7**, 163-174.

Brubaker, G.R.,J.N. Brown, M.K. Yoo, R.A. Kinsey, T.M. Kutchan, and E.A. Mottel, 1970, *Inorg. Chem.*, **18**, 299-302.

Cheng, R.T., M. Corn and J.O. Frohliger, 1971, *Atmos. Environ.*, **5**, 987-1008.

Cotton, F.A. and G. Wilkinson, *Advanced Inorganic Chemistry* (Wiley & Sons, New York, 1980) pp. 811-814.

Dorfman, Ya. A., Z.I. Rogoza and L.V. Kashmikova, 1977, *Zhr. Prikl. Khim.*, **50**, 1709-1714.

Dorfman, Ya. A., Z.I. Rogoza and L.V. Kashmikova, 1978, *Zhr. Prikl. Khim.*, **51**, 1457-1461.

Dushcek, O., and V. Gutmann, 1972, *Z. Anorg. Allg. Chem.*, **394**, 243-253.

Endicott, J.F. K. Kumar, T. Kamasami, and F.P. Rotzinger in *Progress in Inorganic Chemistry Vol.* 30, S.J. Lippard, ed. (Wiley & Sons, New York, 1983) pp. 141-187.

Foffani, A. and M. Menegus-Scarpa, 1953, *Gazz.*, **83**, 1068-1081.

Fuller, E.C. and R.H. Crist, 1941, *J. Am. Chem. Soc.*, **63**, 1644-1650.

Hammock, E.W. and E.H. Swift, 1949, *Anal. Chem.*, **21**, 975-979.

Hathaway, B.J., 1973, *Structure Bonding (Berlin)*, **14**, 49-67.

Heller, H.G. and J.R. Langan, 1981, *J.C.S. Perkin II*, 341-343.

Hoffmann, M.R. and D.J. Jacob in *Acid Rain Precipitation Series Vol.* 3, J.G. Calvert, ed. (Butterworth Publishers, Boston, 1984) p. 109.

Hoffmann, M.R. and A.P. Hong in *Proceedings of the Second Workshop on Environmental and Inorganic Chemistry*, Portugal (April 1985).

Hoselton, M.A., C.-T. Lin, H.A. Schwartz, and N. Sutin, 1978, *J. Am. Chem. Soc.*, **100**, 2383-2388.

Huie, R.E. and P. Neta, 1984, *J. Phys. Chem.*, **88**, 5665-5669.

Hunt, J.P. and H.L. Friedman in *Progress in Inorganic Chemistry Vol.* 30, S.J. Lippard, ed. (Wiley & Sons, New York, 1983) pp. 359-382.

Imamura, T., M. Ryan, G. Gordon, D. Coucouvanis, 1984, *J. Am. Chem. Soc.*, **106**, 984-990.

James, B.R., and R.J.P. Williams, 1961, *J. Chem. Soc.*, 2007-2019.

Keller, P.N. and H.D. Wycoff in *Inorganic Synthesis Vol. II*, W.C. Fernedius, L.F. Audrieth, J.C. Bartar, H.S. Booth, W.C. Johnson, R.E. Kirk and W.C. Schumb, eds. (McGraw-Hill Book Co., New York, 1946) pp. 1-4.

Kierkegaard, P. and B. Nyberg, 1965, *Act. Chem. Scand.*, **19**, 2189-2199.

Kotzias, D., H. Parlar and F. Korte, 1982, *Naturwissenschafter*, **69**, 444-445.

Langford, C.H. and H.B. Gray, *Ligand Substitution Processes* (W.A. Benjamin, Inc., Reading, Mass., 1966).

Latimer, W., *Oxidation Potentials* (Prentice Hall, Englewood Cliffs, N.J., 1952).

Lewin, A.H., R.J. Michl, P. Ganis, U. Lepore and G. Avitabile, 1971, *J. Chem. Soc. Chem. Comm.*, 1400-1401.

Lunak, S., A.M. El-Wakil and J. Veprek-Siska, 1978, *Coll. Czech. Chem. Comm.*, **43**, 3306-3316.

Marquadt, D., 1963, *J. SIAM*, **11**, 431-444.

Mistra, G.C. and R.D. Srivastava, 1976, *Chem. Eng. Sci.*, **31**, 969-971.

Nair, V.R. and G.G.R. Nair, 1971, *Talanta*, **18**, 432-435.

Paulson, A.J. and D.R. Kester, 1980, *J. of Sol. Chem.*, **9**, 269-277.

Ramberg, L., 1910, *Z. Phys. Chem.*, **69**, 512-522.

Reindeers, W. and S.I. Vles, 1925, *Rec. Trav. Chim.*, **44**, 249-268.

Smith, R.M. and A.E. Martell, *Critical Stability Constants, Vol 4: Inorganic Ligands* (Plenum Press, New York, 1976).

Veprek-Siska, J. and S. Lunak, 1974, *Z. Naturforsch.*, **29B**, 689-690.

Yandell, J.K. in *Copper Coordination Chemistry: Biochemical and Inorganic Perspectives*, K.D. Karlin and J. Zubieta, eds. (Adenine Press, New York, 1983), pp. 157-166.

Zeck, O.F. and D.W. Carlyle, 1974, *Inorg. Chem.*, **13**, 34-38.

CHAPTER FOUR

THERMODYNAMICS AND KINETICS OF TRANSIENT Fe(III)-S(IV) COMPLEXES

ABSTRACT

A conditional stability constant for the formation of a Fe(III)-S(IV) complex at μ = 0.4 M and pH 2.1 was determined spectroscopically. Raman measurements indicate that sulfite binds to the metal through oxygen. The mechanism for the internal redox reaction between Fe(III) and S(IV) is discussed. Various pathways for the formation of the Fe(III)-S(IV) species are examined to determine the most probable equilibrium species. Results are interpreted by comparing the formation of Fe(III)-S(IV) species with other Fe(III) complexes. The formation of a discrete Fe(III)-S(IV) complex as a prelude to the Fe(III)-catalyzed autoxidation of S(IV) is discussed.

INTRODUCTION

The initial behavior of the Fe(III)-S(IV) system appeared to parallel the behavior of the Cu(II)-S(IV) system. When a pale yellow Fe(III) solution was mixed with a colorless S(IV) solution, the resultant solution darkened immediately to reddish-brown. The initial color faded quickly (within a few minutes) to a much lighter colored solution. The initial color change was indicative of the formation of a Fe(III)-S(IV) complex. UV/Vis absorbance spectra of this complex are shown in Fig. 4.1 for two S(IV):Fe(III) ratios. The absorbance of these complexes appears as a very broad shoulder between 350 nm and 600

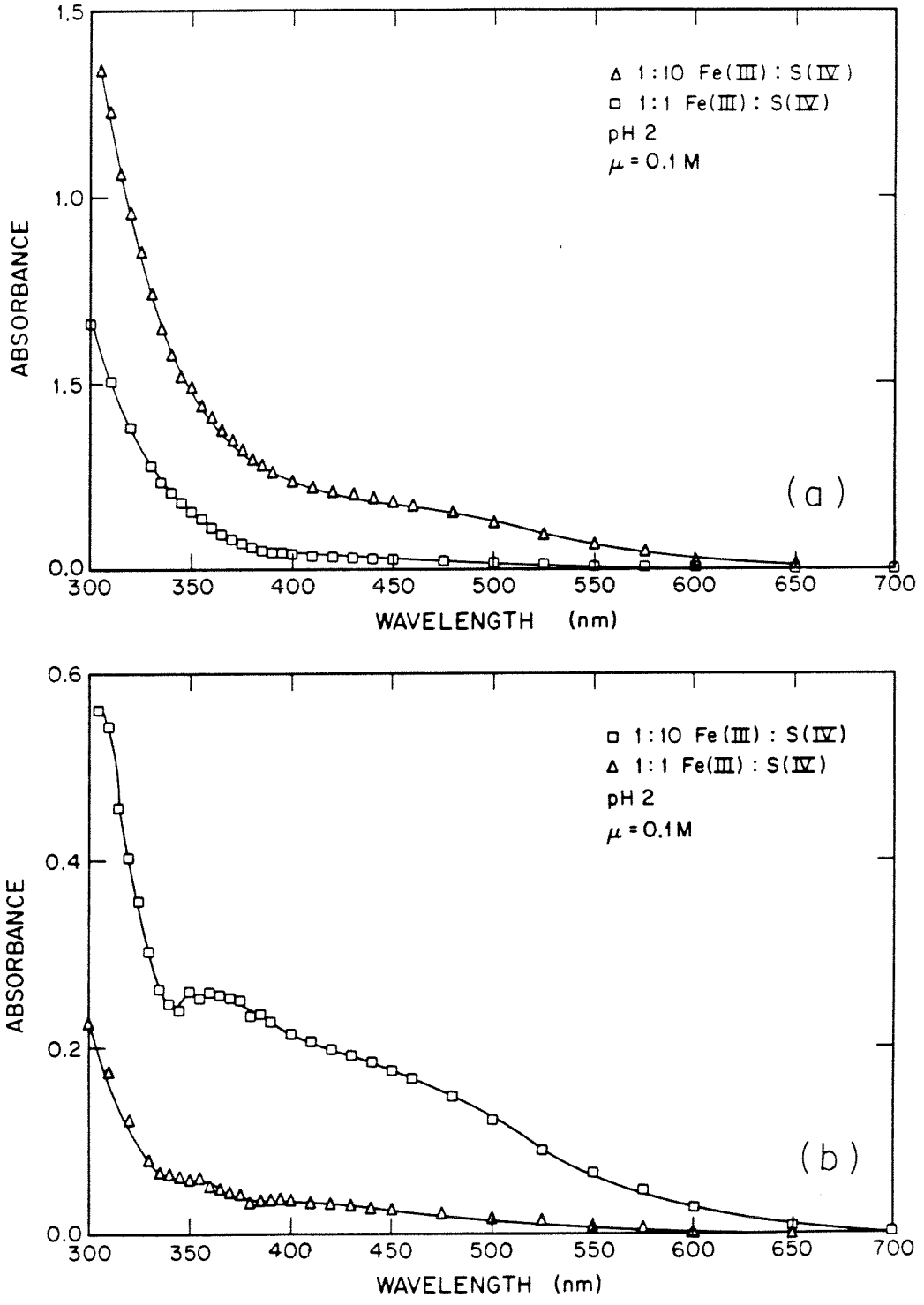

Fig. 4.1 Absorbance spectra of the Fe(III)-S(IV) complex at two Fe(III)-S(IV) ratios (a) absorbance spectra of whole system and (b) difference spectra of the complex (absorbance due to uncomplexed Fe(III) subtracted). ($[Fe(III)]_o$ = 0.5 mM).

nm. These complexes are unstable and undergo a series of redox reactions that result in an aqueous mixture of Fe^{2+}, $S_2O_6^{2-}$ and SO_4^{2-}. The Fe(III)-S(IV) system is more complicated than the Cu(II)-S(IV) system due to the larger number of different Fe(III) species. A significant feature of Fe(III) chemistry in aqueous solutions is the tendency to hydrolyze and to polymerize (Cotton and Wilkinson, 1980). Some important stability constants (μ = 1.0 M) for the Fe(III)-OH^- system are as follows (Stumm and Morgan, 1981).

	Log $^*K$
$Fe(H_2O)_6^{3+} \rightleftharpoons Fe(H_2O)OH^{2+} + H^+$	-3.05
$Fe(H_2O)_6^{3+} \rightleftharpoons Fe(H_2O)(OH)_2^{+} + 2H^+$	-6.31
$2Fe(H_2O)_6^{3+} \rightleftharpoons Fe_2(H_2O)_8(OH)_2^{4+} + 2H^+$	-2.91

The importance of these species can be seen in Fig. 4.2 where speciation is presented as a function of pH for two different iron concentrations (Stumm and Morgan, 1981). The distribution of iron species is a necessary consideration in any kinetic and equilibrium study of the Fe(III)-S(IV) system.

The reduction of Fe(III) by S(IV) at pH 2 is thermodynamically unfavorable.

$e + Fe^{3+} \rightleftharpoons Fe^{2+}$	0.77 V	(Latimer, 1952)
$HSO_3^- \rightleftharpoons H^+ + e + SO_3^{2-}$	-0.84 V	(Huie and Neta, 1984)
$Fe^{3+} + HSO_3^- \rightleftharpoons Fe^{2+} + H^+ + SO_3^-$	-0.07 V	

This reaction becomes less favorable if the ΔG° for formation of $FeSO_3^+$ is included in the calculation. The calculated negative energy change for this reaction implies that either other forms of these species, such as SO_3^{2-} (which is a more powerful reductant than HSO_3^-) or $FeOH^{2+}$

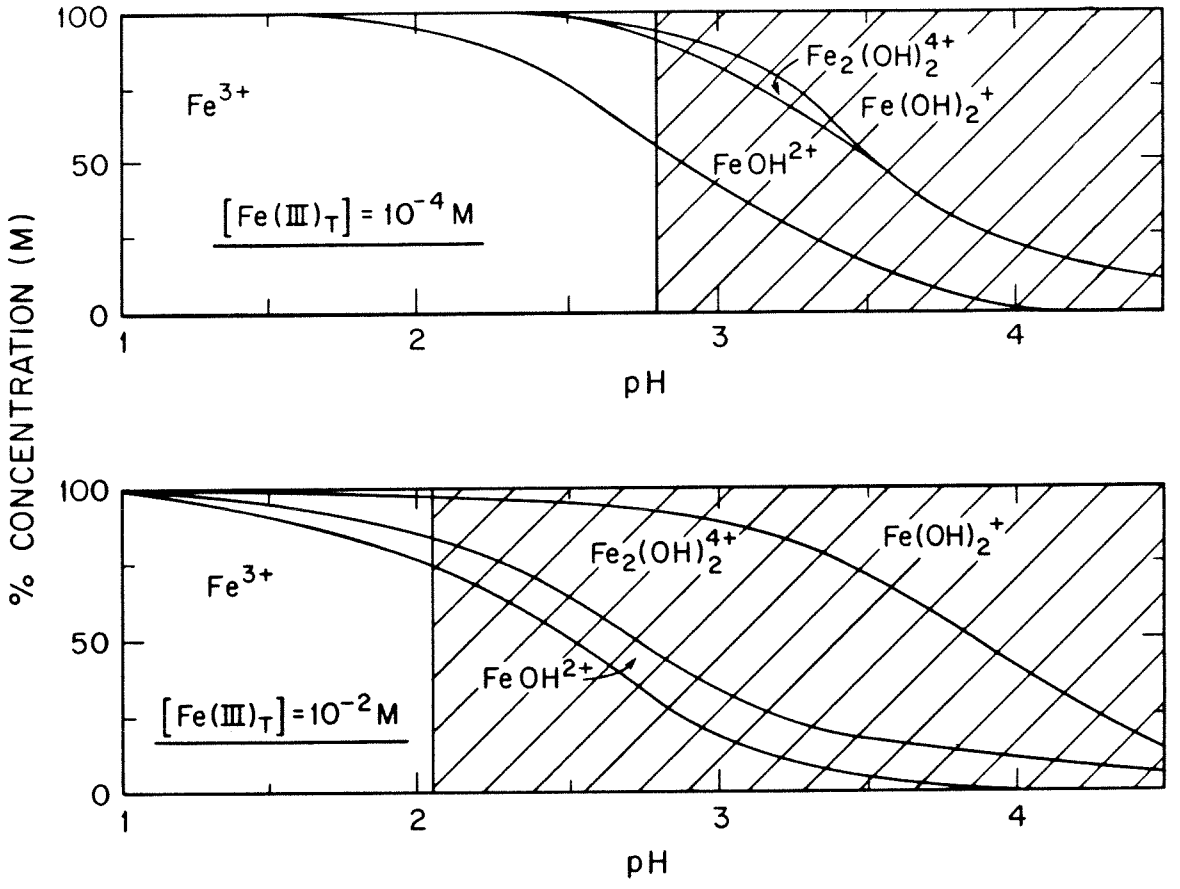

Fig. 4.2 Distribution of Fe(III) species as a function of pH for two different iron concentrations. Shaded area represents saturated solutions (Stumm and Morgan, 1981)

(which is a stronger oxidant than Fe^{3+}), are involved in this reaction or that other energetic changes occur in the system which make the overall reaction favorable. These processes include the stabilization of the products, changes in the Fe(III) reduction potential due to changes in its coordination sphere, and energy released by precipitation.

Gélis (1862) investigated the formation of a red solution when SO_2 was passed into a suspension of ferric hydroxide. His findings confirmed that the red complex decomposed yielding Fe(II) and dithionate. He suggested that the complex was $H_3[Fe(SO_3)_3]$. Gélis' work was repeated by Carpenter (1902) who noted that dithionate was produced in the presence of ferric hydroxide and that sulfate was produced in the presence of ferric chloride. Danilczuk and Swinarski (1961) suggested that $Fe(SO_3)_3^{6-}$ is the most stable Fe(III)-S(IV) species over the pH range 2 to 3 based on photometric titration data collected at 458 nm. However, their work was performed over the concentration range 0.04 to 0.06 M [Fe(III)], for which there is considerable hydrolysis of the ferric ion. Thus, formation of ferric hydroxides and ferric-hydroxy-sulfito complexes may have contributed to the observed absorbance changes.

Investigations of the stoichiometry of the Fe(III)-S(IV) system has shown that the yield of dithionate varied with pH and the nature of the anions present in solution (Albu and Schweinitz, 1932, Bassett and Parker, 1951). Dasgupta et al. (1979) found dithionate was the oxidation product in a perchlorate media, and that increasing amounts of sulfate were produced as the chloride concentration was increased.

The rate of oxidation was also observed to increase as the concentration of Cl^- was increased. The addition of Cu(II) to the system has been found to accelerate the reaction and reduce the production of dithionate (Kuz'minykh and Bomshtein, 1953).

Pollard et al. (1961) have studied the products of the reduction of Fe(III) by S(IV) chromatographically. To obtain measurable quantities of products, high concentrations of reactants were used ($0.04\ M < [Fe(III)]_o < 0.1\ M$, $0.02\ M < [S(IV)]_o < 0.09\ M$ at pH 0.3). However their observations were consistent with those of previous; they found $S_2O_6^{2-}$ to be the principle oxidation product. The presence of Cu(II) in the Fe(III)-S(IV) system resulted in a greater yield of SO_4^{2-}.

Karraker (1963) studied the kinetics of the reduction of Fe(III) by S(IV). To minimize the formation of $S_2O_6^{2-}$, experimental conditions were chosen such that Fe(III) was maintained in 10-40 fold excess. Half-lives of 3 to 14 min for these conditions were reported. The following rate law was suggested:

$$\frac{-d[H_2SO_3]}{dt} = k_1\frac{[Fe^{3+}][H_2SO_3]}{[H^+]} - k_2[Fe^{2+}][HSO_3]. \qquad (4.1)$$

Molecular oxygen was found to enhance the reaction rate, whereas, Fe(II) was found to inhibit the reaction.

Perhaps the most extensive work on kinetics of the reaction of Fe(III) with S(IV) was carried out by Carlyle (1971). Unlike previous workers, Carlyle (1971) and Zeck and Carlyle (1973) examined the rates

of formation and reduction of $FeSO_3^+$. Initial work was done on the rate of aquation of the Fe(III)-S(IV) complex (Carlyle, 1971). Carlyle claimed to study the rate of loss of a coordinated S(IV) group using pH-jump techniques. His rate expression for the rate of aquation (or loss of coordinated S(IV)) was given as

$$\frac{-d[FeSO_3^+]}{dt} = k'[FeSO_3^+] \qquad (4.2)$$

where $k' = k_1 + k_2[H^+] + k_3[HSO_3^-]$.

Kinetic measurements made spectroscopically over the wavelength range of 355 to 470 nm. Observed rate constants ranged from 0.45 to 22.2 sec^{-1}; a curvefitting routine was used to fit the k_1, k_2 and k_3 to the data. Carlyle (1971) estimated an upper bound of 0.4 M for the stability quotient Q_1 ($Q_1 = ([FeSO_3^+][H^+])/([Fe^{3+}][HSO_3^-])$). Using the law of microscopic reversibility, Carlyle determined the rate of formation of the complex using Q_1 and observed rates of aquation. The calculated rate of formation for the reaction $FeOH^{2+} + HSO_3^- \longrightarrow FeSO_3^+$ is $\simeq 270\ M^{-1}sec^{-1}$, which is two to three orders of magnitude lower than typical ligand exchange rates for penta-aquo hydroxy-Fe(III) (see Table 4.1). Carlyle suggested that the $FeSO_3^+$ species contained S-metal bonding, which would explain this discrepancy with measured $FeOH^{2+}$ ligand exchange rates. None of the hydrolysis products of iron were taken into account in Carlyle's interpretation of his observed rate constants.

TABLE 4.1

Rate constants for the formation of mono-complexes of Fe(III) (25 °C)

Ligand (L)	k ($M^{-1}sec^{-1}$) $Fe^{3+} + L$	k ($M^{-1}sec^{-1}$) $FeOH^{2+} + L$
Br^-[a]	20	2.6×10^4
Cl^-[b]	9.4	1.1×10^4
SCN^-[c]	1.27×10^2	1.0×10^4
SO_4^{2-}	(6.37×10^3)[d]	$\simeq 2.4 \times 10^5$[e]
HSO_4^-		$\simeq 2.4 \times 10^4$[e], 1.45×10^5[f]
F^-	(5.0×10^3)[d]	3.2×10^3[g]
HF[g]	11	
N_3^-	(1.6×10^5)[d]	$3 \times 10^3 < k < 4 \times 10^4$[h]
HN_3	4[i]	6.8×10^3[i], 7.4×10^3[h]
H_2O[j]	2.9	7.9×10^4

[a] At 22 ± 2 °C, Connick and Coppel (1959)
[b] Mattheis and Wendt (1961)
[c] Below et al. (1958)
[d] Calculated, Sutin and Seewald (1963)
[e] Wendt and Strelhow (1962)
[f] Davis and Smith (1962)
[g] Pouli and Smith (1960)
[h] Accascina et al. (1967)
[i] Seewald and Sutin (1963)
[j] Rate of water exchange in second-order units, Hunt and Friedman (1983)

Carlyle and Zeck (1973) examined the electron transfer reaction between S(IV) and Fe(III). They found that the rate of disappearance of the colored complex adequately fit a nominal second-order rate law as follws:

$$\frac{-d[Fe(III)]}{dt} = k'[Fe(III)]^2 \qquad (4.3)$$

where $$k' = \frac{a[HSO_3^-]}{[Fe(II)][H^+]} + \frac{b[HSO_3^-]^2/[H^+]^2}{c + [SO_2]}$$

a,b,c are empirically fitted rate constants.

Eqn. 4.3 was found to fit kinetic measurements when [S(IV)] was held in excess. Observed second-order rate constants, that were measured with Fe(III) in excess, were an order of magnitude larger than calculated rate constants. Additional kinetic studies were made with Cu(II) added to the system, with [Cu(II)] at approximately the same concentration as [Fe(III)]. The absorbance was monitored over the wavelength range of 320 to 443 nm. However, since Cu(II)-S(IV) and $FeOH^{2+}$ species absorb in this range, as well as the Fe(III)-S(IV) species, the observed rate of decrease of absorbance over this range may have been wavelength dependent.

The magnitude of an equilibrium constant for the $FeSO_3^+$ complex ($K_1 = [FeSO_3^+]/[SO_3^{2-}][Fe^{3+}]$) has been a matter of some debate. As mentioned above, Carlyle (1971) estimated that the equilibrium quotient, Q_1, had an upper limit of 0.4. Other research groups have attempted to determine the value of K_1. However, uncertainties about experimental technique and lack of consideration of ferric ion

hydrolysis products cast doubt on the validity of this work. Kao (1979), determined log K_1 = 7.1, but ferric hydrolysis products were not included in his calculations and there were possible SO_2 losses during his experiment due to gas transfer. Hansen et al. (1976) determined a stability constant, log K = 9.7, for $([FeSO_3^+][H^+]^2)/([Fe^{3+}][SO_2 \cdot H_2O])$ using calorimetry. This is substantially higher than other estimates; they may have ignored the heat changes due to electron transfer in their data interpretaton.

Sulfur-bonded metal sulfite complexes tend to have larger stability constants than equivalent O-bonded species (see Table 2.1 in which the stability constants for metal-sulfite and metal-sulfate complexes are compared). Based on his investigation on the rate of aquation of $FeSO_3^+$, Carlyle (1971) postulated that there would be metal-sulfur bonds in Fe(III)-S(IV) complexes. Van Eldik (1980) has suggested that metal-O bonded sulfito species of Cr(III) and Rh(III) isomerize to give a metal-S bonded species. He suggested a similar mechanism for labile metal sulfito complexes, such as $FeSO_3^+$ (van Eldik, 1985).

The objectives of this study were to obtain an equilibrium constant for the formation of the Fe(III)-S(IV) complex and to determine the nature of the Fe(III)-S(IV) bonding (e.g. either Fe-S or Fe-O) that dominants in this complex. Kinetic measurements of the rate of electron transfer were made.

EXPERIMENTAL

Reagents and Materials

All reagents were analytical grade. Sodium sulfite (Mallinckrodt) solutions were prepared gravimetrically. Fresh solutions were prepared and stored inside a N_2-atmosphere glovebox (Vacuum Atmospheres Dri-Lab HE-43-2 with HE-493 Dri-Train) for each experiment. The pH of the sulfite solutions was found to decrease only slightly with time ($\Delta[H^+] = 4 \pm 2\times10^{-11}$) for a 0.1 M Na_2SO_3 solution during a two week period. Iron solutions were made from different salts ($Fe(ClO_4)_3$ (G. Frederick Smith) and $FeCl_3 \cdot 6H_2O$ (J. T. Baker Chemical Co.)). The procedure of Tamura et al.(1974) was employed to measure Fe(III) concentrations of the solutions used in the equilibrium studies. Hydroxylamine sulfate was used to reduce Fe(III) to Fe(II) in the analysis. Sulfite solutions were acidified to the desired pH using the corresponding acid of the Fe(III) counterion before they were mixed with the iron solutions. Ionic strength, μ (M), was fixed using filtered $NaClO_4$ solutions (G. Frederick Smith Co.). High-purity water (18 MΩ-cm) was obtained from a Millipore Milli-Q system.

Oxygen-free Techniques

All the kinetic experiments were conducted in an anoxic environment. Dissolved oxygen was removed from solutions using a Schlenk line. In this procedure, a vacuum was drawn above the solution; the solution was then purged with N_2. This vacuum-stripping cycle was repeated three times for each solution. Trace levels of oxygen were scrubbed from the high-purity N_2 by reaction with a packed

column of MnO absorbed on vermiculite. Deoxygenated solutions were placed in a glovebox (Vacuum Atmospheres Dri-Lab HE-43-2 with HE-493 Dri-Train). Oxygen leakage through the gloves was controlled by passing the N_2-atmosphere continuously through a Cu(I) catalyst bed. Measurements that were performed outside the glovebox were made in sealed containers.

Spectrophotometric Studies

The kinetics of the electron transfer reaction between Fe(III) and S(IV) were determined by following the disappearance of the charge-transfer absorption band (350 nm) using a Hewlett-Packard dual beam diode array spectrophotometer (HP 8450A). Absorbance readings were taken in 1 cm quartz cells at at 21.0 $\pm$ 0.4 $^{\circ}$C.

A Dionex Stopped-Flow spectrophotometer (D-100) was used to obtain UV/Visible absorbance spectra of short-lived species. To plot the full spectrum of the Fe(III)-S(IV) complex, the absorbance at t = 10 msec was measured at different wavelengths. The monochromator for the Dionex does not respond linearly with wavelength (probably due to stray light effects). Absorbance readings at different wavelengths were calibrated using the absorbance of K_2CrO_4 solutions of known concentrations (Rao, 1967). Data were collected at 450 and 350 nm at 25°C in a 2 cm Kel-F cell for the equilibrium studies. Variable Fe(III):S(IV) ratios were examined at μ = 0.4 M and pH 2.1. Each data point represented at least three repeatable absorbance readings.

Raman spectra were collected at room temperature on a SPEX model 1402 double-monochromator Raman spectrometer. Spectra were recorded

using the 488 nm line of a Spectra-Physics Model 170 argon ion laser. The laser power incident upon the sample was $\simeq$ 400 mW; a 10 nm interference filter was used to remove stray light, and the spectral resolution was 0.25 cm^{-1}. The frequency was calibrated using known frequencies for carbon tetrachloride and sodium sulfate. Aqueous samples were introduced in a flow-apparatus. Separate solutions of $FeCl_3$ and S(IV) were fed into a junction where they were mixed approximately 30 seconds before they entered the sampling capillary. Ferric chloride was used in the Raman studies since Cl^- does not have a Raman signal (unlike ClO_4^-). All the spectra were represented as a summation of repetitive scans. These spectra were smoothed by a four-point averaging technique.

Electron paramagnetic resonance (EPR) spectra were recorded on a Varian E-Line Century Series spectrometer. Spectra were taken on quick-frozen anoxic solutions at 11 ^{o}K in 5 mm quartz tubes.

RESULTS

Determination of Equilibrium Constant

Equilibrium studies on the Fe(III)-S(IV) system were performed with a Dionex Stopped-Flow spectrophotometer using the same method as that was used for the Cu(II)-S(IV) system (Chapter 2). An equilibrium constant was calculated based on changes in the absorbance at two wavelengths, 350 nm and 450 nm, of the broad shoulder where the complexes absorb (see Fig. 4.1). Two wavelengths were used in this study to see if the absorbance varied with [S(IV)] consistently at both wavelengths. If different behavior had been observed at the two

wavelengths, then more than one species would have been contributing to the absorbance. Formation of a $Fe(SO_3)_n^{3-2n}$ complex could occur by a number of pathways, as follows:

$$Fe^{3+} + nSO_3^{2-} \overset{K_1}{\rightleftharpoons} Fe(SO_3)_n^{3-2n} \quad (4.4)$$

$$Fe^{3+} + nHSO_3^{-} \overset{K_2}{\rightleftharpoons} Fe(SO_3)_n^{3-2n} + nH^{+} \quad (4.5)$$

$$FeOH^{2+} + nHSO_3^{-} \overset{K_3}{\rightleftharpoons} FeOH(SO_3)_n^{3-2n} + nH^{+} \quad (4.6)$$

$$FeOH^{2+} + nSO_3^{2-} \overset{K_4}{\rightleftharpoons} FeOH(SO_3)_n^{3-2n} \quad (4.7)$$

$$Fe(SO_3)_n^{3-2n} + H_2O \rightleftharpoons FeOH(SO_3)_n^{3-2n} + H^{+}. \quad (4.8)$$

where n = 1,2,3... When the total iron concentration is held constant and Beer's Law holds for the system, the method of Newton and Arcand (1953) can be used to relate absorbance changes with increasing S(IV):Fe(III) ratios to an equilibrium constant (similar to the calculation for the Cu(II)-S(IV) system, Chapter 3).

$$A = -K^{-1}\frac{(A - A_0)}{[S(IV)]^n} + A_\infty \quad (4.9)$$

where

A = absorbance;

$K = \dfrac{[Fe(III)\text{-}S(IV)_n]}{[Fe(III)][S(IV)]^n}$;

A_∞ = absorbance of complex, if all the iron was complexed;

In order to determine the meaning of the experimentally obtained stability constant, the S(IV) and the Fe(III) speciation needs to be

considered. Bisulfite and SO_3^{2-} concentrations are related to [S(IV)] by the following relationships (Stumm and Morgan, 1981):

$$HSO_3^- = \alpha_1[S(IV)]$$

and (4.10)

$$SO_3^{2-} = \alpha_2[S(IV)]$$

where

$$\alpha_1 = \frac{1}{[H^+]/K_{a_1} + 1 + K_{a_2}/[H^+]};$$

$$\alpha_2 = \frac{1}{[H^+]^2/K_{a_1}K_{a_2} + [H^+]/K_{a_2} + 1};$$

K_{a_1} and K_{a_2} are the first and second acid dissociation constants of $SO_2 \cdot H_2O$. Since the pH was held constant in this experiment, α_1 and α_2 were constants.

The only assumption about the iron speciation is that the absorbance at the measured wavelength was due to the "uncomplexed" and "complexed" iron, no assumption was made about the speciation of the "uncomplexed" iron. Under the conditions of this investigation, the "uncomplexed" iron would consist of two species, Fe^{3+} and $FeOH^{2+}$; the presence of $Fe(OH)_2^+$ and $Fe(OH)_2Fe^{4+}$ can be neglected. The concentration of Fe^{3+} and $FeOH^{2+}$ can be related to Fe(III) by the first hydrolysis constant, K_b, of iron and a mass balance on iron (Stumm and Morgan, 1981):

$$[Fe^{3+}] = \beta_o[Fe(III)]$$

and (4.11)

$$[FeOH^{2+}] = \beta_1[Fe(III)]$$

where $$\beta_o = \left[1 + \frac{K_b}{[H^+]}\right]^{-1};$$

$$\beta_1 = \beta_o \frac{K_b}{[H^+]};$$

$$^*K_b = \frac{[FeOH^{2+}][H^+]}{[Fe^{3+}]}.$$

Since pH was constant in this experiment, β_o and β_1 were constants.

Fig. 4.3 shows the data collected at different [S(IV)] at the two wavelengths. In Fig. 4.4 the data are plotted using Eqn. 4.9. The linearity of the plots in Fig. 4.4 showed that n = 1. Eqn. 4.9 was found to be valid at [S(IV]:[Fe(III)] ratios above 6:1. Below that ratio, instrument noise and errors in calculating free [S(IV)] led to deviations from linearity.

The values for K which have been determined are K = 76.4 ± 8.7 M^{-1} (450 nm) and K = 57.2 ± 1.7 M^{-1} (350 nm). The best estimate that can be given here is K = 66.8 ± 10.4 M^{-1} at μ = 0.4 M (the average of the two values of K obtained at the different wavelengths). This stability constant is a conditional stability constant, which is characteristic of the system in which it was measured. To interpret the meaning of this stability constant in terms of Eqns. 4.4 to 4.8, the following

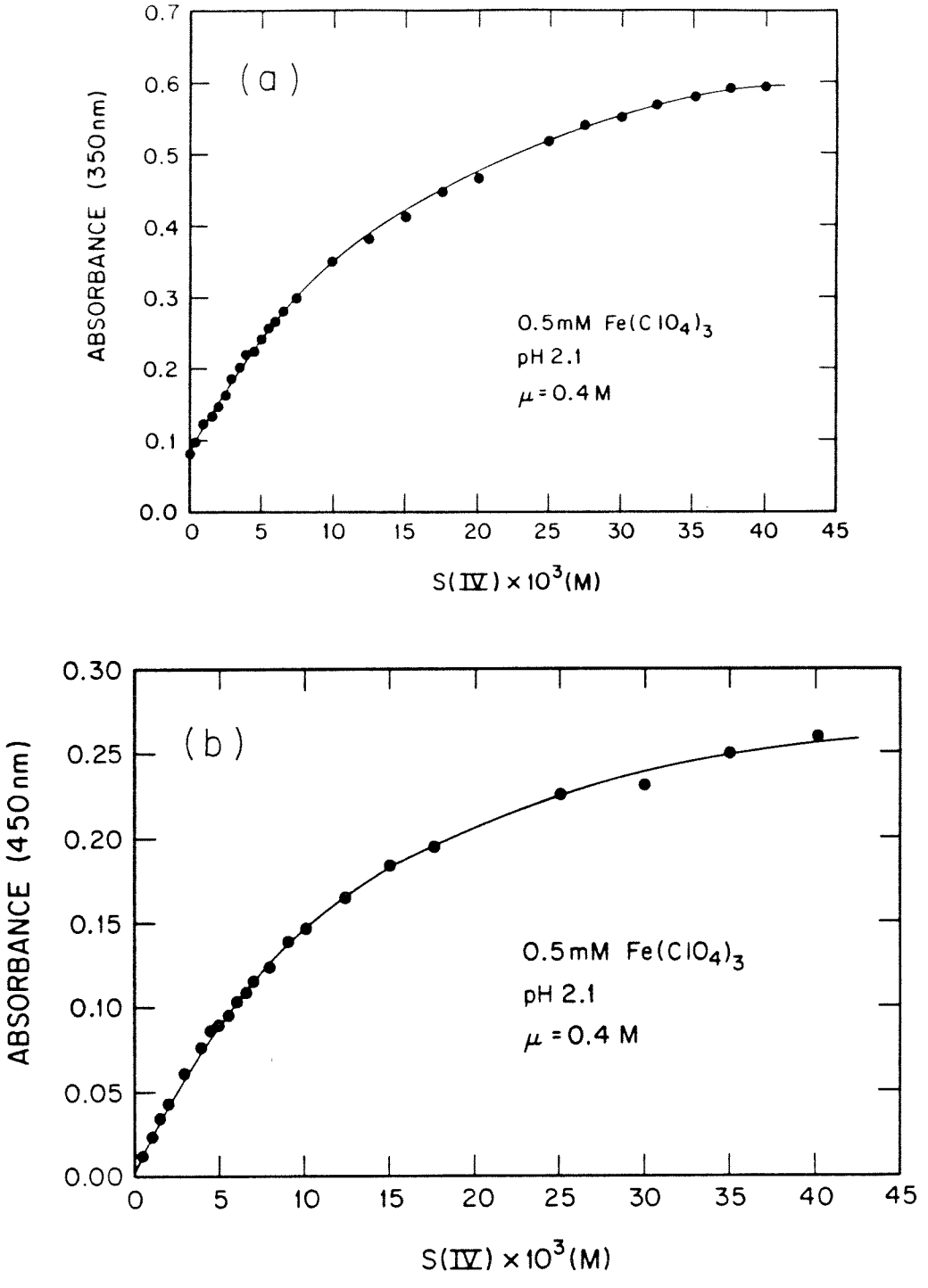

Fig. 4.3 Absorbance of the Fe(III)-S(IV) complex as a function of [S(IV)] at (a) 350 nm and (b) 450 nm.

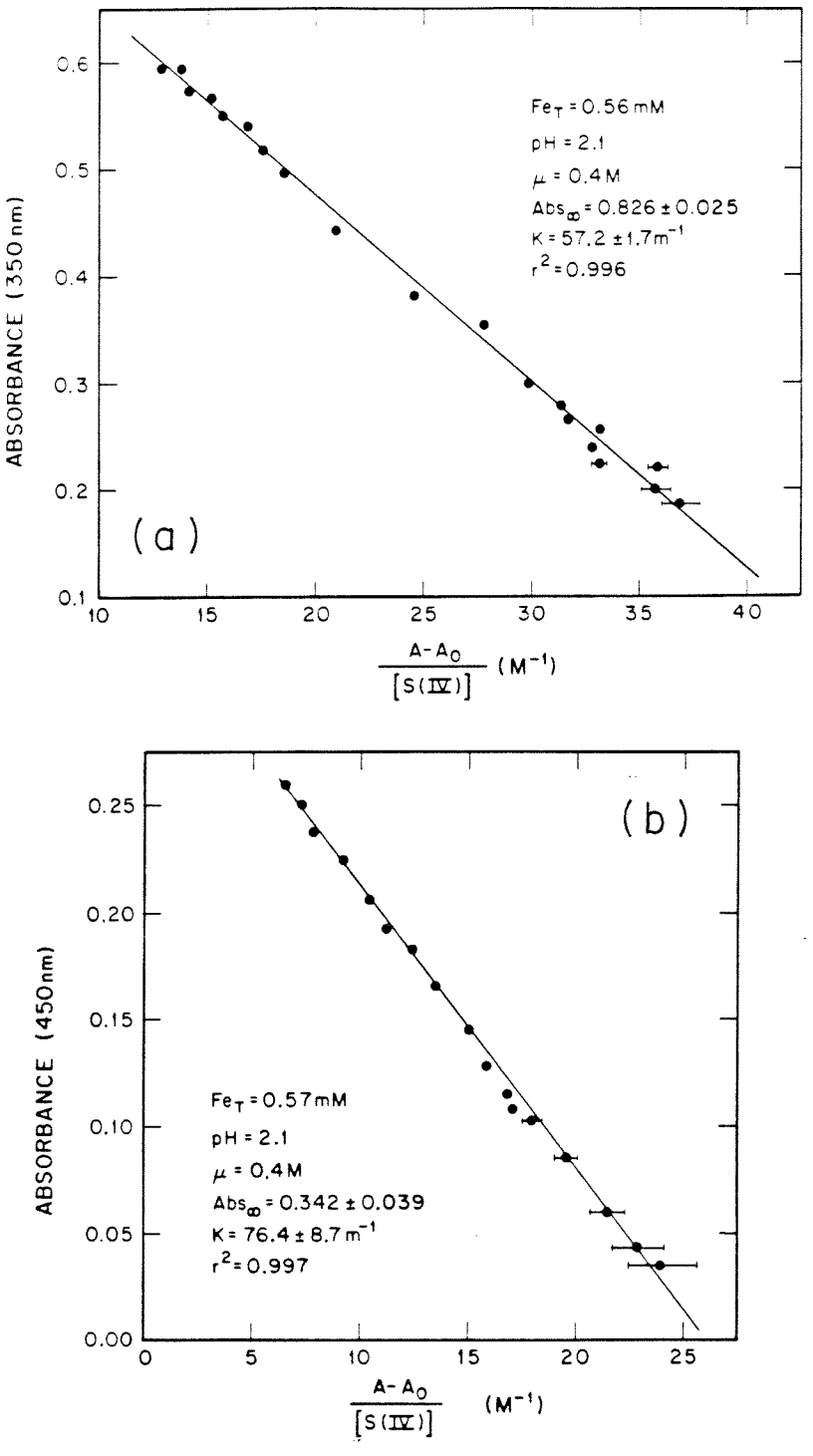

Fig. 4.4 Equation 4.9 applied to data in Figure 4.3 at (a) 350 nm and (b) 450 nm. (Error bars are shown when they exceed symbol size).

stability constants were defined:

$$K_1 = \frac{[FeSO_3^+]}{[Fe^{3+}][SO_3^{2-}]} \quad (4.12)$$

$$K_2 = \frac{[FeSO_3^+][H^+]}{[Fe^{3+}][HSO_3^-]} \quad (4.13)$$

$$K_3 = \frac{[FeOHSO_3^0][H^+]}{[FeOH^{2+}][HSO_3^-]} \quad (4.14)$$

$$K_4 = \frac{[FeHOSO_3^0]}{[FeOH^{2+}][SO_3^{2-}]}. \quad (4.15)$$

Concentrations of the S(IV) species can be calculated using the relationships in Eqn. 4.10. The acid dissociation constants substituted into Eqn. 4.10 for μ = 0.4 M were log K_{a_1} = -1.6 and log K_{a_2} = -6.6 (at μ = 0.0 M, log K_{a_1} = -1.91 and log K_{a_2} = -7.18 (Smith and Martell, 1976)). At pH 2.1, α_1 = 0.62 and α_2 = 1.9 x 10^{-5}. The concentrations for the iron species can be calculated using log $^*K_b$ = -2.73, μ = 0.5 M (Smith and Martell, 1976); β_0 = 0.81 and β_1 = 0.19 at pH 2.1. Using these values, the following stability constants can be calculated: log K_1 = 6.6, log K_2 = 0.024, log K_3 = 0.65, and log K_4 = 7.3. In this case we have assumed for each stability constant that the form of the complex is $FeSO_3^+$ or $FeOHSO_3^0$, and the equilibrium species are HSO_3^- or SO_3^{2-}, and Fe^{3+} or $FeOH^{2+}$.

The relative importance of each the above equilibria could be resolved by studying the pH dependence of the conditional stability constant and by conducting kinetic studies to determine the rate of formation of these different complexes. At pH 2, 20% of Fe(III) was the hydroxide species, at higher pH, $Fe_2(OH)_2^{4+}$ would begin to form,

which would make the system more complicated. However, SO_2 degassed in the stopped-flow cuvette at lower pH; this eliminated a pH dependence study at pH < 2.

Raman Spectroscopy Studies

Raman spectroscopy was used to determine the mode of sulfite bonding to iron(III). High concentrations ($[S(IV)]_o$ = 0.1M, $[Fe(III)]_o$ = 0.25M) of the reactants were needed to obtain well-resolved spectra. At these concentrations, both the Fe(III) and the HSO_3^- are expected to dimerize. Therefore, the speciation of the system may have had an added degree of complexity. The aqueous $FeCl_3$ spectrum indicated there were no peaks that would interfere with the S(IV) spectra.

A Raman spectrum for the Fe(III)-S(IV) aqueous system is shown in Fig. 4.5. The main S-O stretching frequency is a very broad band, similar to those observed in HSO_3^- and SO_3^{2-} solutions. This peak broadening could be due to the solvent effects noted by Davis and Chatterjee (1975) for the S(IV) system. The S-O stretching frequencies moved from 1022 and 1054 cm^{-1} for $NaHSO_3$ and Cu(II)-S(IV) species to 938 cm^{-1} in the Fe(III)-S(IV) system. This peak had comparable S-O stretching frequencies to those reported by Harrison et al. (1983) for first-row transition metal sulfito salts with metal-O bonding (see Table 2.5); therefore metal-O bonding in the Fe(III)-S(IV) complexes appears to be dominant. A weak band at 982 cm^{-1}, which would indicate the presence of some SO_4^{2-}, was noted. No evidence of a peak at 1090 cm^{-1}, corresponding to $S_2O_6^{2-}$ was obtained; this was consistent with SO_4^{2-} being the primary S(IV) oxidation product in the presence of Cl^-

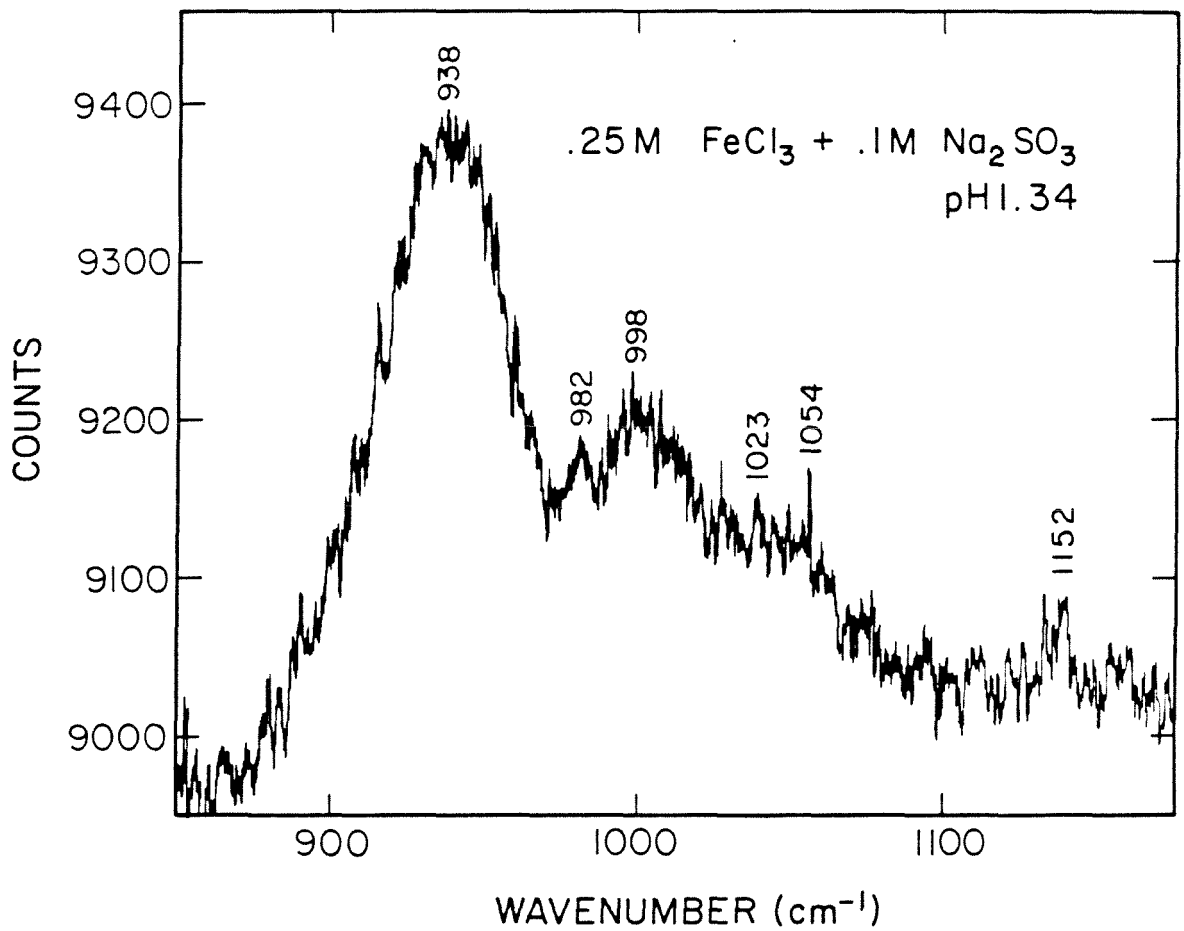

Fig. 4.5 Raman spectrum of Fe(III)-S(IV) system.

Spectrophotometric Kinetic Studies

Mixing Fe(III) with S(IV) solutions resulted in the formation of a red complex that eventually disappeared with time both in the presence and absence of O_2. The water exchange rate for Fe(III) is relatively slow compared to other first row transition metals, $k_{ex} = 1.6 \times 10^2$ sec^{-1} (Hunt and Friedman, 1983). Ligand substitution rates are often controlled by the water exchange rate of the central metal ion (Langford and Gray, 1966). This slow water exchange rate is within the time resolution of a stopped-flow apparatus, so kinetic studies on the formation of the Fe(III)-S(IV) complexes were carried out using a stopped-flow apparatus. Studies of the disappearance of the rapidly formed complex, which occurs on a slower time scale, were conducted using UV/Vis and EPR spectroscopy.

A diagram of a typical stopped-flow kinetic trace ($[Fe(III)]_o$ = 1 mM, $[S(IV)]_o$ = 1 mM, pH = 2) is shown in Fig. 4.6. The initial absorbance increase (i.e. complex formation) occurred faster than the instrument response time (10 msec). After the initial jump in absorbance, there was a continued slow increase in absorbance that was completed within approximately 100 to 120 msec. The rate of this slow increase did not appear to depend on the $[Fe(III)]_o$:$[S(IV)]_o$ ratio for $[S(IV)]_o > [Fe(III)]_o$ ($[Fe(III)]_o$ = 1 mM, $[S(IV)]_o$ = 1, 10, 100 mM). However the magnitude of the total ΔA was dependent on the [S(IV)]:[Fe(III)] ratio. When $[S(IV)]_o < [Fe(III)]_o$ ($[Fe(III)]_o$ = 1 mM, $[S(IV)]_o$ = 0.5 mM), the time to reach the maximum absorbance (A_{max}) was significantly longer ($\simeq$ 600 msec). As the pH was lowered, the

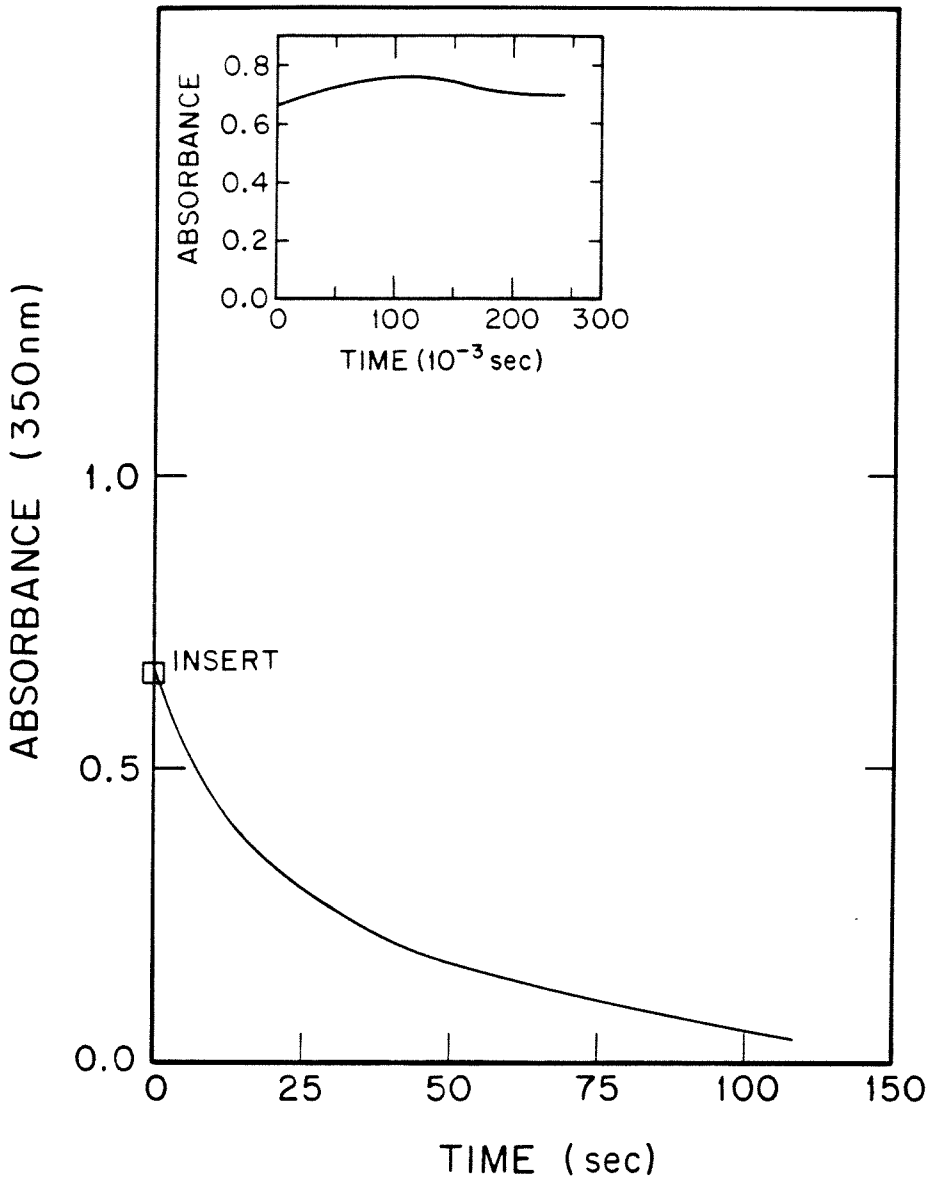

Fig. 4.6 A diagram of a typical kinetic trace obtained with the stopped-flow ($[Fe(III)]_o$ = 1 mM, $[S(IV)]_o$ = 1 mM, pH = 2, μ = 1.3 M).

magnitude of A_{max} decreased and the time to reach A_{max} decreased (to $\simeq$ 60 msec at pH 1, however the initial fast increase was still observed). For all cases, after A_{max} was reached the absorbance began to decrease.

These observations indicated that more than one complex was forming (i.e., the initial complex formed on a fast time scale (< 10 msec) while the second complex formed on a slower time scale (< 120 msec)), or that a complex formed and then underwent some internal changes such as isomerization. The typical observed rates of substitution reactions of Fe^{3+} and $FeOH^{2+}$ complexes are 4 to 10^2 $M^{-1}sec^{-1}$ and 10^3 to 10^5 $M^{-1}sec^{-1}$, respectively (see Table 4.1). Our stopped-flow experiments indicate that $\tau_{1/2}$ for the initial reaction is less that 3 msec and $\tau_{1/2}$ for secondary reaction is less than 30 msec for $[S(IV)]_o > [Fe(III)]_o$ and less than 200 msec for $[Fe(III)]_o > [S(IV)]_o$. The ligand substitution rates would indicate that perhaps the initial reaction is a reaction of $FeOH^{2+}$ and S(IV) (Eqns. 4.6 and 4.7) and the secondary reaction is the reaction of Fe^{3+} and S(IV) (Eqns. 4.4 or 4.5). Carlyle (1971) in his pH-jump experiments observed half-lives of 1540 msec (pH 1.0) to 31 msec (pH 0.7) for cases where either Fe(III) or S(IV) were in excess. These half-lives are greater than the expected half-life for the initial formation step that we observed, although the rates we observed for the secondary reaction falls within this range.

After the Fe(III)-S(IV) complexes formed, the absorbance began to decrease. There is a relatively fast decrease in absorbance (λ = 350 nm) with $\tau_{1/2} \simeq 25$ sec, which parallels the rapid fading of the red color to orange. But this fast decrease does not directly correspond to a

large reduction of the Fe(III) in the system. The slow loss of Fe(III) in the Fe(III)-S(IV) system was verified by measuring the EPR signal in the presence of 1 M HCOOH (*vide infra*).

UV/Vis studies of the disappearance of the complex absorbance (monitored at 350 nm, pH 2, in the presence of 1 M HCOOH) on a slower time scale (1 to 2 hours), indicated that after the initial fast decrease in absorbance there was a continued absorbance loss. Presented in Fig. 4.7 are kinetic traces of the disappearance of Fe(III)-S(IV) complex at different reaction ratios. The solution was kept in the dark and aliquots of the reaction mixture were taken at different times to measure the absorbance. The observed rate data fit a rate expression with two consecutive exponential terms, similar to the Cu(II)-S(IV) system. The observed rates are listed in Table 4.2; they do not vary consistently with increasing S(IV):Fe(III) ratio. The average half-life of these experiments is $\simeq$ 6 min. Kinetic measurements were taken under different irradiation conditions on the HP 8450A. The photon flux into the sample mixture was varied by turning the room lights on or off and by changing exposure time in the HP 8450A spectrophotometer. The results of these experiments are shown in Fig. 4.8, there was no significant change in rate of the disappearance of the complex with at different irradiation levels. The half-life of these reactions is comparable to the data obtained by keeping the solution in the dark, $\tau_{1/2} \simeq 7$ min, however the observed kinetic data do not fit a rate expression with two consecutive exponential terms.

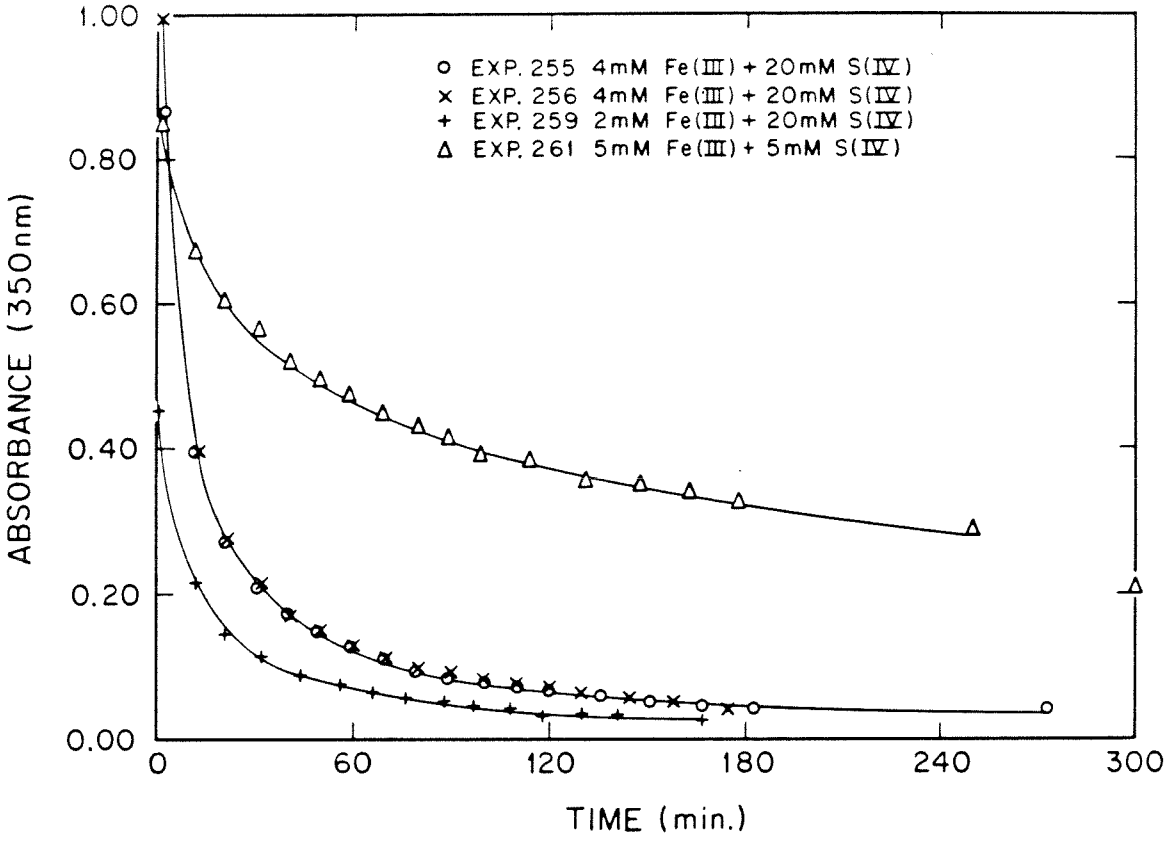

Fig. 4.7 Kinetic data for disappearance of the absorbance (350 nm) due to the Fe(III)-S(IV) charge transfer complexes, at different Fe(III):S(IV) ratios (μ = 1 M, pH 2).

TABLE 4.2

Observed rate constants for the Fe(III)-S(IV) system in in 1 M HCOOH (pH 2)

$[Fe(III)]_o$ (mM^{-1})	$[S(IV)]_o$ (mM^{-1})	Ratio Fe(III):S(IV)	k (sec^{-1})
2	20	1:10	$(2.1 \pm 0.2)x10^{-3}$
4	20	1:5	$(2.7 \pm 0.2)x10^{-3}$
5	5	1:1	$(1.2 \pm 0.2)x10^{-3}$

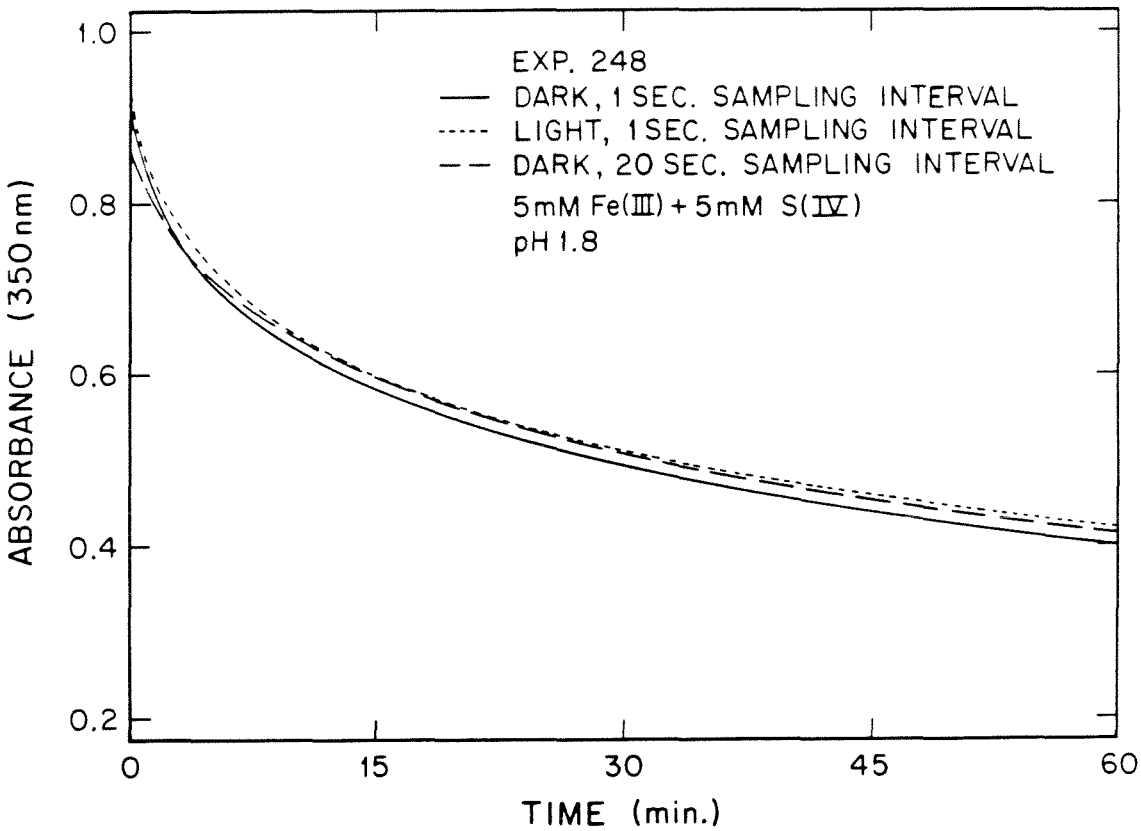

Fig. 4.8 Kinetic data for disappearance of the absorbance (350 nm) due to the Fe(III)-S(IV) complexes under different light conditions. Sampling interval refers to the interval between absorbance measurements when the mixture is exposed to a full spectrum of light (200 to 800 nm). ($[Fe(III)]_o$ = 5 mM, $[S(IV)]_o$ = 5 mM, pH 2, μ = 1 M).

Electron Paramagnetic Resonance Kinetic Studies

EPR studies of the reduction of Fe(III) in the Fe(III)-S(IV) system in the presence of 1 M HCOOH (pH 2) demonstrated the rate of reduction of Fe(III) was comparable to the slow absorbance change at 350 nm discussed above. EPR is a useful technique to study the reduction of Fe(III), since Fe(III) is d^5 and has an EPR signal while Fe(II) is d^6 and has no signal. In Fig. 4.9, EPR spectra are presented of Fe(III) before S(IV) is added and of the Fe(III)-S(IV) system with time. The times listed in the caption are the time the sample was at room temperature (21 $^{\circ}$C) before rapid freezing to take the spectrum. The thawing and freezing process added $\pm$ 30 sec to the indicated times. The species of the Fe(III) in this system was not known. The complex $[FeA_6]^{3-}$, where A represents the formate ion, has been reported for mixtures of $HCOO^-$ and Fe(III) with concentration ratios of at least 12.5 to 1 (Weinland and Reihlan, 1913). Perrin (1959) noted the absence of polynuclear Fe(III)-OH-$HCOO^-$ species in the presence of a large excess of formate. However, in the process of freezing there could be solute-solvent segregation which could result in local pockets of high concentrations of metal ions (up to 10 M, Leigh and Reed, 1971) that might promote the formation of polynuclear species. The spectra which are presented are absorption derivatives of the EPR signal. The numerous species contributing to the signal made it difficult to integrate the signal quantitatively in order to determine the number of Fe(III) centers contributing to the signal. The decrease in the intensity of the signal with time, does give an estimate of the rate of reduction of Fe(III) to Fe(II).

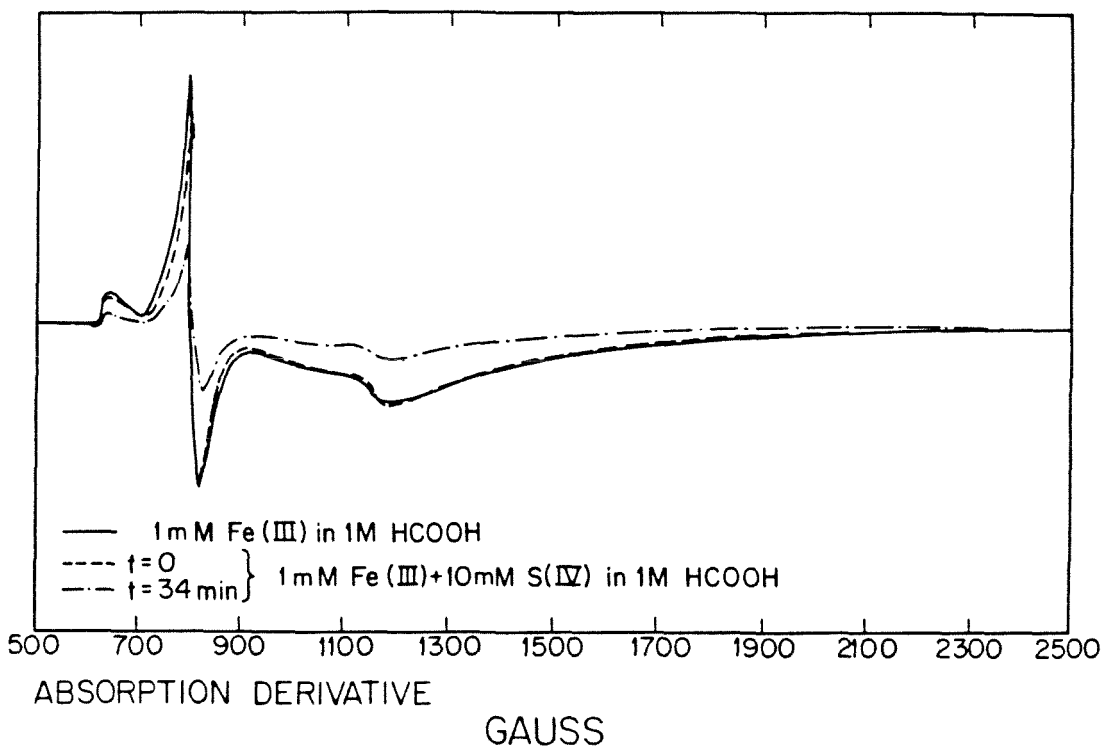

Fig. 4.9 EPR spectrum of 1 mM Fe(III) compared to the EPR spectra of Fe(III)-S(IV) complexes (pH 2).

The shape and the size of the signal do not change significantly when S(IV) is first added to the iron system. An initial decrease in the magnitude of the signal when S(IV) was added would have indicated that there was a rapid reduction of Fe(III) to Fe(II) (within the time it took to mix and freeze the sample t < 30 sec) or that Fe(III)-S(IV) spin-coupled dimers were formed. Apparently neither process occurred. The g-values for the iron species were 4.3 for the strong absorption and 1.9 for a weaker absorption. These spectra are characteristic of Fe(III) with an octahedral coordination environment with a rhombic distortion (Blumberg, 1966). A time series of EPR spectra were taken for the Fe(III)-S(IV) system at different Fe(III):S(IV) ratios (see Fig. 4.10). As the magnitude of the signal decreased with time, there were changes in the shape of the signal. This can be seen in Fig. 4.10. These changes in the shape indicated that there were more than one ferric species in the Fe(III)-S(IV) system, but provided no evidence for their identity. The peak heights of the spectra collected at 10:1 S(IV):Fe(III) as a function of time are shown in Fig. 4.11. The rate of disappearance appeared to be first order. The corresponding half-life was $\simeq$ 8 min. This half-life is comparable to the half-lives obtained by following the disappearance of the absorbance at 350 nm using UV/Vis spectroscopy.

DISCUSSION

The stability constant, K_2 determined for the reaction, $Fe^{3+} + HSO_3^- \rightleftharpoons FeSO_3^+ + H^+$ ($K_2 = 1.1\ M^{-1}$), obtained for a Fe(III)-S(IV)

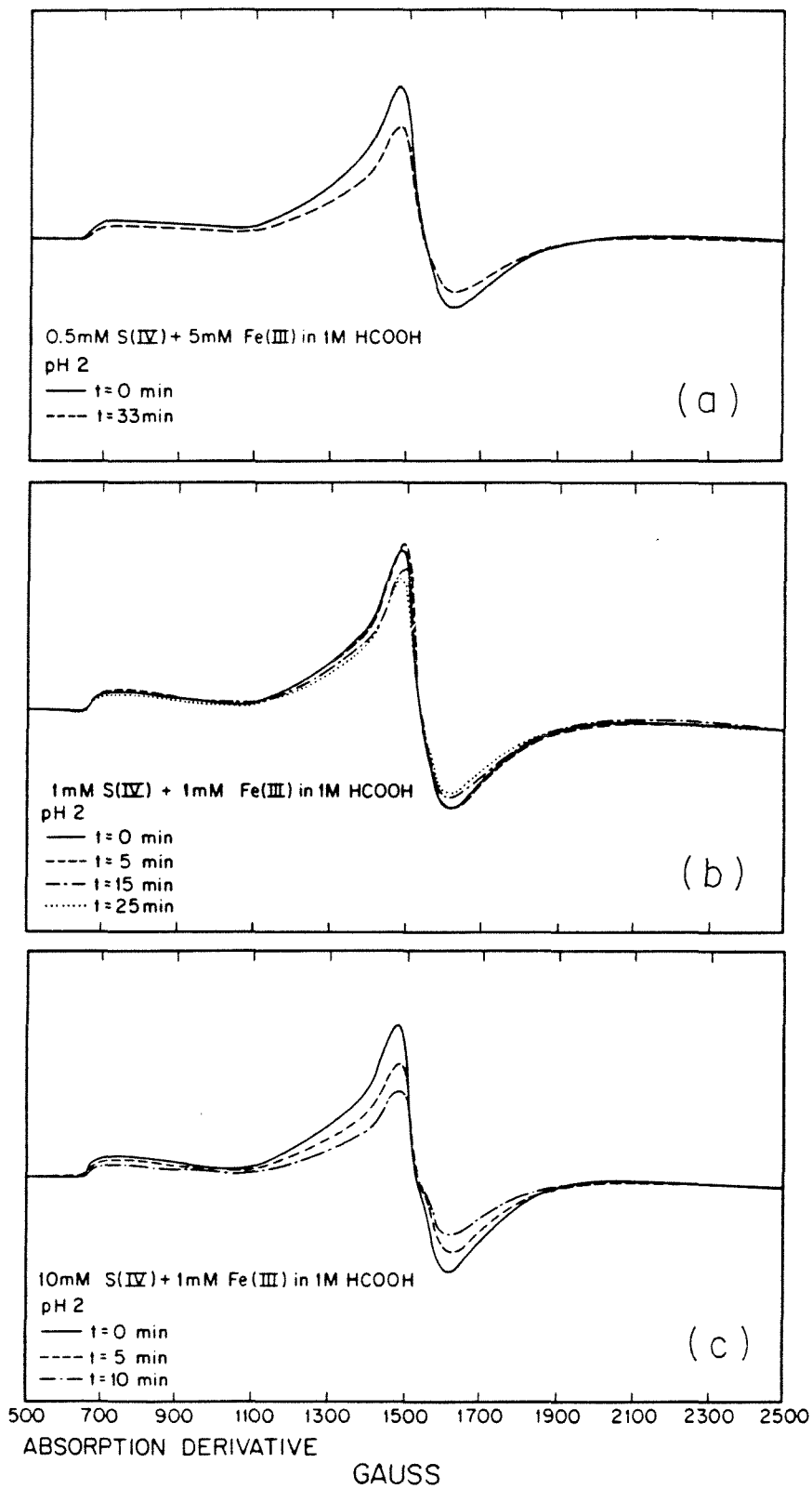

Fig. 4.10 Time series of EPR spectra of the Fe(III)-S(IV) system at different Fe(III):S(IV) ratios (a) 1:2, (b) 1:1 and (c) 1:10.

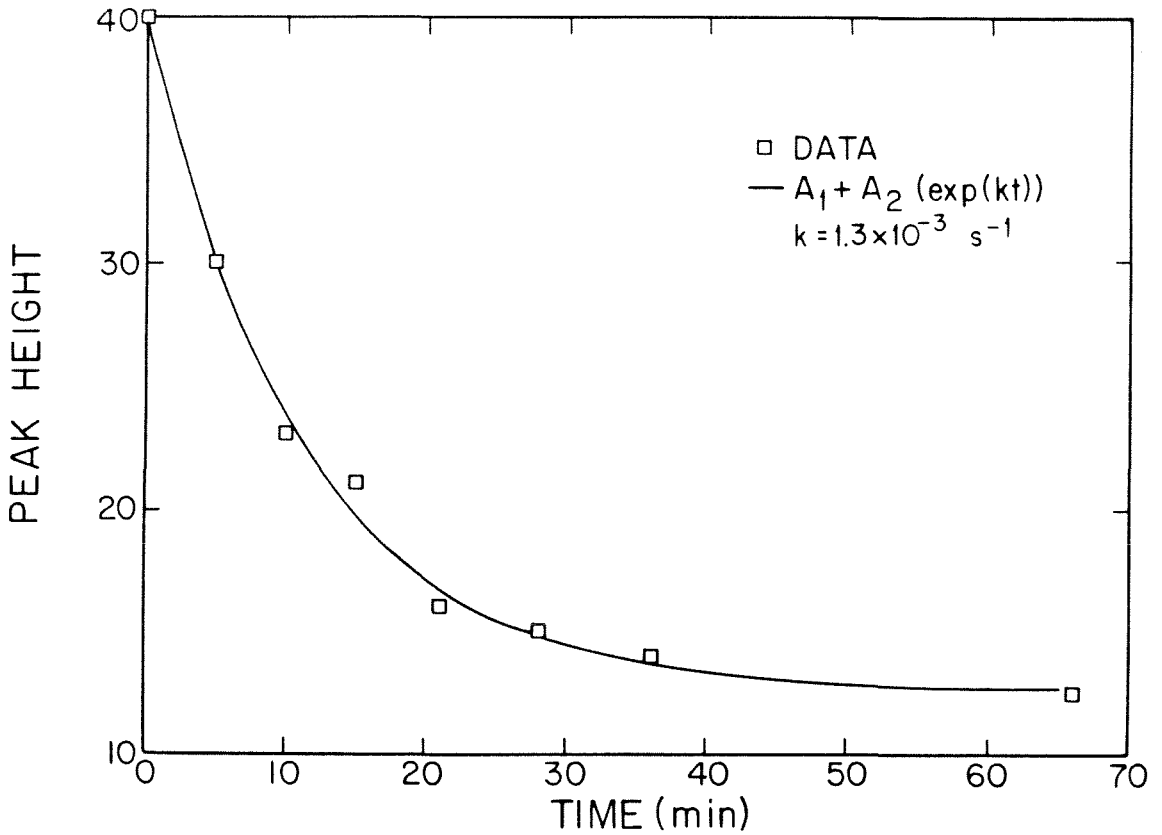

Fig. 4.11 The peak heights of the Fe(III) signal of the time series in Figure 4.7c plotted as a function of time ($[Fe(III)]_o$ = 1 mM, [S(IV)] = 10 mM, pH 2).

species is consistent with the equilibrium quotient determined by Carlyle (1971). Carlyle estimated that the equilibrium quotient Q_1 = $([FeSO_3^+][H^+])/([Fe^{3+}][HSO_3^-]) < 0.4\ M^{-1}$ at μ = 1.0 M (0.36 < pH < 1.37). The pH range used in Carlyle's work (pH 0.36 to 1.37) was a lower pH range than what was employed in this study. His method of determination of the upper bound on the apparent equilibrium constant was to measure the absorbance change at different $[HSO_3^-]/[H^+]$ ratios and to suggest that less than 10% of the iron was complexed (hence the upper bound). Unfortunately, the slow response time in his experimental set-up introduced uncertainty due to Fe(III) reduction. Reduction was slowed by the addition of a 5- to 20-fold excess of [Fe(II)] over [Fe(III)]. The addition of Fe(II) at those levels adds to the uncertainty of his constant.

The rate of formation of Fe(III) complexes has been studied for several different anions, such as Br^-, Cl^-, F^-, SCN^-, SO_4^{2-}, N_3^- (see references in Table 4.1). The rate constants for the formation of Fe(III) complexes appear to be dependent on the nature of the incoming ligand (see Table 4.1) in that the rate increases with an increase in basicity (Acasscina et al., 1967). Two interpretations have been formulated to account for this dependence. Wendt and Strehlow (1962) and Cavasino and Eigen (1064) have suggested formation of an ion pair that subsequently underwent an "inner hydrolysis". They concluded that the extent of ion pair formation depended on the basicity of the ligand. Seewald and Sutin (1963) have proposed an alternative explanation that involved an acid-independent path. In this case the actual reactants were $FeOH^{2+}$ and $HA^{(n-1)-}$. The behavior of the

Fe(III)-S(VI) system may be analogous to the Fe(III)-S(IV) system, since as there appears to be similar bonding (metal-O bonding) in both complexes.

Cavasino (1968) proposed a mechanism for the complexation of Fe(III) by S(VI) that included four possible formation steps as follows:

$$Fe^{3+} + SO_4^{2-} \underset{k_{21}}{\overset{k_{12}}{\rightleftharpoons}} FeSO_4^+ \qquad (4.16)$$

$$FeSO_4^+ + H_2O \underset{k_{42}}{\overset{k_{24}}{\rightleftharpoons}} FeOHSO_4 + H^+ \qquad (4.17)$$

$$FeOH^{2+} + SO_4^{2-} \underset{k_{43}}{\overset{k_{34}}{\rightleftharpoons}} FeOHSO_4 \qquad (4.18)$$

$$Fe^{3+} + HSO_4^- \underset{k_{25}}{\overset{k_{52}}{\rightleftharpoons}} FeSO_4^+ + H^+ \qquad (4.19)$$

$$FeOH^{2+} + HSO_4^- \underset{k_{46}}{\overset{k_{64}}{\rightleftharpoons}} FeOHSO_4 + H^+ \qquad (4.20)$$

Temperature-jump relaxation techniques were used to evaluate the importance of the different pathways under the conditions of $[Fe(III)]_o \simeq 1$ to 4 mM, pH $\simeq$ 0.38 to 2.0, μ = 0.5, 1.2 and 2.0 M. Cavasino's results indicated that reaction 4.18 was the important acid dependent pathway with $k_{34} = 2.31 \times 10^5$ $M^{-1}sec^{-1}$ at μ = 0.5 M, 25 °C. The acid-independent pathway involved Eqns. 4.16 and 4.20. The rate constants were determined to be $3.5 \times 10^3 < k_{12} < 4.6 \times 10^3$ $M^{-1}sec^{-1}$ and $1.9 \times 10^5 < k_{64} < 4.8 \times 10^5$ $M^{-1}sec^{-1}$ at μ = 0.5 M, 25 °C. These rate constants were consistent with known ligand exchange rates for Fe^{3+} and $FeOH^{2+}$ (see Table 4.1). Activation parameters determined by

Cavasino were consistent with k_{12} as the important acid-independent pathway.

In the case of the Fe(III)-S(IV) system the primary S(IV) species are HSO_3^-, $SO_2 \cdot H_2O$ at pH 2. Since $[HSO_3^-] >> [SO_3^{2-}]$ and the since the rate of complexation of $FeOH^{2+}$ is approximately two orders of magnitude greater that that of Fe^{3+}, Eqn. 4.6 appears to be the dominant reaction for the formation of $FeSO_3^+$ under the conditions of this study. This would be consistent with the initial fast increase in absorbance measured on the stopped-flow.

The absorbance increase with increasing [S(IV)]:[Fe(III)] ratio is shown in Fig. 4.3. Expected behavior for a 1:1 complex is that the absorbance does not increase with [ligand]:[metal] ratios greater than one. The observed behavior is consistent with SO_3^{2-} being the complexing ligand as at the pH of these experiments (pH 2.1), $[SO_3^{2-}] = 2 \times 10^{-5}[S(IV)]$. Sulfite as the complexing ligand would indicate that the equilibrium measured would be defined by K_1 ($10^{6.6}$, μ = 0.4 M) or K_4 ($10^{7.3}$, μ = 0.4 M). A stability constant of $\simeq 10^7$ is greater than the stability constant measured for the $CuSO_3$ complex ($K = 10^{4.2}$, μ = 0.4 M), which fits the trend of stability constants for complexes of Fe^{3+} and Cu^{2+} with other ligands (see Table 5.3).

The reaction of ground-state molecular oxygen with S(IV) proceeds at very slow rates in the absence of light or specific catalysts (Hoffmann and Boyce, 1983; Hoffmann and Jacob, 1984). Transition metals, such as Fe(III), which are capable of coordinating S(IV) and/or O_2 accelerate the rate of S(IV) autoxidation. The mechanisms invoked to explain transition metal catalyzed S(IV) autoxidations can be

TABLE 4.3

Stability constants for Cu(II) and Fe(III) complexes (25 °C)[a]

Ligand	Log K		Ionic Strength (M)
	Cu(II)L	Fe(III)L	
CO_3^{2-}	6.75		0
HPO_3^{2-}	4.57	4.92	3.5
SO_3^{2-}	4.2[c]	6.6[d]	0.4
N_3^-	2.86[b]	4.85	0
SO_4^{2-}	2.36	4.04	0
NCS^-	2.33	3.02	0
NO_2^-	2.02		0
F^-	1.2	6.0	0
NO_3^-	0.5	1.0	0
Cl^-	0.4	1.48	0
Br^-	-0.3	0.06	0

[a]From Smith and Martell (1976)

[b]20 °C

[c]This work

[d]This work, assuming that K_1 is the measured equilibrium constant

classified into two categories: i) one-electron free radical reactions and ii) two-electron polar reactions involving ternary complexes comprised of the transition metal, S(IV), and molecular oxygen (Hoffmann and Boyce, 1983; and Hoffmann and Jacob, 1984). A frequently postulated initiation step for the free radical autoxidation of S(IV) as catalyzed by Fe(III) is as follows (Bäckström, 1934; and Hoffmann and Jacob, 1984):

$$Fe^{3+} + SO_3^{2-} \longrightarrow Fe^{2+} + SO_3^{\cdot-}.$$

Bäckström assumed that electron transfer between Fe^{3+} and SO_3^{2-} was an outersphere process. However, formation of an inner-sphere complex appears to be a necessary step in the mechanism. The color change which occurs when Fe(III) is mixed with S(IV) indicates that an inner-sphere complex is formed. Kinetic data obtained in this study indicated that the rate of reduction of Fe(III) was slow, $\tau_{1/2}$ = 8 min. Similar rates were reported by Karraker (1963), .

The catalytic effectiveness of Fe(III) on the autoxidation of S(IV) has been found to increase with pH. The pH dependence of the catalytic reaction is due to the pH dependence of the formation of Fe(III)-S(IV) complexes. A rate law for the iron-catalyzed autoxidation of S(IV) which takes into account the pH dependence of S(IV) speciation is (Hoffmann and Calvert, 1985):

$$\frac{-d[S(IV)]}{dt} = k[Fe(III)][S(IV)]\alpha_2$$

where α_2 has been defined in Eqn. 4.10. Hoffmann and Calvert applied this equation to published experimental data for the Fe(III) catalyzed autoxidation of S(IV) (Aubuchon, 1976; Fuzzi, 1978; Brimblecombe and Spedding, 1974; and Neytzwell-de Wilde and Taverner, 1958) and found good agreement. Their recommended rate constant for this reaction is k = $(1.2 \pm 0.32) \times 10^6$ $M^{-1}sec^{-1}$. At a typical atmospheric concentration of Fe(III), 20 μM, and S(IV) as the limiting reagent (typical atmospheric SO_2 concentration are 20 ppb in Los Angeles) this rate constant indicates a half-life of 30 msec. The Fe(III) catalyzed autoxidation reaction is significantly faster than the rate of electron transfer.

Freiburg (1975) has proposed ternary complexes of Fe(III), S(IV) and O_2 as a prelude to electron transfer for the Fe(III) catalyzed autoxidation of S(IV):

$$Fe^{3+} + HOSO_2^- \rightleftharpoons FeOSO_2H^{2+}$$

$$FeOSO_2H^{2+} + SO_3^{2-} \rightleftharpoons Fe(OSO_2)_2H$$

$$Fe(OSO_2)_2H + O_2 \rightleftharpoons Fe(OSO_2)_2HO_2$$

$$Fe(OSO_2)_2HO_2 \xrightarrow{H_2O} Fe^{3+} + 2SO_4^{2-} + H^+.$$

Based on our results, oxidation of S(IV) via formation of a ternary complex appears to be a more probable pathway than a free radical chain reaction. Analogous catalytic species to those proposed for the Cu(II)-S(IV) system (Chapter 3) may be the reactive species in the

Fe(III)-S(IV) system in the presence of O_2. This catalytic intermediate would be of the form:

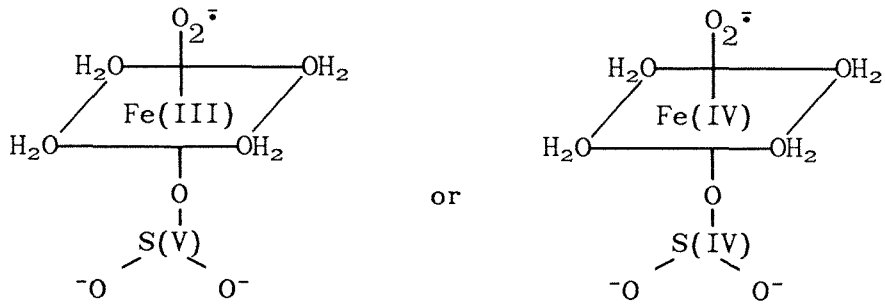

Although Fe has been found in high ($\simeq$ 100 μM) concentrations in atmospheric droplets (see Table 1.1), much of this iron would be in form of solid particles. Ferric oxides, such as Fe_2O_3, have been identified as components of airborne particles (Fukasawa, 1980). Other sulfite complexes, such as α-hydroxyalkylsulfonates, have larger stability constants than the Fe(III)-S(IV) complexes (K for the HSO_3^-/HCHO adduct = $[HOCH_2SO_3^-]/[HCHO][HSO_3^-]$, = 10^7, Munger et al., 1986). Thus, given the stability constant $K_1 = 10^{6.6}$ for $FeSO_3^+$, the ratio of $[Fe(III)]_T:[HCHO]_T$ would have to be approximately 30 at pH 2 or $3x10^2$ at pH 5 for comparable concentrations of $FeSO_3^+$ to coexist with $HOCHSO_3^-$. Aldehydes have been found in much higher concentrations (Munger et al., 1984, 1986) than Fe(III) in cloud-, fog- and rainwater systems, therefore S(IV) speciation is likely to be dominated by $RC(OH)SO_3^-$ chemistry rather than $Fe(SO_3)_n^{3-2n}$.

REFERENCES

Accascina, F., F.P. Cavasino and S. D'Alessandro, 1967, *J. Phys. Chem.*, **71**, 2474-2481.

Albu, H.W. and H.D. von Schweintz, 1932, *Ber., Deutsch. Chem. Ges.*, **B65**, 729-737.

Aubuchon, C., *The Rate of Iron Catalyzed Oxidation of Sulfur Dioxide by Oxygen in Water* (Ph.D. Thesis, John Hopkins U., Baltimore, MD, 1976).

Bäckström, H.L.J., 1934, *Z. Phys. Chem. (Leipzig)*, **25B**, 122-138.

Bassett, H. and W.G. Parker, 1951, *J. Chem. Soc*, **46**, 1540-1560.

Below, Jr., J.F., R.E. Connick and C.P. Coppel, 1958, *J. Am. Chem. Soc.*, **80**, 2961-2967.

Blumberg, W.E. in *Magnetic Reasonance in Biological Systems*, A. Ehrenberg, B.G. Malmström, eds. (Pergamon Press, Oxford, 1960) pp. 119-133.

Brimblecombe, P. and D.J. Spedding, 1974, *Atmos. Env.*, **8**, 937-945.

Carlyle, D.W., 1971, *Inorg. Chem.*, **10**, 761-764.

Carlyle, D.W. and O.F. Zeck, 1973, *Inorg. Chem.*, **12**, 2978-2983.

Carpenter, H.C.H., 1902, *J. Chem. Soc.*, **24**, 1-14.

Cavasino, F.P. and M. Eigen, 1964, *Ric. Sci. Rend.*, **A4**, 509-522.

Cavasino, F.P., 1968, *J. Phys. Chem.*, **72**, 1378-1384.

Connick, R.E. and C.P. Coppel, 1959, *J. Am. Chem. Soc.*, **81**, 6389-6394.

Cotton, F.A. and G. Wilkinson, *Advanced Inorganic Chemistry* (J. Wiley & Sons, New York, 1980).

Danilczuk, E. and A. Swinarski, 1961, *Rocz. Chem.*, **35**, 1563-1572.

Davis, A.R. and Chatterjee, 1975, *J. of Sol. Chem.*, **4**, 399-412.

Davis, G.G. and W. MacF. Smith, 1960, *Can. J. Chem.*, **38**, 1836-1845.

Dasgupta, P.K., P.A. Mitchell, P.W. West, 1979, *Atmos. Env.*, **13**, 775-782.

Donally, L.H., 1933, *Ind. Eng. Chem. Anal. Ed.*, **5**, 91.

Eigen, M., K. Kustin and G. Maass, 1961, *Z. Phys., Chem. (Frankfurt)*, **30**, 130-136.

Freiburg, J., 1975, *Atmos. Env.*, **9**, 661-672.

Fukasawa, T., M. Iwaatsuki, S. Kawabuko and K. Niyazaki, 1980, *Anal. Chem.*, **52**, 1784-1787.

Fuzzi, S., 1978, *Atmos. Env.*, **12**, 1439-1442.

Gélis,M.A. ,1862, *Ann. Chim. Phys.*, **65**, 222.

Hansen, L.D., Whiting, D.J. Eatough, T.E. Jensen, R.M. Izatt, 1976, *Anal. Chem.*, **48**, 634-638.

Harrison, W.D., J.B. Gill and D.C. Goodall, 1983, *Polyhedron*, **2**, 153-156.

Hoffmann, M.R. and S. D.Boyce in *Trace Atmospheric Const., Adv. Env. Sci. & Tech.*, **12**, S.E. Schwartz, ed. (J. Wiley & Sons, New York, 1983) pp. 147-189.

Hoffmann, M.R. and D.J. Jacob in *Acid Rain Precipitation Series Vol.* 3, J.G. Calvert, ed. (Butterworth Publishers, Boston, 1984) p. 109.

Hoffmann, M.R. and J.G. Calvert, *Chemical Transformation Modules for Eulerian Acid Deposition Models, Vol. II, The Aqueous Chemistry.* (U.S. E.P.A., N.C.A.R. Interagency Agreement DW 930237, 1985).

Hoffmann, M.R. and A.P. Hong in *Proceedings of the Second Workshop on Environmental and Inorganic Chemistry*, Portugal (April, 1985).

Huie, R.E. and P. Neta, 1984, *J. Phys. Chem.*, **88**, 5665-5669.

Hunt, J.P. and H.L. Friedman in *Progress in Inorganic Chemistry, Vol.* 30, S.J. Lippard, ed. (Wiley & Sons, New York, 1983) pp. 359-382.

Kao, C.F., *Thermodynamic and Kinetic Studies of the Iron-Sulfite System by Electrochemical Methods* (Ph.D. thesis, Henry Krub School of Mines, Columbia University, New York, New York., 1979).

Karraker, D.G., 1963, *J. Phys. Chem.*, **67**, 871-874.

Kuz'minykh, I.N. and T.B. Bomshtein, 1953, *Zh. Priklad. Khim.*, **26**, 3-8.; *Chem. Abs.*, 1953, **47**, 5832.

Langford, C.H. and H.B. Gray, *Ligand Substitution Processes* (W.A. Benjamin, Inc., Reading, Mass., 1966).

Latimer, W., *Oxidation Potentials* (Prentice Hall, Englewood Cliffs, N.J., 1952).

Leigh, Jr., J.S. and G.H. Reed, 1971, *J. Phys. Chem.*, **75**, 1202-1204.

Matthies, P. and H. Wendt, 1961, *Z. Phys. Chem. (Frankfurt)*, **30**, 137-140.

Munger, J.W., C. Tiller, M.R. Hoffmann, 1986, *Science*, **231**, 247-249.

Newton, T.W. and G.M. Arcand, 1953, *J. Am. Chem. Soc.*, **75**, 2449-2453.

Neytzell-de Wilde, F.G. and L. Traverner in *2nd U.N. Intl. Conf. Peaceful Uses for Atomic Energy Proc. Vol.* 3 (1958), pp. 303-317.

Perrin, D.D., 1959, *J. Chem. Soc.*, 1710-1717.

Pollard, F.H., P. Hanson, and G. Nickless, 1961, *J. Chromatogr.*, **5**, 68-73.

Pouli, D. and W. MacF. Smith, 1960, *Can. J. Chem.*, **38**, 567-575.

Rao, C.N., 1967, *Ultra-Violet and Visible Spectroscopy, Chemical Applications* (Plenum Press, New York, 1967).

Seewald, D. and N. Sutin, 1963, *Inorg. Chem.*, **2**, 643-645.

Smith, R.M. and A.E. Martell, *Critical Stability Constants Vol. 4: Inorganic Ligands* (Plenum Press, New York, 1976).

Stumm, W. and J.J. Morgan, *Aquatic Chemistry* (Wiley & Sons, New York, 1981) pp. 134-137.

Tamura, H., K. Goto, T. Yotsuyanagi, and M. Nagayama, 1974, *Talanta*, **21**, 314-318.

Van Eldik, R, 1980, *Inorgan. Chem. Act.*, **42**, 49-52.

Van Eldik, R., 1985, personal commumication.

Weinland, R.F. and H. Reihlen, 1913, *Ber.*, **40**, 3144-3150; *Chem. Abst.*, 1914, **8**, 637-638.

Wendt, H. and H. Strehlow, 1962, *Z. Elektrochem.*, **66**, 228-234.

CHAPTER FIVE

SUMMARY

Cu(II)-S(IV) SYSTEM

When aqueous Cu(II) and S(IV) solutions are mixed transient complexes form at pH $\leq$ 6. At pH > 6 an unstable Cu(II)-S(IV) solid forms. This solid was identified as $Cu_2SO_3(OH)_2 \cdot H_2O$. The Cu(II)-S(IV) complexes are redox-active; Cu(II) is reduced to Cu(I) and S(IV) is oxidized to S(VI). The redox reaction in the Cu(II)-S(IV) system is unusual as the end products are an equilibrium mixture of Cu(II), Cu(I), S(IV) and S(VI), and a mixed valence precipitate, $Cu^{II}SO_3Cu^{I}_2SO_3 \cdot 2H_2O$.

The stability complex for $CuSO_3$ was measured spectroscopically. The calculated value is $K = 1.8 \pm 0.6 \times 10^4\ M^{-1}$ (μ = 0.4 M, 25 °C). Raman and IR measurements of the Cu(II)-S(IV) aqueous system and $Cu_2SO_3(OH)_2 \cdot H_2O$, respectively, indicate the presence of Cu-S bonds. The formation of Cu-S bonds may account for an increase in stability of $CuSO_3$ complexes over $CuSO_4$.

Postulated redox-active species in the Cu(II)-S(IV) system appear to be copper dimers that are bridged by SO_3^{2-} (i.e. $Cu_2SO_3^{2+}$ and $Cu_2SO_3OH^+$). These dimers appear to be in equilibrium with $CuSO_3$, the dominant Cu(II)-S(IV) species at high $[SO_3^{2-}]$:[Cu(II)] ratios. The existence of reactive copper(II) dimers is consistent with the observation of bi-phasic kinetics and the production of a two-electron transfer oxidation product, SO_4^{2-}. EPR studies of the system indicate

that the Cu(II) signal was damped by Cu(II)-Cu(II) coupling in the dimeric species. The hyperfine structure of the Cu(II) changed considerably during the course of the redox reaction, indicating some changes to the Cu(II) coordination sphere as the reaction progresses.

The postulated mechanism involved two consecutive reductions of copper in the Cu(II) dimers. The estimated rate constants for the reduction of Cu(II) in $Cu_2SO_3^{2+}$ are $k_5 \simeq 5.7 \times 10^{-3}$ sec^{-1} and $k_7 \simeq 5.1 \times 10^{-4}$ sec^{-1} and while for $Cu_2SO_3OH^+$ they are $k_6 \simeq 1.8 \times 10^{-2}$ sec^{-1} and $k_8 \simeq 1.8 \times 10^{-3}$ (Chapter 3). The results are interpreted in terms of the initial formation of an inner-sphere complex which is followed by rate-determining electron-transfer steps. The pH dependence of reduction of Cu(II) in this system supports the model of two active redox species in the system. Different anions were found to affect the rate electron transfer; Cl^- was found to enhance the rate, whereas SO_4^{2-} was found to inhibit the rate. These effects were interpreted in terms of stabilizing either Cu(I) or Cu(II) in the system.

Fe(III)-S(IV) SYSTEM

The initial behavior of the Fe(III)-S(IV) system is similar to the Cu(II)-S(IV) system. Transient complexes form readily when Fe(III) and S(IV) are mixed. The spectra obtained for these complexes show the existence of a broad shoulder between 325 and 675 nm. The shape of the shoulder changes as the ratio of [S(IV)]:[Fe(III)] is increased. This behavior suggests that more than one Fe(III)-S(IV) complex forms. A conditional stability constant for the formation of a 1:1 Fe(III)-S(IV)

complex was determined (log K = 1.8 ± 1.0 M^{-1} at μ = 0.4 M, 25 °C, pH 2.1). Raman results indicate the dominance of metal-O bonds in Fe(III)-S(IV) species.

Stopped-flow kinetic studies of the formation of the Fe(III)-S(IV) complex indicate the likely path of formation is the complexation of $FeOH^{2+}$ by HSO_3^-. EPR kinetic data on the subsequent reduction of Fe(III) in the Fe(III)-S(IV) system indicate that this is a slow reaction with a half-life of ≃ 7 min. The same half-life is obtained by spectrophotometrically monitoring the disappearance of the complex. The kinetic mechanism appears to be similar to the Cu(II)-S(IV) system, in that the formation of complexes are followed by rate-limiting electron-transfer steps.

COMPARISON BETWEEN THE Cu(II)- AND Fe(III)-S(IV) SYSTEMS

Internal redox reactions for transient Cu(II)-S(IV) complexes and Fe(III)-S(IV) complexes have been shown to be slow, with characteristic half-lives between 1 and 7 min. The Fe(III)-S(IV) system appears to be much more complicated than the Cu(II)-S(IV) system. Iron hydrolysis products are present in the pH range over which the Fe(III)-S(IV) complexes are formed. In the Cu(II)-S(IV) system, the change in the absorbance of the complex as a function of [S(IV)] can be used to determine an equilibrium constant for $CuSO_3$. However, in the Fe(III)-S(IV) system, the number of possible equilibria is far greater. Consequently, similar studies yield only a conditional equilibrium constant.

The redox kinetics of the Fe(III)-S(IV) system are expected to follow a similar mechanism to the Cu(II)-S(IV) system, with electron transfer reactions taking place by a series of parallel and consecutive reactions. However in the case of Fe(III)-S(IV) system the number of possible species that can be involved has increased significantly from the Cu system and could involve $FeOHSO_3$, $FeSO_3^+$, $Fe(SO_3)_2^-$, etc. Dimeric Fe(III)-S(IV) complexes are less likely to be the active redox species since the primary oxidation product is $S_2O_6^{2-}$, which is formed as the result of a one-electron transfer.

IMPLICATIONS FOR ATMOSPHERIC SYSTEMS

The slow rate of internal electron transfer reactions of Cu(II)-S(IV) and Fe(III)-S(IV) complexes makes these reactions improbable initiation steps for a free radical chain oxidation of S(IV) (Bäckström, 1934). The second-order rate constant for the iron catalyzed autoxidation of S(IV) is $1.2 \pm 0.32 \times 10^6$ $M^{-1}sec^{-1}$ (Hoffmann and Calvert, 1985). At [Fe(III)] = 20 μM (and gas phase concentrations of SO_2 = 20 ppb), this reaction has a half-life of 30 msec which is substantially faster than the rate of reduction of Fe(III) ($\tau_{1/2} \simeq 7$ min) observed in this study. Veprek-Siska and Lunak (1971) proposed that the metal catalyzed autoxidation of S(IV) proceeded via the formation of metal-O_2-SO_3^{2-} complexes. Their proposed intermediate for the Cu(II)-S(IV) catalytic system was $O_2Cu(I)(SO_3)_n^{-2n+1}$. However, the slow rate of reduction of Cu(II) to Cu(I) would rule out this mechanism. Instead, a more likely pathway is the one proposed by Hoffmann and Hong (1984) for the sulfito cobalt(II)-

tetrasulfophthalocyanine (Co(II)TSP) system, in which the active catalytic species was a ternary O_2-CoTSP-SO_3^{2-} species. Analogous O_2-Fe(III)-SO_3^{2-} and O_2-Cu(II)-SO_3^{2-} catalytic intermediates could form in cloud-, rain- and fogwater systems.

The Fe(III)- and Cu(II)-S(IV) complexes are transitory in the presence and absence of O_2. These species may be important equilibrium species in the presence of a continued source of S(IV) and the absence of other competing complexes of S(IV). The stability constants determined for these two systems are relatively large for inorganic complexes of Cu(II) and Fe(III) ($K_{CuSO_3} = 10^{4.2}$, $K_{FeSO_3^+} = 10^{6.6}$, see Table 4.3). Other reversible sulfite complexes, such as α-hydroxyalkylsulfonates, $HOCH_2SO_3^-$, have larger stability constants than the Fe(III)-S(IV) and Cu(II)-S(IV) complexes ($K = [HOCH_2SO_3^-]/([HSO_3^-][HCHO]) = 10^7$, Munger et al., 1986). For comparable concentrations of $CuSO_3$ and $FeSO_3^+$ to exist with $HOCH_2SO_3^-$ in a system with 1 mM S(IV), the ratio of the concentration of metals to HCHO must be $[Fe(III)]_T:[HCHO]_T \simeq 30$ at pH 2 or $3x10^2$ at pH 5 and $[Cu^{2+}]_T:[HCHO]_T \simeq 10^7$ at pH 2 or 6 at pH 5. These conditions may exist in the remote troposphere in the absence of photochemical smog. In Southern California, aldehydes have been found in much higher concentrations (Munger et al., 1984, 1986) than Fe(III) and Cu(II) in cloud-, fog- and rainwater systems, therefore S(IV) speciation is likely to be dominated by $RC(OH)SO_3^-$ in this area.

SUGGESTIONS FOR FUTURE RESEARCH

In this thesis, the thermodynamics, kinetics and mechanisms of reactions of S(IV) with Cu(II) and Fe(III) have been addressed. An equilibrium constant for $CuSO_3$ has been determined and a mechanism for the reduction of Cu(II) by S(IV) has been proposed. A conditional stability constant has been obtained for the Fe(III)-S(IV) system. The following areas of research may prove to be fruitful for gaining a better insight of metal-S(IV) chemistry.

Much of the fundamental research on ligand substitution kinetics and redox reactions of transition metals has been investigated using substitution inert ($k_{ex(H_2O)} \simeq 10^{-6}$ sec^{-1}) metals such as Co(III) and Cr(III). The degrees of freedom in labile ($10^3 < k_{ex(H_2O)} < 10^9$ sec^{-1}) metal systems such as the Fe(III) and Cu(II) systems can be reduced by the formation of complexes with well-characterized binding sites, such as metallophthalocyanines and porphyrins. A study of the formation and redox kinetics of these metal sulfito macromolecules would provide valuable insights to the mechanisms of the reduction of the hexaquo metals in the presence of S(IV). This technique should be valuable for the Fe(III)-S(IV) system, since the Fe(III) speciation in a macromolecular complex could be controlled.

Results of this research suggest that the catalytically active metal-S(IV) species could be ternary metal-S(IV)-O_2 species which form as a prelude to the oxidation of S(IV). Kinetic measurements on the redox chemistry of the Fe(III)-S(IV) system in the presence of oxygen when oxygen is the limiting reagent are desired. These experiments must be performed on a stopped-flow spectrophotometer in an anoxic

environment. Rigorously controlled levels of O_2 are necessary, since preliminary experiments on this system yielded erratic results due to oxygen leakage into the syringes of the stopped-flow.

Numerous studies have alluded to the apparent synergism between Fe(III) and Cu(II) on the catalytic rate of oxidation of S(IV) (Albu and Schweinitz, 1932; Bassett and Parker, 1951; Dasgupta et al., 1979). The addition of copper to the Fe(III)-S(IV) system may change the reaction mechanism. In the absence of O_2, the principle oxidation product for Fe(III)-S(IV) is S(V), however, when Cu(II) is added, the primary product becomes S(VI) and the oxidation of S(IV) is enhanced. A typical mechanism which has been proposed to explain this reaction is as follows (Carlyle and Zeck, 1973):

$$\text{Fe(III)} + \text{S(IV)} \rightleftharpoons \text{Fe(II)} + \text{S(V)}$$

$$\text{Fe(III)} + \text{S(V)} \rightleftharpoons \text{Fe(II)} + \text{S(VI)}$$

$$\text{Cu(II)} + \text{S(V)} \rightleftharpoons \text{Cu(I)} + \text{S(VI)}$$

$$\text{Fe(III)} + \text{Cu(I)} \rightleftharpoons \text{Fe(II)} + \text{Cu(II)}.$$

This mechanism fails to consider $CuSO_3^o$, which is likely to form in a mixed catalytic system. Understanding the interactions between different metals in the presence of S(IV) is relevant to tropospheric chemistry, since both Cu(II) and Fe(III) in addition to a variety of other metals are present at significant levels in clouds, rain, fogs and haze aerosol.

REFERENCES

Albu, H.W. and H.D. von Schweintz, 1932, *Ber., Deutsch. Chem. Ges.*, **B65**, 729-737.

Bäckström, H.L.J., 1934, *Z. Phys. Chem. (Leipzig)*, **25B**, 122-138.

Bassett, H. and W.G. Parker, 1951, *J. Chem. Soc*, **46**, 1540-1560.

Carlyle, D.W. and O.F. Zeck, 1973, *Inorg. Chem.*, **12**, 2978-2983.

Dasgupta, P.K., P.A. Mitchell, P.W. West, 1979, *Atmos. Env.*, **13**, 775-782.

Hoffmann, M.R. and J.G. Calvert, *Chemical Transformation Modules for Eulerian Acid Deposition Models, Vol. II, The Aqueous Chemistry.* (U.S. E.P.A., N.C.A.R. Interagency Agreement DW 930237, 1985).

Hoffmann, M.R. and A.P. Hong in *Proceedings of the Second Workshop on Environmental and Inorganic Chemistry*, Portugal (April, 1985).

Munger, J.W., D.J. Jacob, and M.R. Hoffmann, 1984, *J. Atmos. Chem.*, **1**, 335-350.

Munger, J.W., C. Tiller and M.R. Hoffmann, 1986, *Science*, **231**, 247-249.

Veprek-Siska, J. and S. Lunak, 1974, *Z. Naturforsch.*, **29B**, 689-690.

APPENDIX A

ALTERNATIVE EXPERIMENTAL TECHNIQUES USED FOR INVESTIGATING THE Cu(II)-S(IV) SYSTEM

ELECTRON SPECTROSCOPY FOR CHEMICAL ANALYSIS

Purpose

Electron spectroscopy for chemical analysis (ESCA) was used to investigate the Cu(I):Cu(II) ratios in the red crystalline precipitate (identified as $Cu^{II}SO_3Cu^{I}_2SO_3 \cdot 2H_2O$, a mixed valence salt of Cu(I) and Cu(II)) obtained from Cu(II)-S(IV) mixtures. These ratios were of interest as crystals obtained from Cu(II)-S(IV) solutions with different anions present (e.g., NO_3^- or SO_4^{2-}) appeared to have slightly different shapes.

Method

Spectra were taken on a Hewlett-Packard 5950A electron spectrometer. Samples were prepared by grinding the crystals and then mounting the powder on an etched piece of silicon using a hexane and vaseline mixture (20:1). The sample was placed in the probe and degassed for 30 min before placing probe into the spectrometer. The temperature was then lowered to 240 $^{\circ}K$. Spectra were initially taken without the floodgun, and the peaks shifted and changed shape with time (i.e., the signal smeared). The floodgun was used to reduce the smearing.

Results

A broad sweep (1280 eV, with the central binding energy at 640 eV), showed peaks corresponding to Cu_{2p}, S_{2p}, C_{1s}, O_{1s}, and Na_{2s} (see

Fig. A.1). The C_{1s} peak was from the mounting mixture and was used for the reference peak (i.e., for monitoring any signal shift with time). The presence of Na in the sample indicated that Na^+ probably randomly substituted for Cu^+ in the crystal; sodium has approximately the same ionic radius as Cu^+.

Individual peaks were then investigated at greater resolution. Numerous sweeps ($\simeq$ 100 per peak) were necessary to obtain enough information to analyze the spectra. Typical spectra for Cu(II) and S(IV) are shown in Fig. A.2; two peaks for Cu were apparent at this higher resolution. The Cu(I) and Cu(II) peaks were not resolved from these spectra as the two peaks are very close; approximately 1 eV apart. To resolve these peaks, spectra of model compounds containing Cu(II) and Cu(I) must be used to analyze the signal. However, in the spectra obtained, the Cu(II) signal changed with time (see Fig. A.3); the change in time of the relative heights of $Cu_{2p3/2}$ and $Cu_{2p1/2}$ peaks indicate photoreduction was occurring in the sample. Even greater photoreduction was observed when the floodgun was used.

Conclusions

The sample photoreduced in the electron spectrometer, causing the Cu(II):Cu(I) ratio to change with time. Electron spectroscopy techniques were therefore of limited use. The presence of a Na peak indicated that Na^+ substitutes into $Cu^{II}SO_3Cu_2^{I}SO_3 \cdot 2H_2O$.

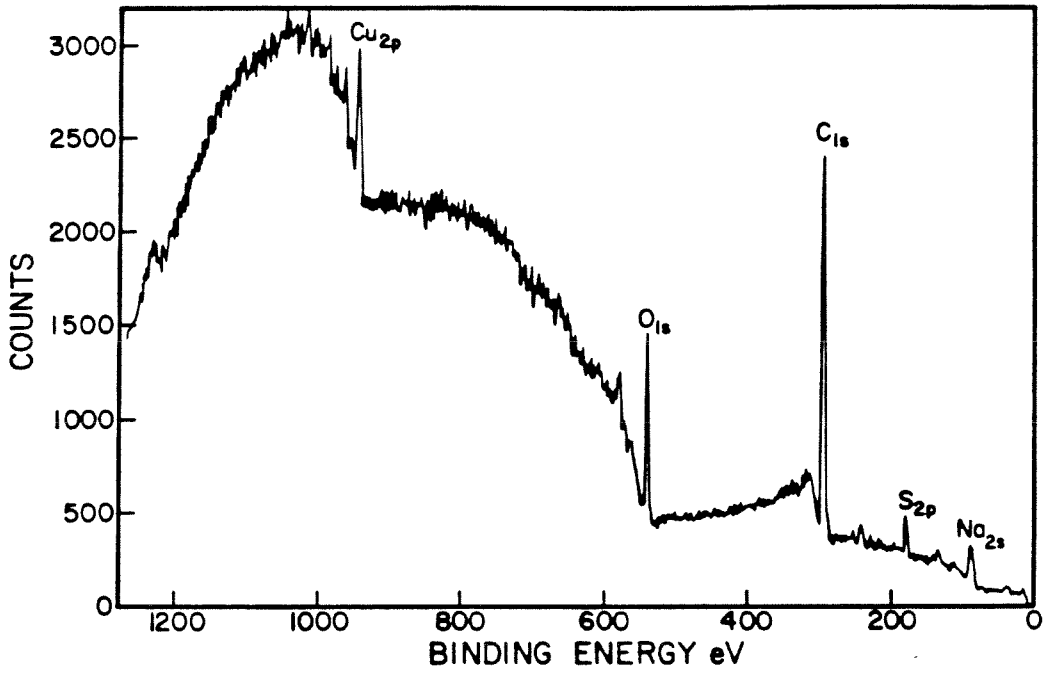

Fig. A.1 ESCA spectrum of $Cu^{II}SO_3Cu_2^{I}SO_3 \cdot 2H_2O$ sample (broad sweep, 1280 eV).

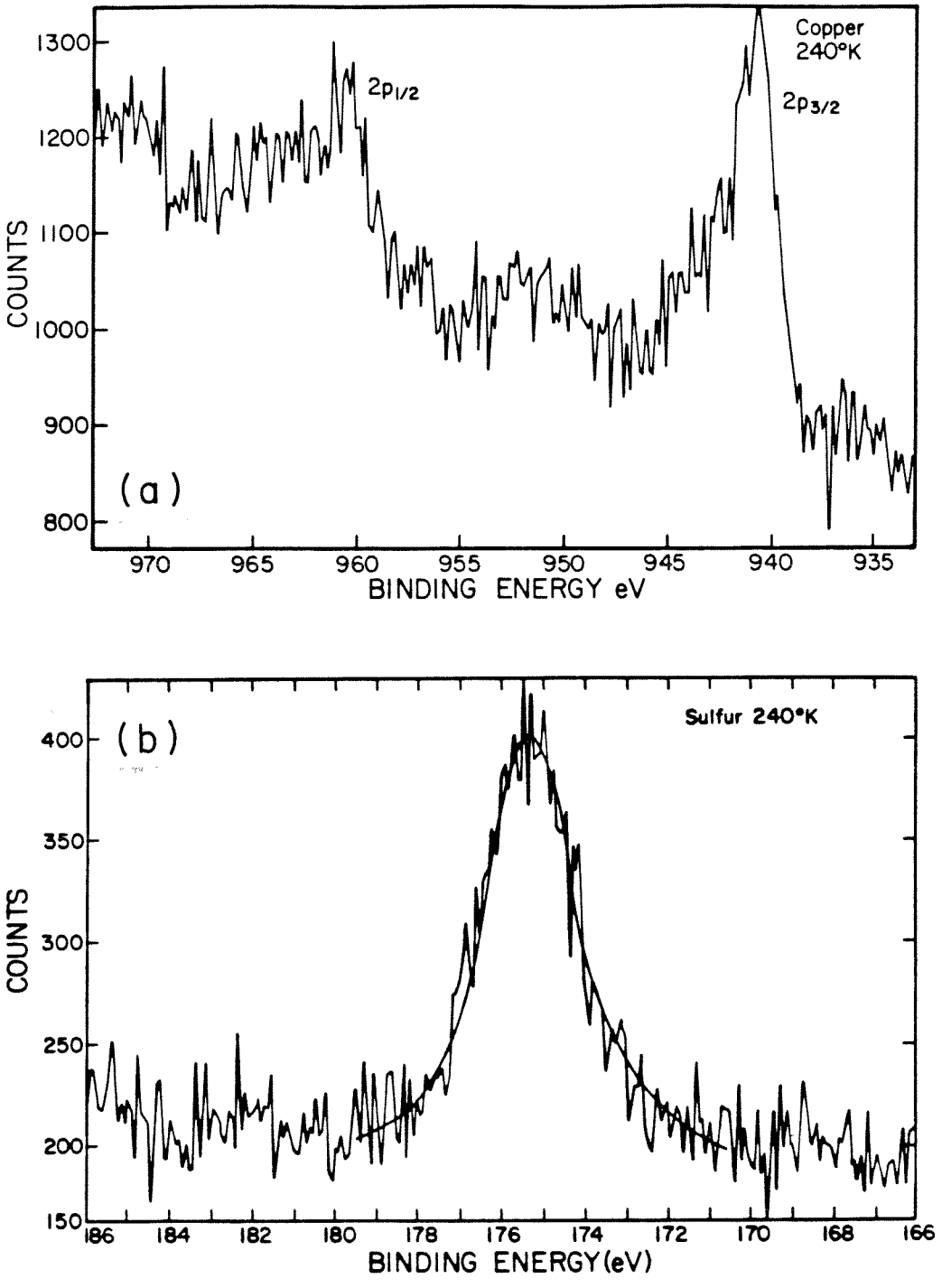

Fig. A.2 ESCA spectra of $Cu^{II}SO_3Cu_2^{I}SO_3 \cdot 2H_2O$ sample (a) copper peak and (b) sulfur peak (narrow sweeps).

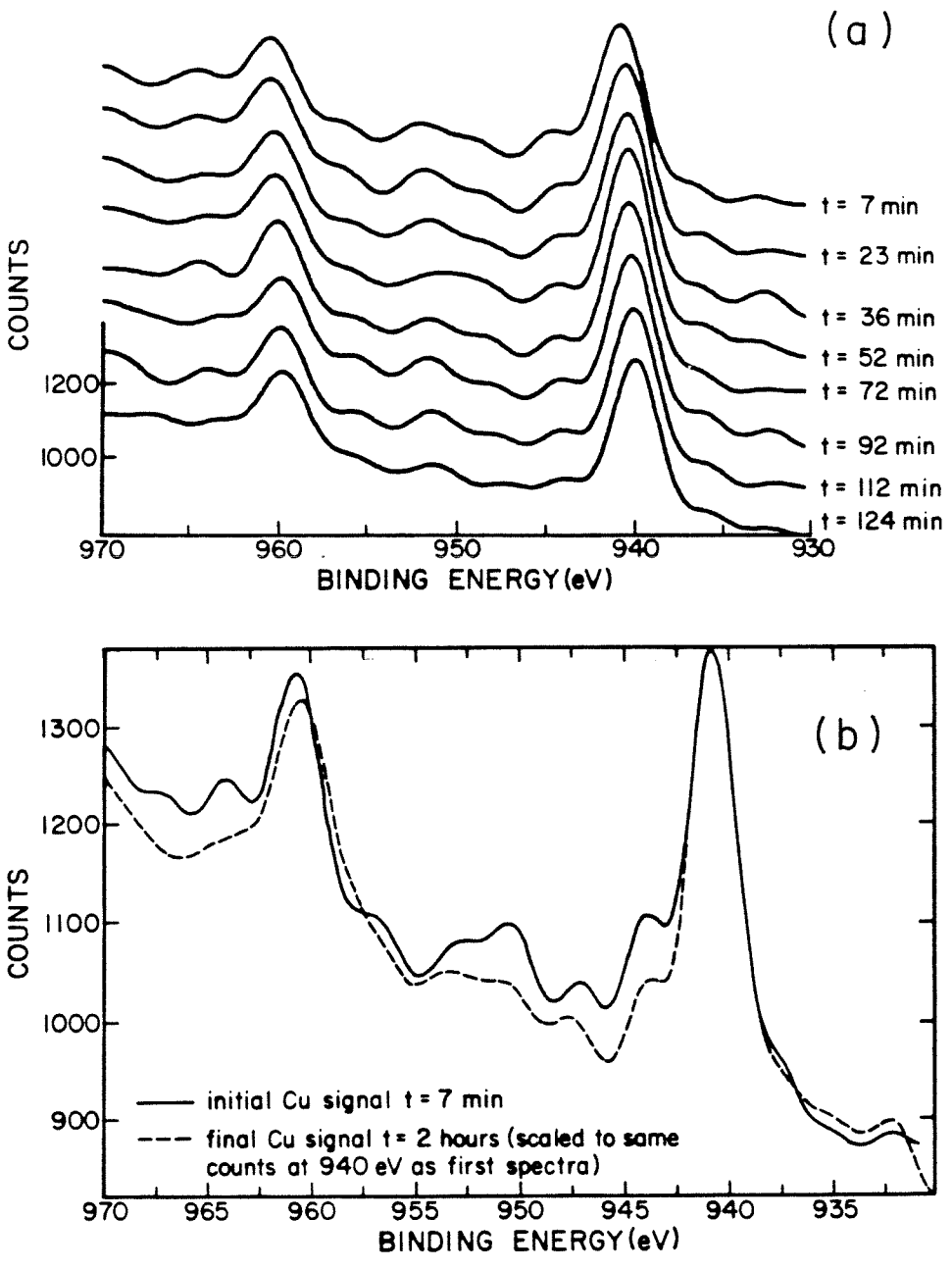

Fig. A.3 The copper peak of Fig. A.2 ,smoothed, (a) shown as a function of time and (b) the peaks from (a) are compared for t = 7 min and t = 124 min to show the change in signal shape.

FOURIER TRANSFORM INFRARED SPECTROSCOPY

Purpose

Fourier transform infrared spectroscopy (FTIR) was used to investigate the bonding in aqueous-phase Cu(II)-S(IV) complexes.

Method

FTIR spectra were collected with a single beam Sirius 100 Mattson spectrometer using BaF_2 cells with a 0.025 mm pathlength. Aqueous mixtures were injected into the cells and the cells were then sealed. Copper chloride solutions were used since Cl^- does not have an IR signal. The metal-S(IV) solutions (0.25 M of each reactant) were mixed just before injecting into the cells. To obtain a well-resolved spectrum, numerous scans were taken and added together, taking $\simeq$ 25 min per spectrum.

Results

The baseline spectrum of H_2O (shown in Fig. A.4a) showed that an absorbance range between 1200 and 500 cm^{-1} could be studied. The spectrum of 0.25 M $NaHSO_3$ (at pH 4) is shown in Fig. A.4b, the SO stretching frequencies (1023 and 1065 cm^{-1}) were close to the stretching frequencies for HSO_3^- observed using Raman spectroscopy (1022 and 1054 cm^{-1}, Chapter 2). The SO stretching frequencies were higher for the Cu(II)-S(IV) mixture (0.25 M of each reactant, pH 1, see Fig. A.4b), however this shift might have been be due to the formation of $BaSO_3$. The H_2O spectrum after the cell was exposed to the Cu(II)-S(IV) mixture was similar to the spectrum of the Cu(II)-S(IV) mixture, and was thus evidence that the cell surface had been modified on exposure to the Cu(II)-S(IV) solution.

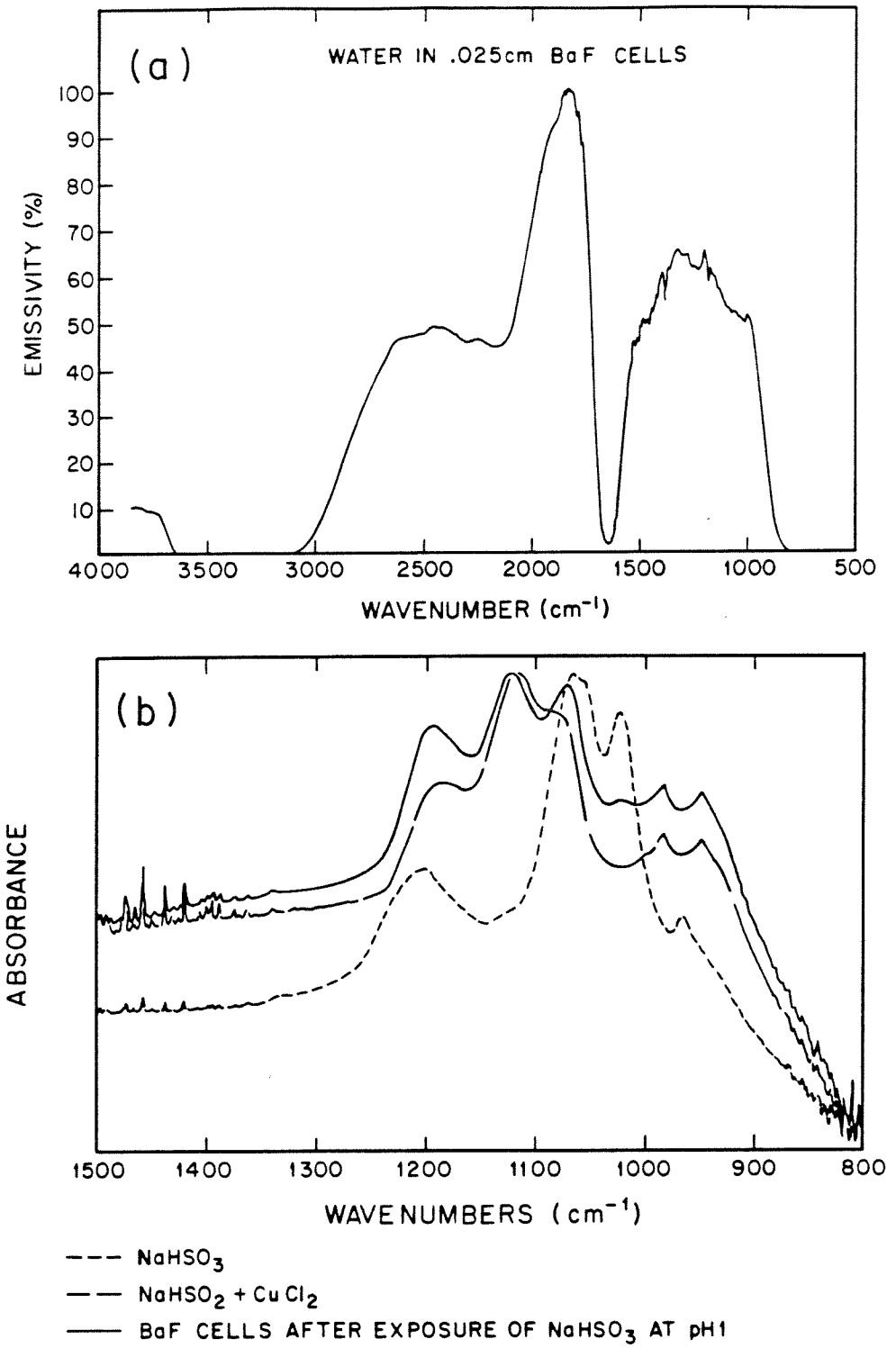

Fig. A.4 FTIR spectra of (a) H_2O in BaF_2 cells and (b) 0.25 M HSO_3^-, 0.25 M HSO_3^- + 0.25 M Cu(II), pH 1 and H_2O in BaF_2 cells after the cells were exposed to the Cu(II)-S(IV) mixture.

Conclusions

The large number of scans required by this technique and interference problems with BaF_2 cells made it an inappropriate method for studying the Cu(II)-S(IV) system. If this technique were to be applied to this system, an inert cell material such as germanium must be used. Additional transient effects would have to be addressed since Cu(II)-S(IV) complexes are unstable and their structure would change significantly over the time period needed to obtain a well-resolved spectrum.

TITRATIONS

Purpose

Both Cu(II) and pH titrations were used to try to determine equilibrium constants for $CuSO_3$.

Results

Radiometer electrodes with a KCl filling solution were used for the pH titrations. Plating of Cu(I)Cl on the pH electrode frit caused the electrode response to change after exposure ($\simeq$ 1 min) to Cu(II)-S(IV) mixtures. Soaking the electrode in HNO_3 ($\simeq$ 0.1 M) restored the electrode response.

Copper(I) is known to change the response of solid state Ag_2S/Cu(II)S electrodes (Westall et al., 1979). Attempts to use an Orion Cu(II) specific electrode in Cu(II)-S(IV) solutions showed that the response of this electrode changed as the Cu(II) was reduced to Cu(I).

Conclusions

Titrations using pH and Cu(II) specific electrodes can not be used on Cu(II)-S(IV) mixtures. Furthermore, pH measurements on Cu(II)-S(IV) mixtures should be made with great care; the electrode should be calibrated before each measurement.

CYCLIC VOLTAMMETRY

Purpose

Cyclic voltammetry was used to investigate the redox reaction in Cu(II)-S(IV) mixtures and to determine a stability constant for $CuSO_3$.

Method

Cyclic voltammetry measurements were made on Cu(II)-S(IV) solutions purged with Ar. The potential of a graphite electrode vs. SCE (Pt working electrode, NaCl saltbridge) was monitored.

Results

The electrode response changed during the course of the reaction. A freshly cleaved electrode surface had a different response than a surface that had been exposed to the Cu(II)-S(IV) mixture. This can be seen by the continually changing signal obtained for the Cu(II)-S(IV) system (see Fig A.5). The existence of a Cu^0 stripping peak superimposed on the Cu^{2+}/Cu^{+} couple indicated Cu^0 was deposited on the electrode surface. A separate peak near the Cu^{2+}/Cu^{+} couple indicated that the complex had a lower exchange rate than Cu^{2+}. The equilibrium constant could not be measured as an irreversible reduction was occurring in the system.

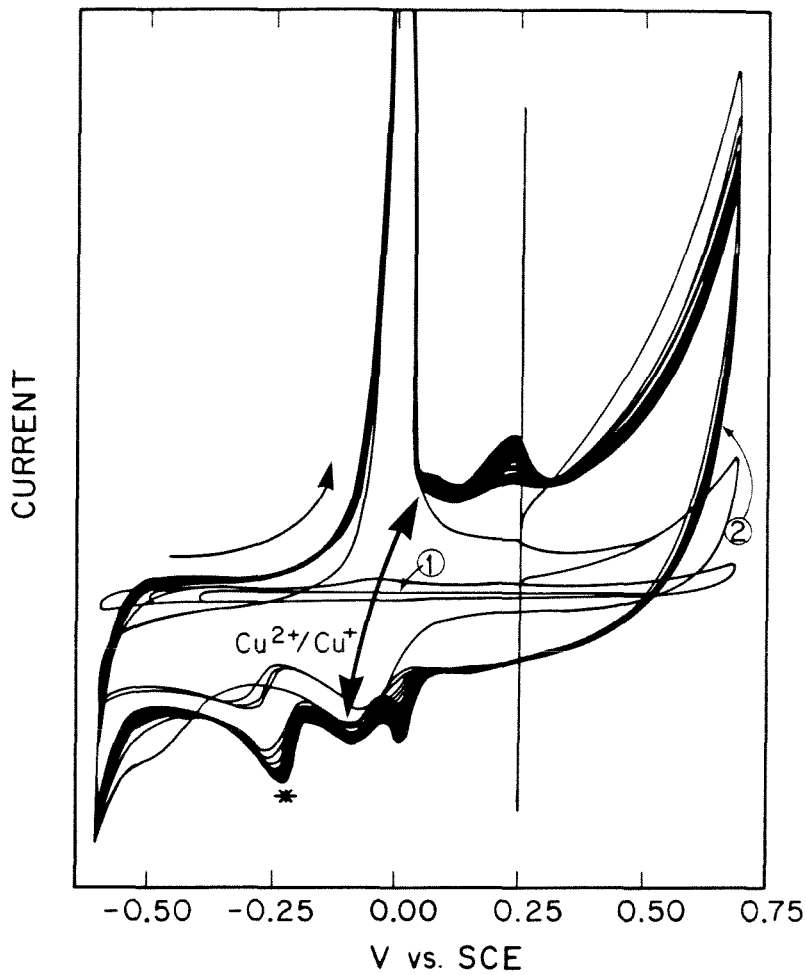

① 1 mM S(IV) (μ = 0.1 M, pH 5)
② 1 mM S(IV) + 1 mM Cu(II) (μ = 0.1 M, pH 5)

NOTE: (i) Cu^0 stripping peak superimposed on Cu^{2+}/Cu^{+} couple
(ii) Peak marked * was due to an irreversible reduction reaction. The existence of a separate peak indicated that the complex has a lower ligand exchange rate than Cu^{2+}.
(iii) Trace shape changed with time, i.e. the electrode response must be changing with time.

Fig. A.5 Cyclic voltammetry signal obtained for Cu(II)-S(IV) mixture.

Conclusions

An irreversible reduction occurred in the Cu(II)-S(IV) system. The existence of a separate peak from the Cu^{2+}/Cu^{+} couple indicated that the ligand exchange rate was lower for the complex than for Cu^{2+}. However, the trace was too complicated to analyze quantitatively.

ELECTRON PARAMAGNETIC RESONANCE

Purpose

Electron Paramagnetic Resonance (EPR) was used to investigate the disappearance of Cu(II) in the Cu(II)-S(IV) system and to obtain information about changes in the Cu(II) coordination environment during the course of the reduction of Cu(II) in this system.

Method

EPR spectra were recorded on a Varian E-Line Century Series spectrometer. Spectra were taken on quick-frozen anoxic solutions at 77 ^{o}K in 5 mm quartz tubes. Spectra were integrated using the equations of Aasa and Vänngard (1975).

Background and Results

EPR is a powerful tool to study metal centers which have unpaired electrons. The interaction of the unpaired electron with a magnetic field yields information about the g-value, the symmetry of the compound of interest, the number of spins contributing to the signal and the electron relaxation processes. Copper(II), d^{9}, has an EPR signal, whereas Cu(I), d^{10}, does not; EPR was used to investigate the reduction of Cu(II) in the Cu(II)-S(IV) system.

The position of the resonance, or g-value is defined as

$$g = \frac{h\upsilon}{\beta H_z} \qquad (A.1)$$

where h = Planck's constant (6.63×10^{-27} erg sec);

υ = frequency of radio waves (typically 9.2 GHz);

β = Bohr magneton (0.92732×10^{-2} $\frac{erg}{gauss}$);

H_z = magnetic field (the z direction is the direction of laboratory apparatus).

The g-value or g-factor quantifies the strength of interaction of a given electron with an applied magnetic field. It is the spectroscopic gauge of the magnitude of the magnetic moment, μ, of the electron under study:

$$\mu = -g\beta\sqrt{s(s+1)} \qquad (A.2)$$

where s = spin of particle ($s = 0, \frac{1}{2}, 1, \frac{3}{2}...$).

Eqns. A.1 and A.2 apply to both free and unbound electrons. The g-value of unbound electrons is 2.002319; unpaired electrons in different environments have different g-values which depend on the electronic structure of their environment.

The structure super-imposed on the basic spectral envelope can give insight into the coordination environment of the metal center. This super-imposed structure can be caused from contributions from the the nuclear moment (hyperfine interactions), or from the electron-electron interactions if there is more that one paramagnetic

center present. These paramagnetic centers can interact two ways: dipole-dipole interactions (when the centers are close enough for the orbits of two unpaired electrons to overlap) or by exchange interactions (when the two centers interact through a bridging ligand).

Quantitative information can be obtained about the number of spins contributing to the observed resonance. This can be determined by comparing the area under the sample signal to the area under the signal of a sample of known concentration. The spectra obtained are actually absorption derivatives of the paramagnetic signal and must be integrated twice to obtain the area under the curves (which is directly proportional to the number of paramgnetic centers contributing to the spectra). The area under the signal may give a number lower than the actual paramagnetic spins in the system; the signal from a paramagnetic center can be quenched from dipole-dipole interactions or exchange interactions.

The total magnetic moment will have a combined contribution from spin and orbital magnetism. The signal varies with the direction of a molecule in a magnetic field. If the molecule has less than cubic symmetry, the g-factor will be orientation dependent or anisotropic. Typical spectra are taken on frozen solutions and powders. In these media, the metal center adopts random orientations, so that all possible orientations are present. A molecule oriented arbitrarily with respect to the magnetic field will exhibit a g-value:

$$g = g_x^2 l_x^2 + g_y^2 l_y^2 + g_z^2 l_z^2$$

where l_x^2, l_y^2, and l_z^2 are the normalized direction cosines of the g tensor coordinate frame onto the direction of the magnetic field, H_z, and $g_x^2 l_x^2$, $g_y^2 l_y^2$, $g_z^2 l_z^2$ are 3 directionally weighted contributions to the g-value. There are special cases for different values of g; when two values are the same $g_x = g_y < g_z$ or $g_x = g_y > g_z$, it is known as the axial case. The unique g value is known as $g_{\parallel}$, while the identical pair are known as $g_{\perp}$. When all three g-values are the same, it is an isotropic case. The lowest spin cases ($s = \pm\frac{1}{2}$) exhibits EPR spectra with $g_{\perp} = 6$ and $g_{\parallel} = 2$. Fig. A.6 shows the effect of different g_n-values on EPR spectra (taken from Palmer, 1980)

If there are two paramagnetic centers, there can be electron-electron interactions between the two centers. As mentioned earlier, these can be due to exchange interactions or space interactions via dipole-dipole coupling. Both of these states lead to a redefinition of the wave functions of individual electrons. The resultant states may be different than those for the individual paramagnetic centers. In the case of two paramagnetic centers interacting with a spin of $\frac{1}{2}$ each, the resultant states are $s = 1$ $(\frac{1}{2} + \frac{1}{2})$ or $s = 0$ $(\frac{1}{2} - \frac{1}{2})$ neither of which is paramagnetic. As different transitions are allowed for the new spin states, there are drastic changes in the EPR spectra. The exchange interaction is weaker than the dipole-dipole interaction and is usually attentuated ten-fold by each sigma bond.

Another possible consequence of dipolar interaction is an apparent loss of intensity in the EPR spectra. If the magnitude of the dipolar term is substantial, an EPR signal will only be observed from molecules

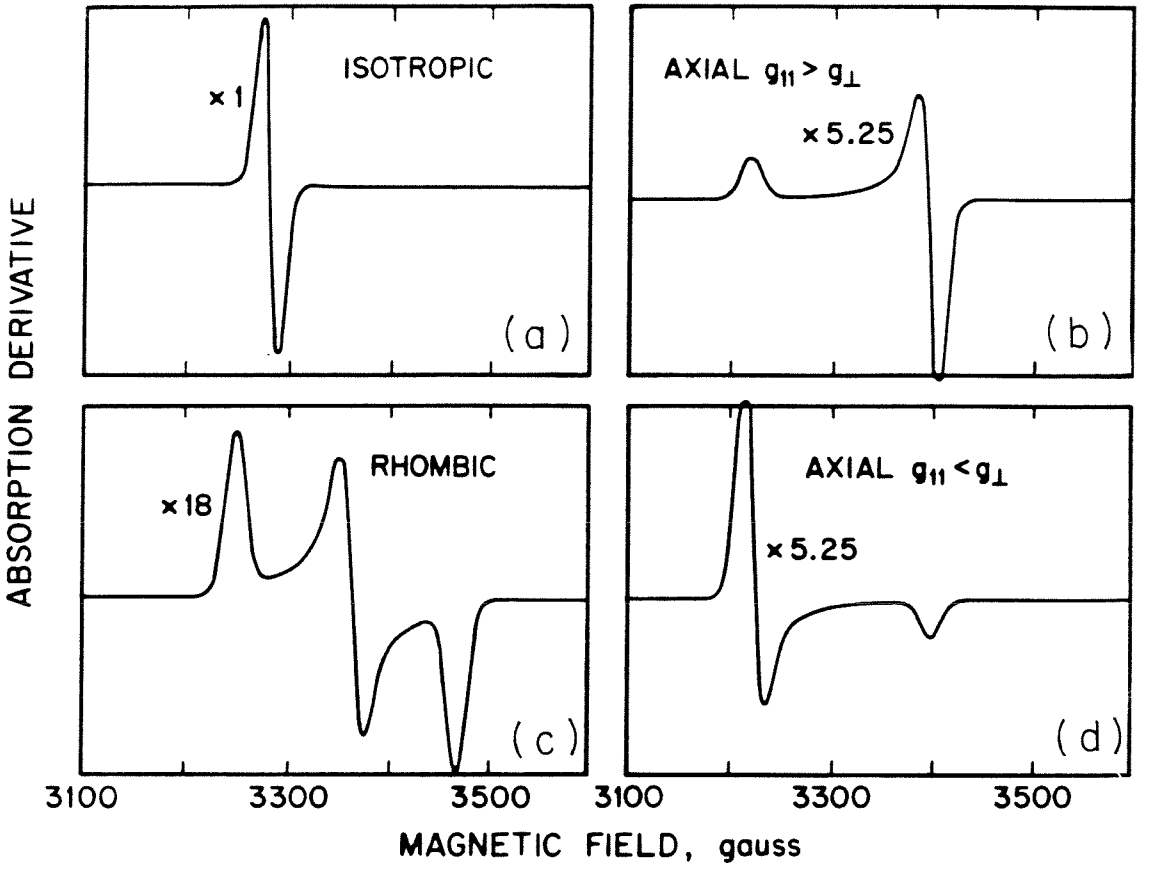

Fig. A.6 Theoretical line shapes for s = ½ EPR spectra (a) isotropic case, $g_x = g_y = g_z$, (b) axial case, $g_{\parallel} > g_\perp$, (c) rhombic case, $g_x \neq g_y \neq g_z$, and (d) axial case, $g_{\parallel} < g_\perp$. (Taken from Palmer, 1980).

which are not affected. These molecules can be a small percentage of the total. As the distance between the molecules increases, a greater number contribute to the unperturbed EPR. The relative intensity of the EPR can give some idea of the separation between the paramagnetic centers. The effects of dipole-dipole interactions have to be carefully interpreted. In Figure A.7, there are a series of spectra showing the effects of relative orientations between the g-tensors for two paramagnets (the scaling factor alongside the spectra denote the vertical expansion used in each spectra, taken from Palmer, 1980). The important features to note are: relatively little increase in width, the change in detail of the spectra, and the sensitivity of the spectra to orientation.

By understanding the nature of these dipole-dipole interactions, information can then be extracted from the EPR spectra for the Cu(II)-S(IV) system. The initial integrated EPR spectra obtained were gaussian in shape (see Fig. A.8a). This was caused by the "slow-freezing" of samples in an aqueous media. This freezing process usually promotes ice crystal formation with subsequent solute-solvent segregation (Leigh and Reed, 1971). The segregated solutes do not freeze until a eutectic composition is reached, resulting in local concentrations of up to 10 M solute. Quick-freezing partially alleviated this problem, but it was difficult to freeze fast enough to totally overcome these effects. Four approaches were used to overcome this problem in aqueous solution: quick-freezing, using high ionic strength, forming a better glass in a solution of 30% ethylene glycol and using a polydextran gel matrix (Pharmica Sephadex G-50) The

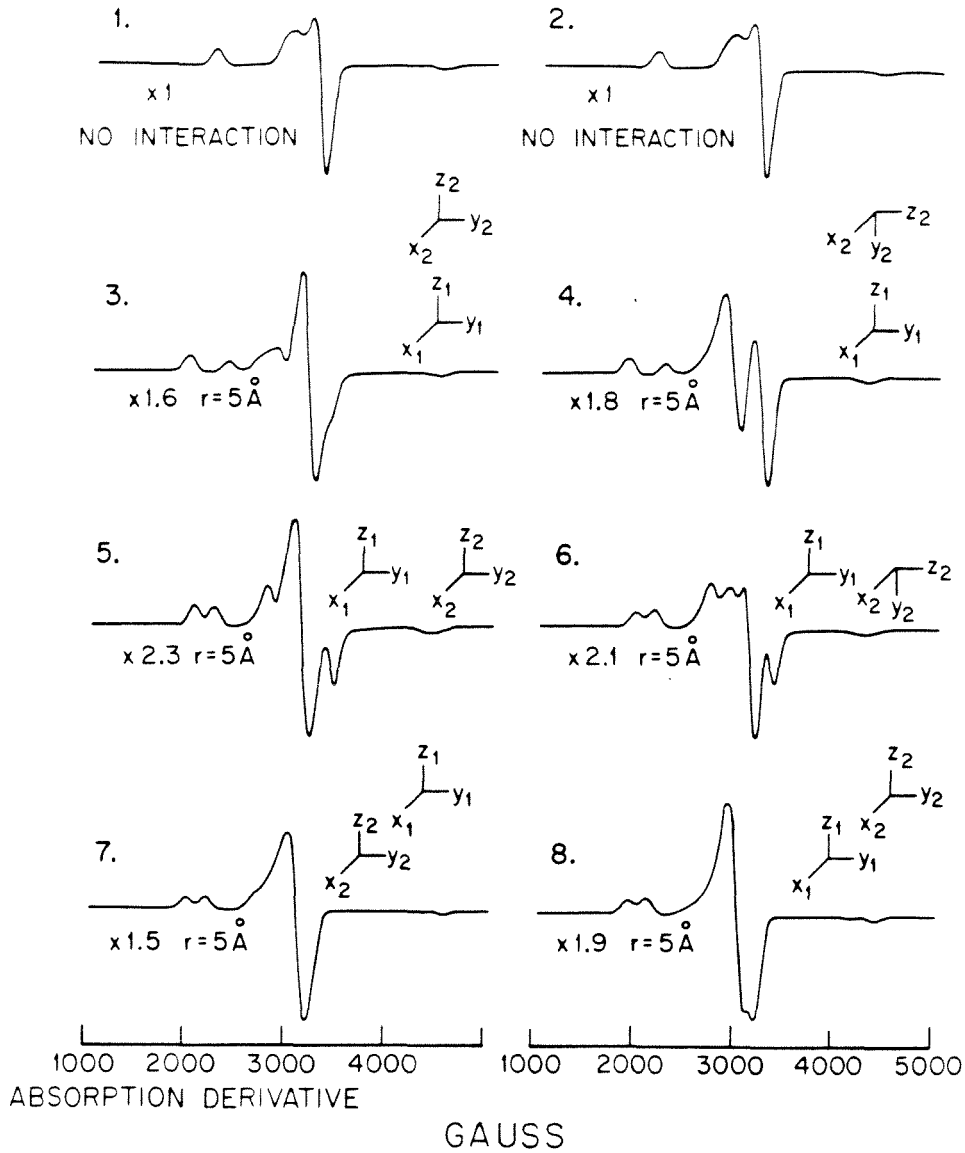

Fig. A.7 Simulation of magnetic dipolar interaction between two paramagnets (g_x = 1.5, g_y = 2.2, g_z = 3.5, and g_x = 2.0, g_y = 2.0, g_z = 2.17) at a distance of 5 Å and at various orientations of the g-tensors. The multiplicative factors were employed to scale the spectra to the same size. (Taken from Palmer, 1980).

objective was to minimize perturbations in the equilibrium of species of interest. Increasing the ionic strength can shift the equilibrium away from the species of interest. Ethylene glycol was found to interfere with Cu(II)-S(IV) complex formation. Preliminary results using a polydextran gel, suggested by Leigh and Reed (1971), were the most promising; hyperfine structure was apparent at low ionic strength. However, the majority of EPR spectra were taken of aqueous mixtures of Cu(II)-S(IV) in the presence of $NaNO_3$, $NaClO_4$, or NaCl. The total number of spins in $Cu(NO_3)_2$ solutions was found not to vary with pH (from pH 3 to 6), with ionic strength or with the presence of ethylene glycol, although the hyperfine structure could only be seen for solutions with higher ionic strength and in the presence of ethylene glycol. In Fig. A.8 spectra of Cu-S(IV) mixtures at 3 ratios of S(IV):Cu(II) are shown. As the ratio increased, and the ionic strength of the solution increased, the hyperfine structure became more evident.

EPR spectra of the Cu(II)-S(IV) system in the presence of ClO_4^- and NO_3^- are shown in Fig. A.9. These spectra are typical Cu(II) EPR spectra with a g-value of 2.1 and four hyperfine structures. There was an immediate decrease in the magnitude of the Cu(II) signal when S(IV) was added (within the 30 seconds it took to mix and freeze the solutions); see Table A.1. The times given for each spectrum are the total time for which the sample was at room temperature (21 $^{\circ}C$) before quick-freezing to take the spectrum. The freezing and thawing added $\pm$ 30 sec to the indicated times. As the reaction progressed, the hyperfine structure changed, indicating that there were changes in the inner-coordination sphere of the copper. However, there was no

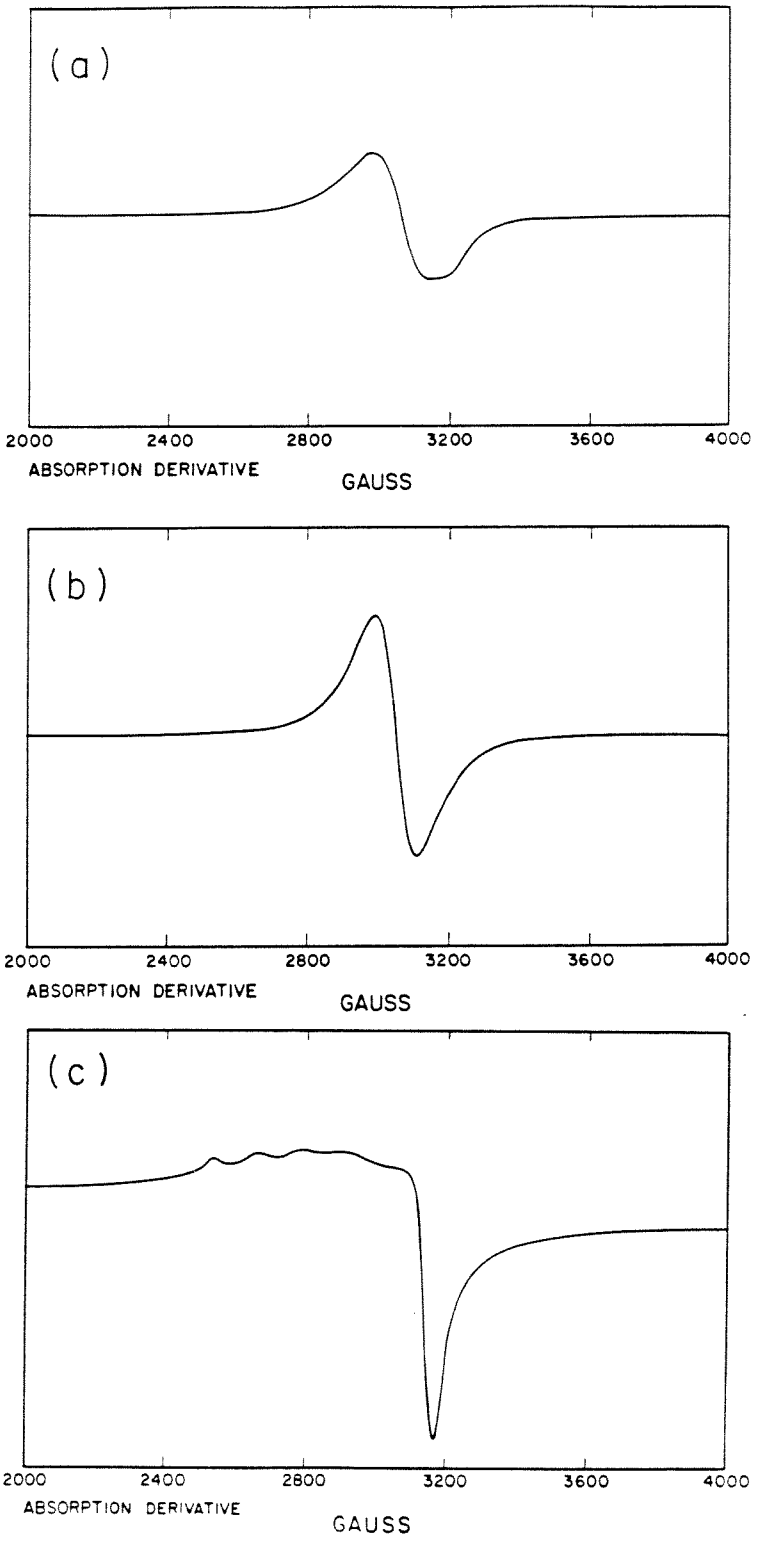

Fig. A.8 EPR spectra of Cu(II)-S(IV) mixtures at different ratios (a) S(IV):Cu(II) = 1, (b) S(IV):Cu(II) = 2 and (c) S(IV):Cu(II) = 10. ($[Cu(II)]_T$ = 2 mM, pH = 5).

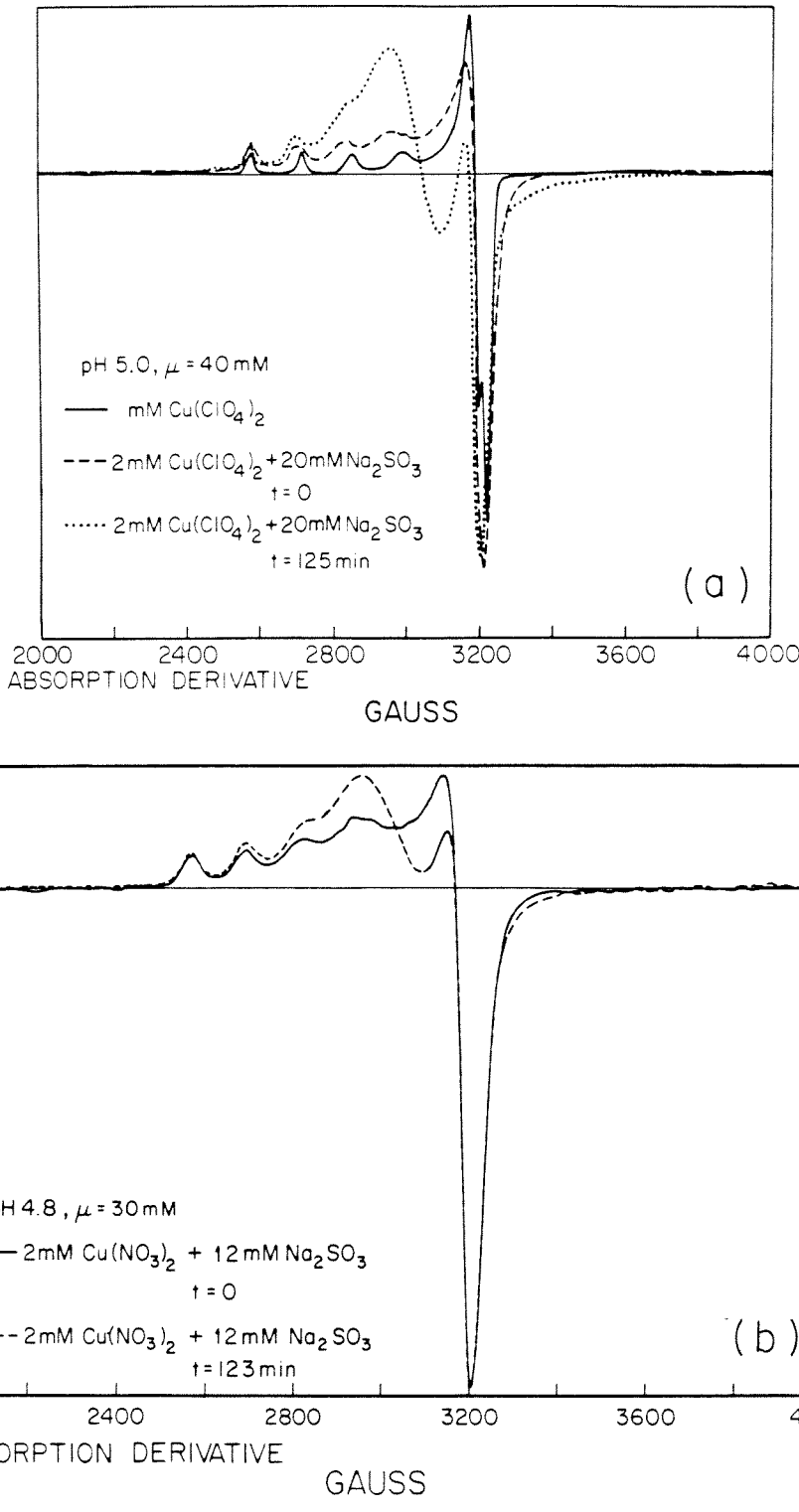

Fig. A.9 Cu(II) EPR spectrum for the Cu(II)-S(IV) system in the presence of (a) ClO_4^- and (b) NO_3^-.

TABLE A.1

Data based on changes in the areas under the recorded EPR spectra of the Cu(II)-S(IV) system presented in Fig. B.9 as a function of time

ClO_4^-		NO_3^-	
Time[a]	% $[Cu(II)]_o$[b]	Time[a]	% $[Cu(II)]_o$[b]
0	51	0	59
25	46	18	64
50	44	42	62
75	49	86	64
100	51	123	62
125	49	>12 hours	58
>26 hours	40		

[a] $[Cu(II)]_o$ was determined from the area under a [Cu(II)] spectrum with no S(IV) present.

[b] Times refer to the length of time the sample was at room temperature before quick-freezing to take spectrum.

significant decrease in the number of Cu(II) centers contributing to the spectra (see Table A.1). The initial decrease indicated that either there was a rapid reduction of the Cu(II) when S(IV) was added to the solution, or else there was spin-coupling of the copper centers by the formation of sulfite-bridged copper dimers.

Conclusions

The Cu(II)-S(IV) system can be studied using EPR. To obtain the maximum information from the EPR spectra, techniques should be used to minimize interference from the freezing process. In the experiments analyzed for this project, the number of paramagnetic centers contributing to the signal was investigated. Information can also be obtained by investigating the changes which occur in the Cu(II) coordination environment during the course of the reaction between Cu(II) and S(IV).

REFERENCES

Aasa, R. and T. Vanngard, 1975, *J. Mag. Res.*, **19**, 308-315.

Leigh, Jr., J.S. and G.H. Reed, *J. Phys. Chem.*, **75**, 1202-1204.

Palmer, G. in *Advances in Inorganic Biochemistry, Vol. 12*, D.W. Darnall and R.G. Wilkins, ed. (Elsvier/North Holland, Inc., New York, 1980) pp. 153-182.

Westall, J.C., F.M. Morel and D.N. Hume, 1979, *Anal. Chem.*, **51**, 1792-1798.

APPENDIX B

EXPERIMENTAL DATA FOR CHAPTER THREE

TABLE B.1

EXPERIMENTAL DATA FOR TABLE 4.3

$[S(IV)]_o$ = 0.01 M
$[Cu(II)]_o$ = 0.004 M
pH = 4.7

t (min)	absorbance (340 nm)
0	0.298
21	0.160
33	0.134
43	0.138
56	0.107
85	0.094
146	0.091
211	0.080
361	0.066
936	0.040
1360	0.028
1686	0.027

$[S(IV)]_o$ = 0.02 M
$[Cu(II)]_o$ = 0.002 M
pH = 5.0

t (min)	absorbance (340 nm)
0	1.224
20	0.646
38	0.519
62	0.440
80	0.401
97	0.373
115	0.352
138	0.332
187	0.298
222	0.281
282	0.262
343	0.271
1025	0.266
1045	0.260
1713	0.216

$[S(IV)]_o$ = 0.005 M
$[Cu(II)]_o$ = 0.005 M
pH = 4.5

0	0.786
18	0.504
37	0.421
55	0.361
71	0.334
94	0.310
113	0.290
138	0.274
190	0.249
251	0.228
318	0.213
422	0.198
551	0.188
1284	0.160
1588	0.151
2013	0.138

$[S(IV)]_o$ = 0.01 M
$[Cu(II)]_o$ = 0.004 M
pH = 4.9

0	0.511
15	0.270
32	0.216
56	0.180
76	0.154
103	0.142
126	0.131
153	0.119
177	0.114
223	0.104
265	0.094
289	0.095
345	0.097
376	0.085
621	0.093
641	0.091
3034	0.043

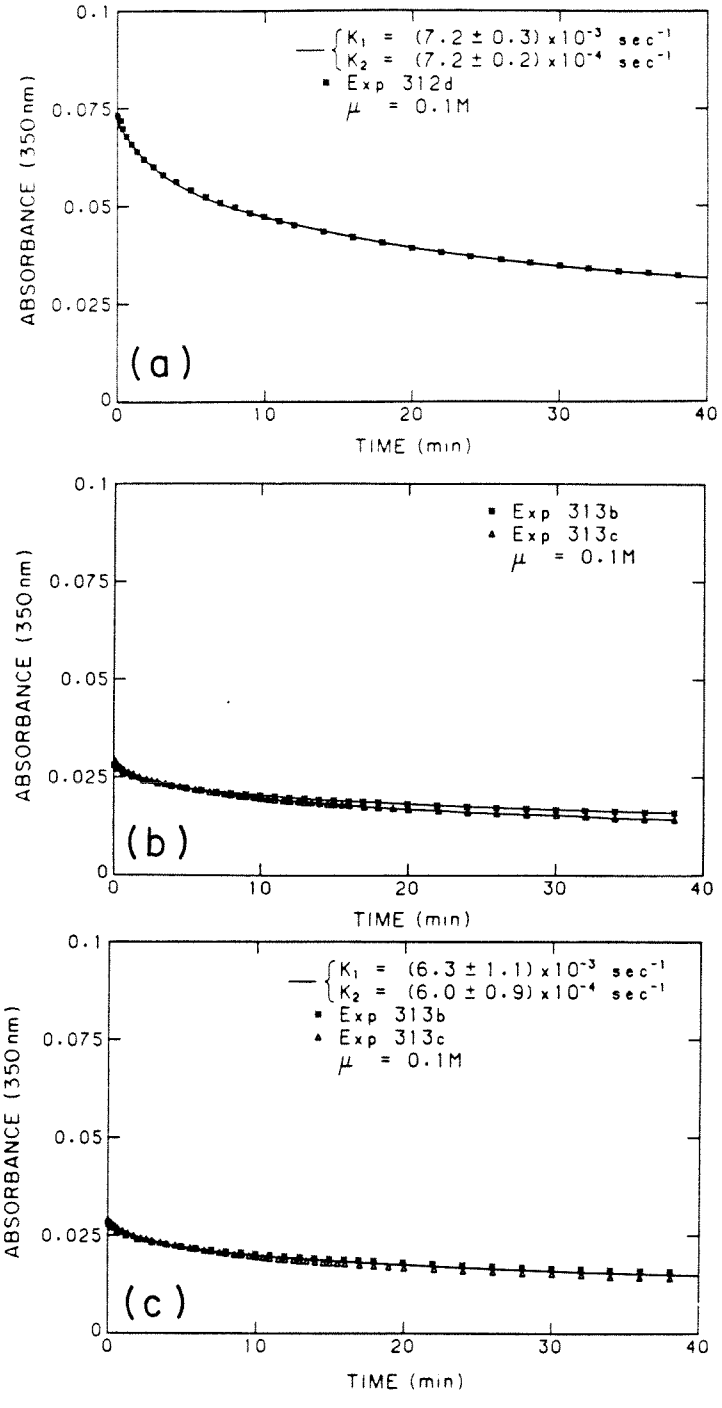

Fig. B.1 Kinetic data obtained at 350 nm for the Cu(II)-S(IV) system (a) pH 4.9, (b) pH 4.4, and (c) pH 4.4. (The solid line in (c) was fit to the data using a nonlinear least squares double-exponential fitting routine). ($[S(IV)]_o$ = 10 mM, $[(Cu(II)]_o$ = 1 mM).

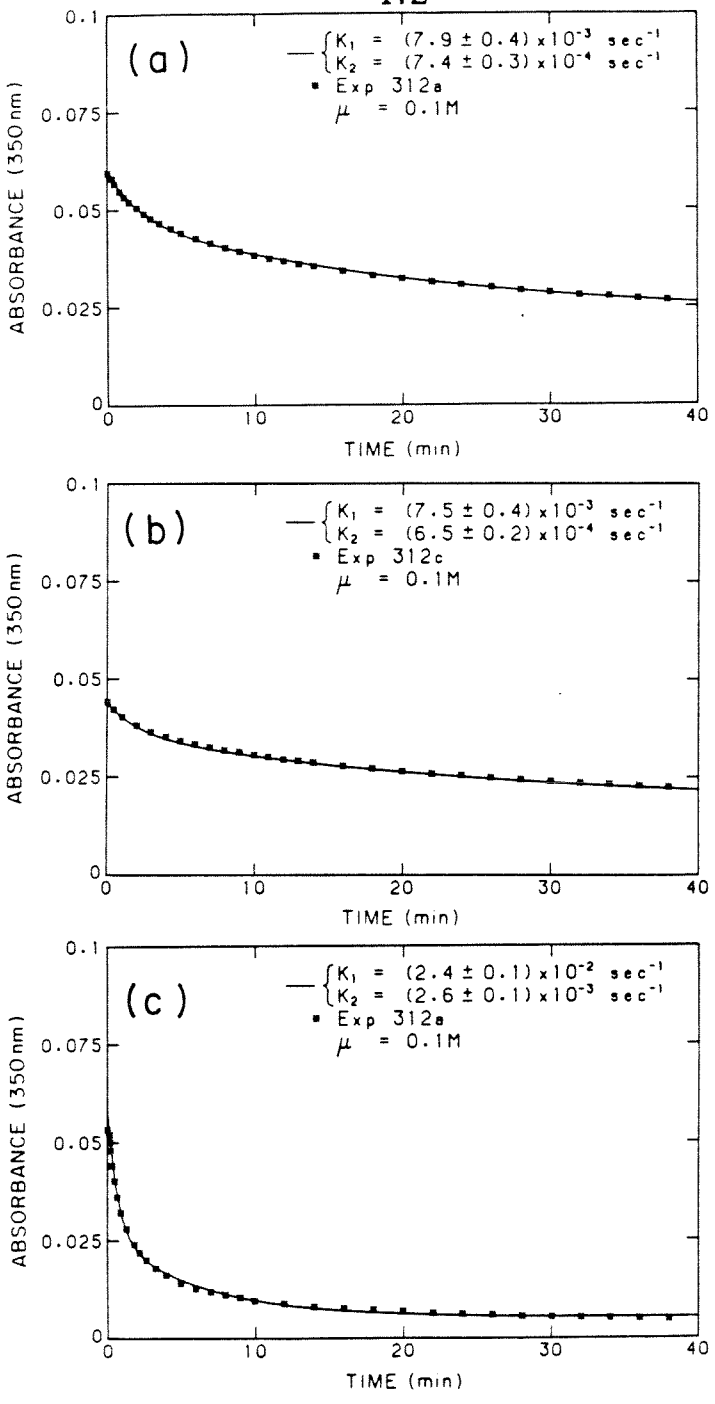

Fig. B.2 Kinetic data obtained at 350 nm for the Cu(II)-S(IV) system with different anions present (a) ClO_4^-, pH 4.8 (b) SO_4^{2-}, pH 4.9, and (c) Cl^-, pH 4.9. (The solid line was fit to the data using a nonlinear least squares double-exponential fitting routine). ($[S(IV)]_o$ = 10 mM, $[(Cu(II)]_o$ = 1 mM).

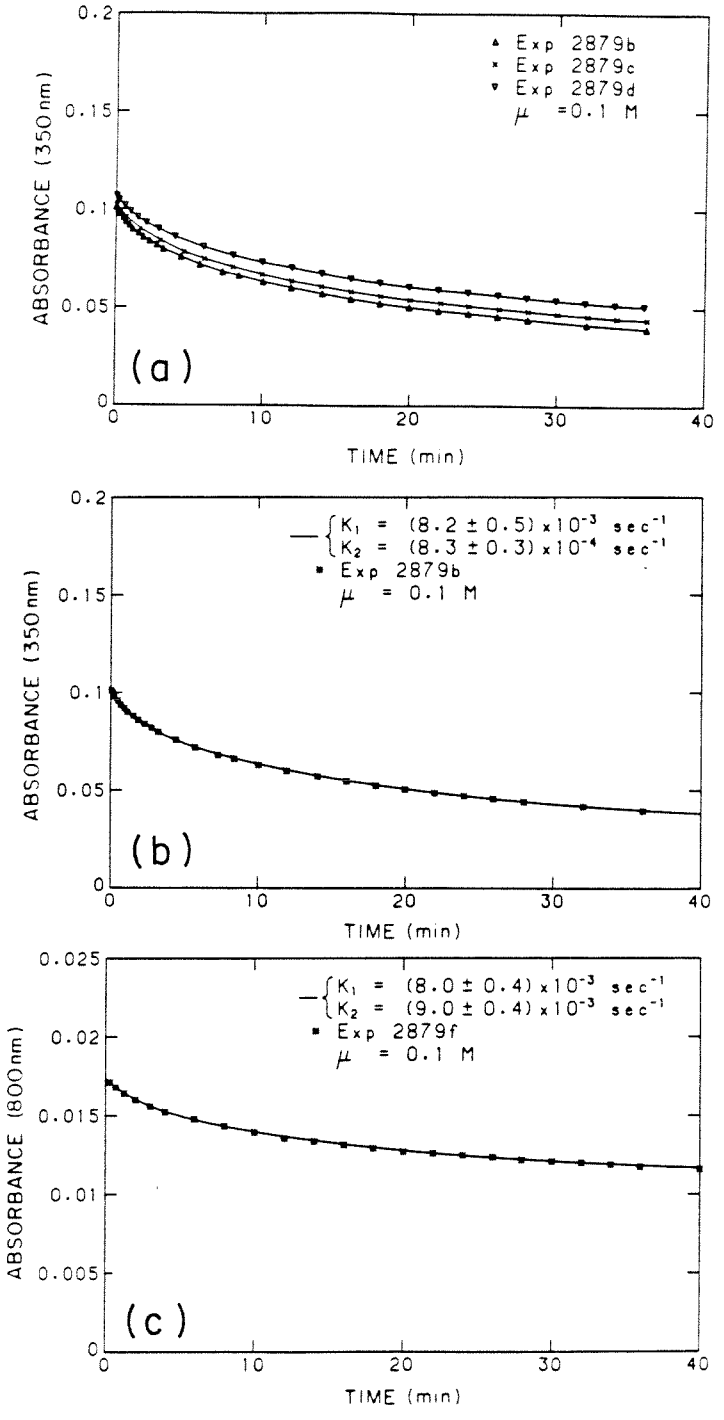

Fig. B.3 Kinetic data obtained for the Cu(II)-S(IV) system at pH 5.2 (a) 350 nm, (b) 350 nm, and (c) 800 nm. (The solid lines in (b) and (c) were fit to the data using a nonlinear least squares double-exponential fitting routine). ($[S(IV)]_o$ = 10 mM, $[(Cu(II)]_o$ = 1 mM).

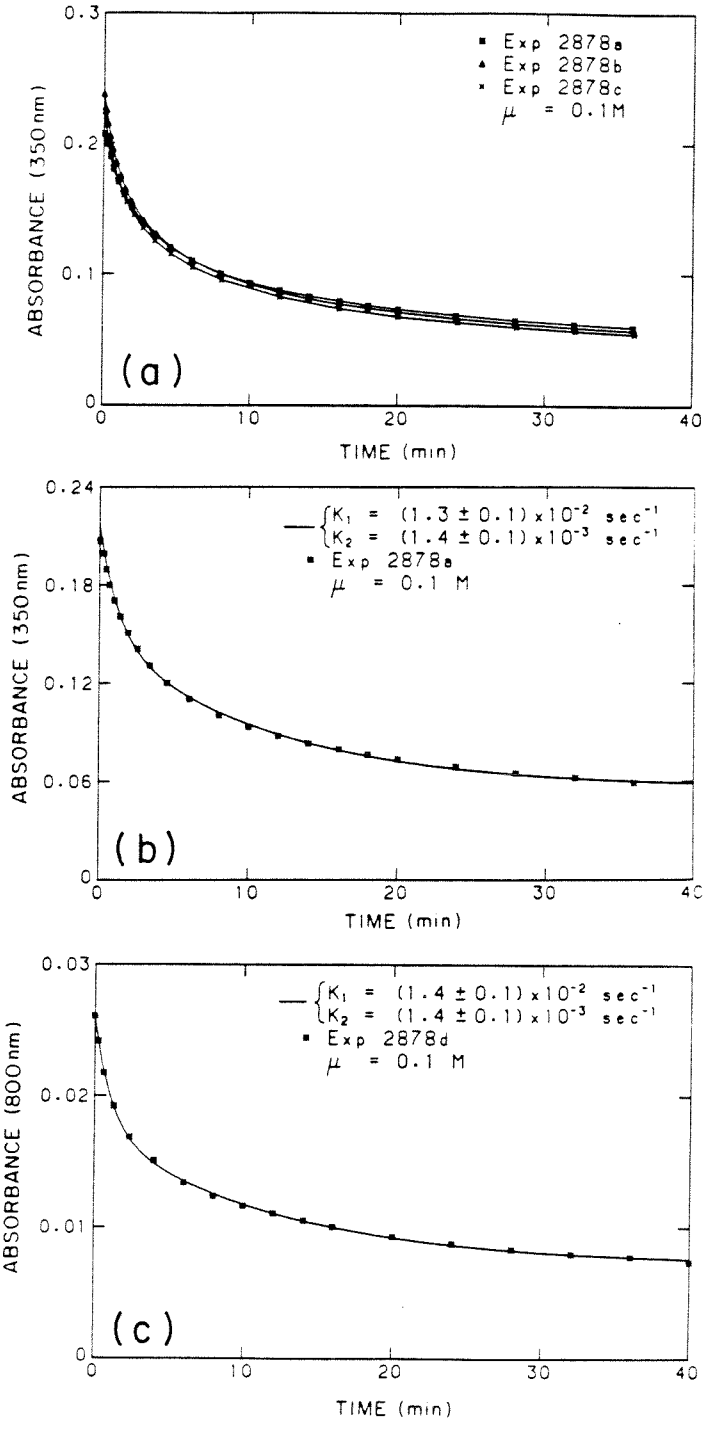

Fig. B.4 Kinetic data obtained for the Cu(II)-S(IV) system at pH 5.7 (a) 350 nm, (b) 350 nm, and (c) 800 nm. (The solid lines in (b) and (c) were fit to the data using a nonlinear least squares double-exponential fitting routine). ($[S(IV)]_o$ = 10 mM, $[(Cu(II)]_o$ = 1 mM).

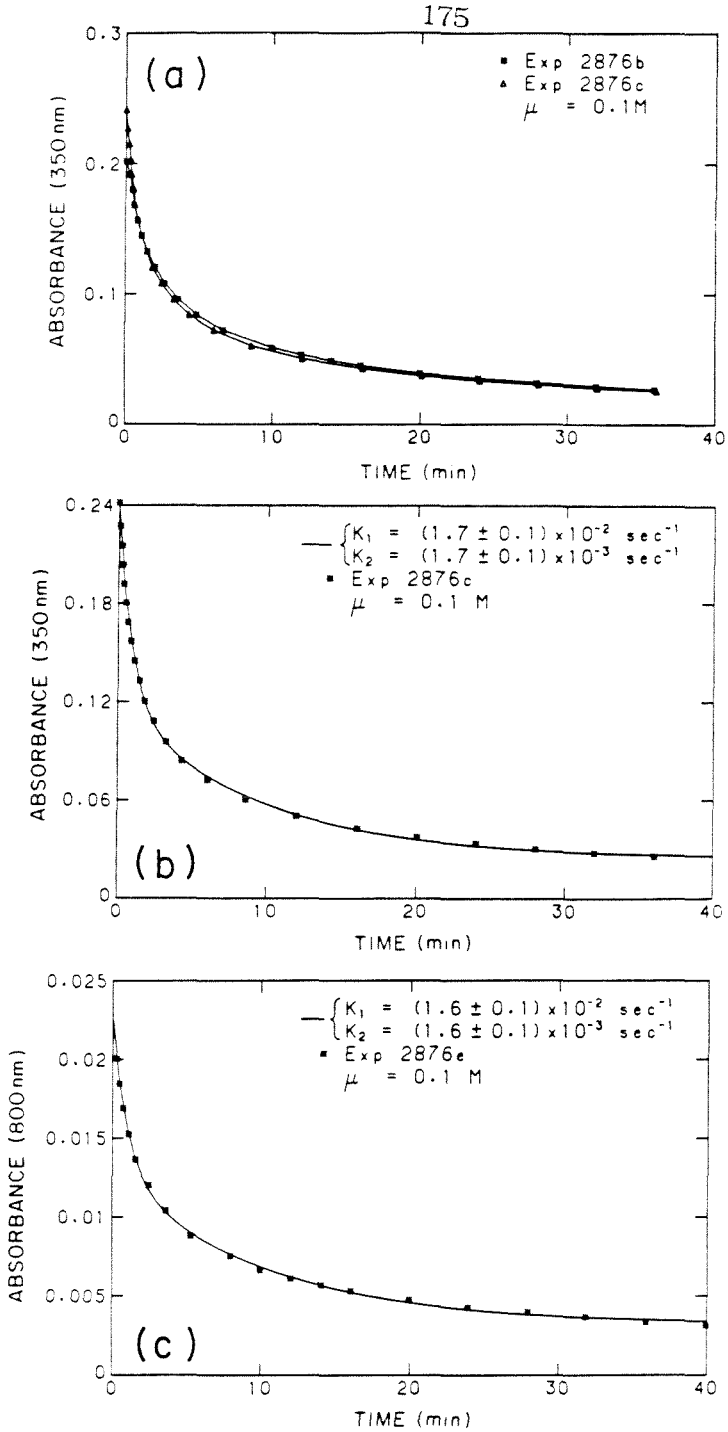

Fig. B.5 Kinetic data obtained for the Cu(II)-S(IV) system at pH 6.2 (a) 350 nm, (b) 350 nm, and (c) 800 nm. (The solid lines in (b) and (c) were fit to the data using a nonlinear least squares double-exponential fitting routine). ($[S(IV)]_o$ = 10 mM, $[(Cu(II)]_o$ = 1 mM).